NON-LOOSE TORUS KNOTS

JOHN B. ETNYRE, HYUNKI MIN, AND ANUBHAV MUKHERJEE

ABSTRACT. We give a complete coarse classification of Legendrian and transverse torus knots in any contact structure on S^3.

CONTENTS

1. Introduction

The study of Legendrian and transverse knots in contact 3–manifolds has gone hand in hand with the development and application of contact geometry, with many key features (like tightness) and constructions (like Legendrian and transverse surgery) relying on them. Moreover, over the last 20 or so years, a rich and beautiful theory of Legendrian and transverse knots has developed. However, there has been surprisingly little work on Legendrian knots in overtwisted contact manifolds. This might partially be due to the fact that overtwisted contact structures are classified and are determined by their algebraic topology [13]. However, non-loose Legendrian and transverse knots in overtwisted contact structures, which are those with tight complements, are of great interest. For example, Legendrian surgery on a non-loose Legendrian knot might produce tight contact structures and hence be the key to the classification of tight contact structures on certain manifolds. Indeed, in a forthcoming paper by the first two authors and Tosun [20], the results in this paper will be used to classify tight contact structures on some small Seifert fibered spaces where such a classification has remained elusive. The result in this paper will also be used in joint work of the first two authors and Piccirillo and Roy [19] to construct explicit symplectic embeddings of rational homology balls into $\mathbb{C}P^2$ and its blowups. In addition, the results in this paper will illuminate many new features of non-loose knots, showing that there is as rich a structure to them as for the much studied Legendrian and transverse knots in tight contact manifolds.

In this paper, we give a complete coarse classification of non-loose Legendrian and transverse torus knots in any overtwisted contact structure on S^3. Combining with the results of [16] and [15], this completes the coarse classification of Legendrian and transverse torus knots in any contact structure on S^3. We note, in particular, that this gives the first classification of Legendrian knots that involves Giroux torsion in their complement. The existence of such knots was shown in [15], but all previous classification results only considered the case without Giroux torsion.

Previously, non-loose knots were only completely classified for Legendrian and transverse representatives of the unknot [14]. There have been several partial classifications for other knots [15] and in particular torus knots [25, 43]. In Section 3, we will give a simple algorithm to classify non-loose Legendrian and transverse torus knots. In Section 1.3 and 1.4, we will also give closed form classifications for non-loose Legendrian and transverse $(2, \pm(2n+1))$–torus knots and $(5, \pm 8)$–torus knots.

The proofs of our main results relay on two main ingredients, convex surfaces and the geometry of the Farey graph. While convex surface theory is now a well-known part of

contact geometry, we have to develop several new techniques. The most interesting might be the ability to add Giroux torsion to some virtually overtwisted contact structures, see Lemma 6.15 and its associated lemmas, which relies on what appears to be a novel application of Honda's work on tricky non-rotative layers [36]. To the authors' knowledge, all previous work involving Giroux torsion — its existence or adding it to an existing contact structure — has been restricted to universally tight contact structures. So we give the first examples of the existence of Giroux torsion for tight but virtually overtwisted contact structures. (These examples are on the complement of some torus knots, but in a future work, the first two authors will give examples on closed 3–manifolds). Another interesting technique is the ability to detect non-loose knots by carefully applying the state transition technique in overtwisted contact structures. This allows us to determine when all Legendrian (p, q)-knots are non-loose without relying on contact surgery diagrams or invariants from Heegaard Floer homology. This is done for (p, q)-torus knots with $\mathrm{tb} < pq$ in Proposition 7.5 and 7.13 and the same arguments work for $\mathrm{tb} = pq$ as well; moreover, Propositions 7.16 and 7.20 show that all non-loose knots with $\mathrm{tb} > pq$ are destabilizations of ones with $\mathrm{tb} = pq$, so the non-looseness can also be seen without contact surgery diagrams or invariants from Heegaard Floer homology. Concerning the geometry of the Farey graph, we develop new ways to analyze pairs of paths in the Farey graph that approach a given fraction from different directions, see Section 2.3. From this, we can, among other things, determine when two non-loose knots stabilize to become equivalent, see Propositions 7.10 and 7.15. We can also use this to calculate the classical invariants of non-loose torus knots without relying on contact surgery diagrams, see Lemma 2.19; and this, in particular, allows us to distinguish non-loose Legendrian knots after adding Giroux torsion to their complements, see Lemma 6.19 (there does not seem to be a way to do this using the more classical surgery diagram approach to computing rotation numbers).

1.1. **Basic notations and prior classification results.** So far, with the exception of [15, 24], non-loose Legendrian knots have only been studied in S^3. To discuss these results, we recall that Eliashberg classified overtwisted contact structures on all 3–manifolds, and on the 3–sphere they are in one-to-one correspondence with the integers, [13]. We will denote by ξ_n, for $n \in \mathbb{Z}$, the overtwisted contact structure on S^3 with $d_3(\xi_n) = n$. See Section 2.5 for the definition of the d_3-invariant.[1]

We denote the Thurston-Bennequin invariant of a Legendrian knot L by $\mathrm{tb}(L)$ and its rotation number by $\mathrm{rot}(L)$. For a transverse knot T we denote its self-linking number by $\mathrm{sl}(T)$. We also denote the amount of convex Giroux torsion in the complement of a standard neighborhood of a Legendrian knot L by $\mathrm{tor}(L)$. See Section 2.2 for the definition of convex Giroux torsion. Note that all classification results so far, except those in [15], only considered Legendrian knots with $\mathrm{tor} = 0$. We say knots are *coarsely classified* if they are classified up to co-orientation preserving contactomorphism, smoothly isotopic to the identity. It is well-known that loose knots are coarsely classified by the classical invariants

[1] We adopt the convention that the d_3-invariant of contact structures on S^3 are integers and the standard tight contact structure has d_3-invariant 0. This differs from the original definition in [32] by 1/2. We also note that some papers enumerate overtwisted contact structures with their Hopf invariant which is the negation of the d_3-invariant.

[15, Theorem 1.4]. We say two Legendrian knots L_1 and L_2 are *equivalent* if there is a coorientation preserving contactomorphism, smoothly isotopic to the identity, sending L_1 to L_2, and similarly for transverse knots.

Previously, the only knot type for which there was a complete coarse classification of non-loose knots was the unknot. In [14], Eliashberg and Fraser showed that only the contact structure ξ_1 supports non-loose unknots and the non-loose representatives are: $L^i_\pm$ for $i \geq 2$ and L^1 such that

$$\mathrm{tb}(L^i_\pm) = i \text{ and } \mathrm{rot}(L^i_\pm) = i-1,$$
$$\mathrm{tb}(L^1) = 1 \text{ and } \mathrm{rot}(L^1) = 0,$$

and satisfy

$$S_\pm(L^i_\pm) = L^{i-1}_\pm \text{ and } S_\pm(L^2_\pm) = L^1,$$
$$S_\mp(L^i_\pm) \text{ and } S_\pm(L^1) \text{ are loose.}$$

From this one can see that there are no non-loose transverse unknots.

To visualize the classical invariants of Legendrian knots we consider the *mountain range* of Legendrian knots for a given smooth knot type. Given a smooth knot type K and a fixed contact structure ξ, we denote by $\mathcal{L}(K)$ the set of Legendrian knots in ξ up to coarse equivalence[2] and consider a map $\Phi : \mathcal{L}(K) \to \mathbb{Z}^2$ that sends $L \in \mathcal{L}(K)$ to $(\mathrm{rot}(L), \mathrm{tb}(L))$. The image of Φ is called the *mountain range* of K. We can also restrict Φ to the subset $\mathcal{L}_{nl}(K)$ of non-loose Legendrian knots realizing K; and since we completely understand loose Legendrian knots isotopic to K, we will refer to the mountain range of K in some overtwisted contact structure, as the image of Φ restricted to $\mathcal{L}_{nl}(K)$.

If one considers the non-loose unknots discussed above, we see that their image under Φ is an infinite V with vertex at $(0,1)$. We will say a mountain range for a knot type *contains a V with vertex at* (a,b) if the image of Φ contains Legendrian knots as above where the vertex of the V has invariants (a,b). See the right drawing of Figure 4 for example.

In [25], Geiges and Onaran gave the next coarse classification results for some torus knots with specific classical invariants. They considered only "strongly exceptional" knots. The term exceptional is what we are calling non-loose, and strongly means there is no Giroux torsion in the complement. In this paper we will say such knots are non-loose without convex Giroux torsion, or non-loose knots with tor = 0. Their results are as follows.

Left-handed trefoil: There are exactly two non-loose Legendrian representatives without convex Giroux torsion with tb = −5 or tb < −6, and there is at least one with tb = 1 and at least two for all other values of tb. All these examples are in ξ_2.

Right-handed trefoil: There are exactly four non-loose Legendrian knots having tor = 0 and tb = 7. Two have rot = ±4 and live in ξ_1 and the other two have rot = ±8 and live in ξ_{-1}. They also constructed non-loose Legendrian knots in ξ_{-1} with tb realizing any integer less than or equal to 5 and such Legendrian knots in ξ_1 with tb realizing any integer greater than or equal to 6.

[2]Usually, $\mathcal{L}(K)$ denotes the set of Legendrian knots up to Legendrian isotopy. In this paper however, since we only consider coarse classification, we adopt this definition.

Other torus knots: For $p \geq 2$ and $n \geq 1$, there are exactly $2p$ non-loose Legendrian $(p, np+1)$-knots having tor $= 0$ and tb $= np^2 + p + 1$. If $n \geq 2$, then there are exactly $2(p-1)(n-1)$ such non-loose Legendrian $(p, -(np-1))$–torus knots having tor $= 0$ and tb $= -np^2 + p - 1$. They also worked out the rotation numbers of these knots and which overtwisted contact structures in which they live.

Geiges and Onaran also produced interesting surgery descriptions for all their examples. One thing they did not do is to indicate how their examples are related by stabilization; thought through personal communication, in some cases, such as for the left handed trefoil with tb < -6 they are able to see this relation. Though in other cases, this is not clear, such as what happens to the non-loose Legendrian left-handed trefoil with tb $= 1$ when it is stabilized? Is it non-loose? (We see below, that there are actually three such knots and each has different behavior under stabilization.)

In [43], Matkovič coarsely classified non-loose negative (p, q)–torus knots with tb $< pq$ and with tor $= 0$. The classification is in terms of specific contact surgery descriptions in Figure 2, and to determine if a given surgery description is non-loose one must determine if Legendrian surgery on the knot produces a tight contact manifold. This is translated into information about the rotation numbers in the contact surgery diagram; which, in turn, is equivalent to our "pairs of decorated paths" description used in our classification algorithm given in Section 3.

While we do not consider links in this paper, we do mention that Geiges and Onaran have coarsely classified all non-loose Legendrian Hopf links (including ones with tor $>$ 0) in [26]. This and Eliashberg and Fraser's result above are the only complete coarse classification of non-loose representatives of a link type.

The only results involving the classification, and not just the coarse classification, of non-loose Legendrian knots is the work of Vogel, [44]. He showed that for each tb and rot realized by a non-loose unknot above, there are exactly two non-loose unknots up to Legendrian isotopy. We believe that some of our results below can also be upgraded to classifications up to Legendrian isotopy, but that will be the subject of future work.

We also note that in addition to the above works, there have been many constructions of non-loose knots, see for example [27, 28, 40].

1.2. **General non-loose torus knots.** From now on, we always assume that $|q| > p > 0$. In Section 3, we will give a simple algorithm to classify non-loose Legendrian representatives of any (p, q)–torus knot. In this section, we discuss the properties of the classifications that have a simple closed form. In particular, we will see that for non-loose Legendrian (p, q)–torus knots having tor $= 0$ and tb $\geq pq$, there is a simple classification and such knots with tb $< pq$ always destabilize. Thus the intricacies in our algorithm involve understanding when the representatives with tb $= pq$ become the same or loose under stabilization. We will also see that there is always a simple classification for non-loose Legendrian knots with tor > 0.

The first observation from our classification concerns destabilizing non-loose Legendrian knots.

Theorem 1.1. *Any non-loose (p,q)–torus knot destabilizes except when* $\mathrm{tb} = pq$ *or one Legendrian representative when* $pq < 0$ *and* $\mathrm{tb} = |pq| - |p| - |q|$. *Non-loose Legendrian knots with* $\mathrm{tb} = pq$ *sometimes destabilize and sometimes do not.*

We can also restrict the potential d_3-invariants of overtwisted contact structures that support non-loose torus knots.

Theorem 1.2. *Suppose ξ is an overtwisted contact structures on S^3 supporting a non-loose Legendrian (p,q)–torus knot L with* $\mathrm{tor}(L) = n$, *then*

$$d_3(\xi) = \begin{cases} \text{odd} & \text{if } pq > 0 \text{ and } n \in \mathbb{Z}, \text{ or } pq < 0 \text{ and } n \text{ is a half-integer,} \\ \text{even} & \text{if } pq < 0 \text{ and } n \in \mathbb{Z}, \text{ or } pq > 0 \text{ and } n \text{ is a half-integer.} \end{cases}$$

To state our classification, we first let q/p be a rational number with $|q/p| > 1$. If $pq < 0$, we have the continued fraction

$$\frac{q}{p} = [a_1, \dots, a_m] = a_1 - \cfrac{1}{a_2 - \frac{1}{\dots - \frac{1}{a_m}}}$$

where $a_i \le -2$ for $1 \le i \le m$. If $pq > 0$, we consider the continued fraction

$$\left(\frac{p}{q} - 1\right)^{-1} = [a_1, \dots, a_m].$$

In either case, we consider the continued fraction

$$\left(\frac{q}{p} - \left\lceil \frac{q}{p} \right\rceil\right)^{-1} = [b_1, \dots, b_n].$$

We now set

$$m(p,q) = |(a_1+1)\cdots(a_{m-1}+1)a_m| \cdot |(b_1+1)\cdots(b_{n-1}+1)b_n|$$

and

$$n(p,q) = |(a_1+1)\cdots(a_m+1)| \cdot |(b_1+1)\cdots(b_n+1)|$$

We will see in Section 2.2 that $m(p,q)$ is the number of tight contact structures on a solid torus with convex boundary having two dividing curves of slope q/p times the number of such contact structures with dividing slope p/q, and $n(p,q)$ is the number of tight contact structures on $L(p,-q)\#L(q,-p)$, where we use the convention that $L(p,q)$ is $-p/q$–surgery on the unknot.

We can now enumerate all the non-loose Legendrian (p,q)–torus knots with $\mathrm{tb} > pq$ and $\mathrm{tor} = 0$.

Theorem 1.3. *Suppose $|q| > p > 1$. There are exactly $2n(p,q)$ non-loose (p,q)–torus knots with* $\mathrm{tb} = i > pq$ *and* $\mathrm{tor} = 0$ *which we denote by*

$$L^i_{\pm,k} \text{ for } 1 \le k \le n(p,q)$$

except when $pq < 0$ *and* $i = |pq| - |p| - |q|$. *In this case, there are* $2n(p,q)+1$ *non-loose representatives and this extra Legendrian knot is denoted by* L_e. *We also know that*

$$S_\pm(L^i_{\pm,k}) = L^{i-1}_{\pm,k} \text{ for } i > pq+1,$$
$$S_\mp(L^i_{\pm,k}) \text{ is loose for } i > pq.$$

Moreover, $S^j_\pm(L^{pq+1}_{\pm,k})$ *is non-loose for any* $j > 0$. *For the extra Legendrian* L_e *when* $pq < 0$, *we have*

$$S_\pm(L_e) = L^{|pq|-|p|-|q|-1}_{\pm,1}.$$

Any $L^i_{\pm,k}$ *can be realized as a Legendrian knot shown in Figure 1. Also,* $\mathrm{rot}(L^i_{+,k}) = -\mathrm{rot}(L^i_{-,k})$ *and* $\mathrm{rot}(L_e) = 0$ *and* L_e *lives in the contact structure* $\xi_{|pq|-|p|-|q|+1}$.

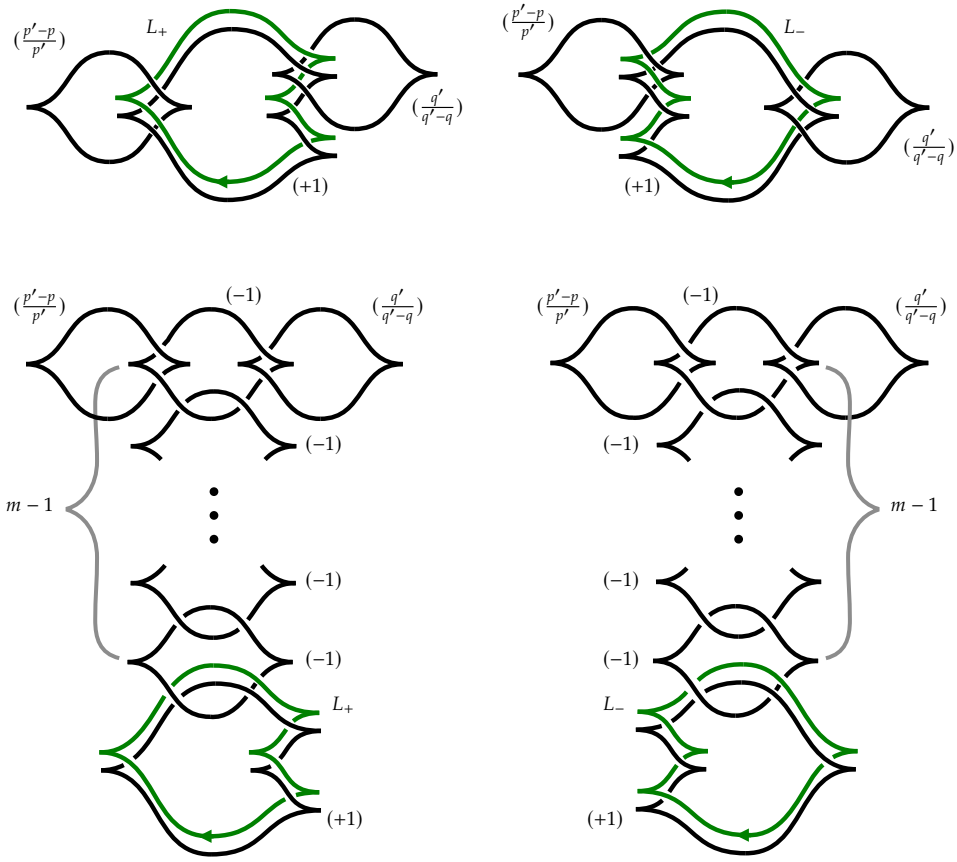

FIGURE 1. Half of the $2n(p,q)$ of non-loose Legendrian (p,q)–torus knots with tb $= pq+1$ and tor $= 0$ are shown on the top left and the other half on the top right. Similarly, half of the $2n(p,q)$ of non-loose Legendrian (p,q)–torus knots with tb $= pq+m$ for $m > 1$ and tor $= 0$ are shown on the bottom left and the other half on the bottom right. Here, q'/p' is the largest rational number such that $pq' - p'q = 1$.

In Section 2.5, we show how to compute the rotation number of $L^i_{\pm,k}$ and the d_3-invariant of the contact structure on which it lives, but we note that $L^i_{+,k}$ and $L^i_{-,k}$ live in the same contact structure. We note that surgery diagrams as in Figure 1 first appeared in work of Geiges and Onaran [25] for specific torus knots, but it is clear from their work that one can construct examples of non-loose (p,q)-torus knots with tb $> pq$ for any p and q. Our work shows that all such knots, except one when $pq < 0$, come from these diagrams.

We can similarly enumerate non-loose Legendrian knots with tb $= pq$ and tor $= 0$.

Theorem 1.4. *Suppose $|q| > p > 1$. The number of non-loose Legendrian (p,q)–torus knots with* tb $= pq$ *and* tor $= 0$ *is exactly*

$$\begin{cases} m(p,q) & \text{if } pq > 0, \\ m(p,q) - 2\left\|\left\lceil \frac{q}{p} \right\rceil\right\| & \text{if } pq < 0 \end{cases}$$

and any such Legendrian knot can be realized as a Legendrian knot shown in Figure 2.

In Section 2.5, we show how to compute the rotation numbers of these knots and the d_3-invariants of the contact structures in which it lives. We note that the surgery diagram in Figure 2 first appeared in work of Lisca and Stipsicz [41] in the context of small Seifert fibered spaces, and then in work of Lisca, Ozsváth, Stipsicz, and Szabo [40] to construct some non-loose Legendrian torus knots using Heegaard-Floer theory.

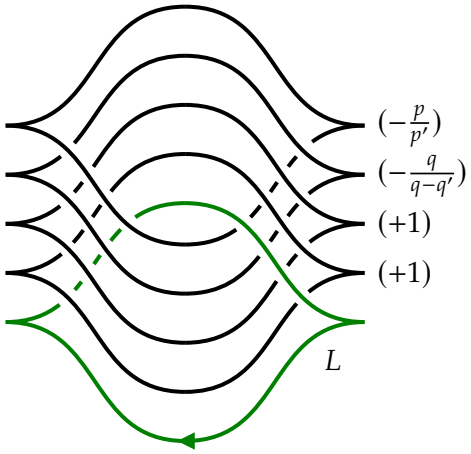

FIGURE 2. L is a non-loose torus knot with $\mathrm{tb}(L) = pq$ and $\mathrm{tor}(L) = 0$. Here, q'/p' is the largest rational number such that $pq' - p'q = 1$.

Remark 1.5. We will see there are always $m(p,q)$ Legendrian (p,q)-knots with tb $= pq$ and tor $= 0$, but when $pq < 0$, it turns out that $2\left\|\lceil q/p \rceil\right\|$ of those are in (S^3, ξ_{std}).

The algorithm in Section 3 will give a complete classification of non-loose Legendrian and torus knots, but we can easily describe the qualitative features of the classification through mountain ranges. In particular, for all but one of the overtwisted contact structures supporting non-loose Legendrian (p,q)–torus knots, the mountain range for the non-loose representatives with tor $= 0$ will be as in Figure 3. Notice that each mountain range

contains an infinite X. We call the grey shaded regions in the figure *wings*. The number of peaks in the wings will depend on (p, q) and decorated paths in the Farey graph from ∞ to q/p and then to 0, see Section 3.

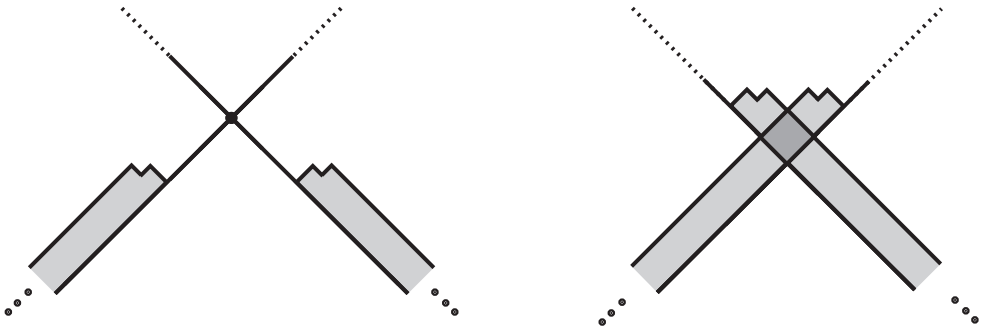

FIGURE 3. Generic mountain ranges for non-loose Legendrian (p, q)–torus knots with tor $= 0$. On the left is the case where $pq < 0$ and on the right is where $pq > 0$. The peaks occur at tb $= pq$. Each integral point in the lightly shaded region, whose coordinates sum to be odd, is realized by a unique non-loose Legendrian knot, while in the darker shaded region on the right and crossing point on the left there are exactly two representatives with those invariants.

However we observe the following about the wings.

Theorem 1.6. *Given any positive integers n and $m_1, \ldots, m_{n-1}$ there is some (p, q)–torus knot whose mountain range in some overtwisted contact structure has $2n$ peaks, and the distance between the i^{th} and $(i+1)^{st}$ peak is at least m_i (we label the peaks according to their distance from the infinite X).*

There exists one overtwisted contact structure for each (p, q)–torus knot where the classification of non-loose representatives is different, see Figure 4.

We note that it might be possible that for some (p, q)–torus knot, two or more of the mountain ranges shown in Figures 3 and 4 occur in the same overtwisted contact structure. In which case the Legendrian knots depicted in each figure are never equivalent to those in another. In all our computed examples we see that this never occurs and conjecture that it never does.

Conjecture 1.7. *In each overtwisted contact structure that supports non-loose (p, q)–torus knots, the mountain range of such knots is given by only one of the diagrams indicated in Figures 3 and 4.*

In [43] Matkovič classified non-loose Legendrian (p, q)-torus knots with $pq < 0$ and tb $< pq$, from this she could classify all non-loose transverse knots, without convex Giroux torsion, as well. She could then show that if two non-loose transverse knots were not related by stabilization, then they were in distinct overtwisted contact structures. This verifies our conjecture for negative torus knots.

We now consider the number of contact structures supporting non-loose Legendrian (p, q)–torus knots.

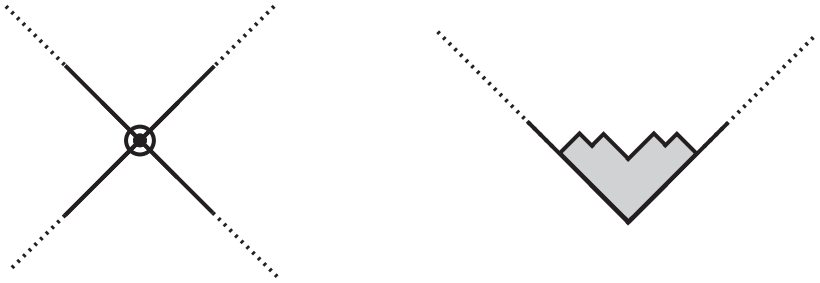

FIGURE 4. The mountain range of non-loose Legendrian (p,q)–torus knots with tor = 0 for the exceptional contact structures. On the left is the mountain range for a negative (p,q)–torus knot in $\xi_{|pq|-|p|-|q|+1}$. The crossing is at $(\mathrm{rot},\mathrm{tb}) = (0, |pq| - |p| - |q|)$ and there are three distinct non-loose Legendrian knots. On the right is the mountain range for a positive (p,q) torus knot in ξ_1. The lower vertex is at $(\mathrm{rot},\mathrm{tb}) = (0, pq - p - q + 2)$.

Theorem 1.8. *There are at most $n(p,q)$ overtwisted contact structures supporting non-loose Legendrian (p,q)–torus knots with* tor = 0*. And at most*

$$n(p,q) + |(a_1+1)\cdots(a_{m-1}+1)| \cdot |(b_1+1)\cdots(b_{n-1}+1)|$$

overtwisted contact structures supporting any non-loose Legendrian (p,q)–torus knots.

We note that if Conjecture 1.7 is true, then the upper bound in Theorem 1.8 gives the exact number of such contact structures.

We also give some qualitative properties of non-loose torus knots with tor > 0.

Theorem 1.9. *Let L be a non-loose Legendrian (p,q)–torus knot with* $\mathrm{tor}(L) > 0$*. Then*

(1) $\mathrm{tor}(L)$ *is finite and well-defined,*
(2) *there exists a unique Legendrian knot L' with* $\mathrm{tb}(L') = pq$ *and* $\mathrm{tor}(L') = 0$ *such that the complement of L is obtained by attaching a convex Giroux torsion layer in the complement of L'.*

We now turn to transverse knots. As is well-known [16, Theorem 2.10], the classification of transverse knots is equivalent to the classification Legendrian knots up to negative stabilization. Thus our algorithm for classifying non-loose Legendrian (p,q)–torus knots will also classify non-loose transverse (p,q)–torus knots.

Theorem 1.10. *Suppose ξ is an overtwisted contact structure supporting non-loose transverse (p,q)–torus knots. If we suppose Conjecture 1.7 is true, then in ξ, either*

(1) *there are a finite number of non-loose transverse knots $T_1, \dots T_n$, the stabilization of T_i is T_{i+1} for $i < n$, and the stabilization of T_n is loose; or*
(2) *there are an infinite number of non-loose transverse knots with the same self-linking number and they are distinguished by the Giroux torsion in their complement.*

In the former case all the T_i have zero Giroux torsion in their complement. If Conjecture 1.7 is not true, then the non-loose transverse knots in ξ could be a union of several copies of non-loose knots of type (1) and (2) above.

We note that in [43], Matkovič proved that negative torus knots (with no Giroux torsion in their complements) are transversely simple and gave an algorithm that could be used to obtain the above results for these knots.

1.3. **Non-loose $(2, \pm(2n+1))$–torus knots.** Here we give an explicit classification of non-loose Legendrian and transverse $(2, \pm(2n+1))$–torus knots for $n \in \mathbb{N}$. We begin with Legendrian $(2, 2n+1)$–torus knots.

Theorem 1.11. *The $(2, 2n+1)$–torus knot has non-loose Legendrian representatives only in ξ_1, ξ_0, and ξ_{1-2n}. The classification in each of these contact structures is as follows.*

(1) *In (S^3, ξ_0), there are non-loose Legendrian $(2, 2n+1)$–torus knots $L_\pm^{i,k+\frac{1}{2}}$ for $i \in \mathbb{Z}$ and $k \in \mathbb{N} \cup \{0\}$ such that*

$$\mathrm{tb}(L_\pm^{i,k+\frac{1}{2}}) = i, \text{ and } \mathrm{rot}(L_\pm^{i,k+\frac{1}{2}}) = \mp(i - 2n + 1),$$

and

$$\mathrm{tor}(L_\pm^{i,k+\frac{1}{2}}) = \begin{cases} k + \frac{1}{2} & \text{if } i > 2n-1, \\ k+1 & \text{if } i \leq 2n-1. \end{cases}$$

We also have

$$S_\pm(L_\pm^{i,k+\frac{1}{2}}) = L_\pm^{i-1,k+\frac{1}{2}} \text{ and } S_\mp(L_\pm^{i,k+\frac{1}{2}}) \text{ is loose.}$$

(2) *In (S^3, ξ_{1-2n}), there are non-loose Legendrian $(2, 2n+1)$–torus knots $L_\pm^{i,k}$ for $i \in \mathbb{Z}$ and $k \in \mathbb{N} \cup \{0\}$ such that*

$$\mathrm{tb}(L_\pm^{i,k}) = i, \text{ and } \mathrm{rot}(L_\pm^{i,k}) = \mp(i + 2n - 1)$$

and

$$\mathrm{tor}(L_\pm^{i,k}) = \begin{cases} k & \text{if } i > 2n-1, \\ k + \frac{1}{2} & \text{if } i \leq 2n-1. \end{cases}$$

We also have

$$S_\pm(L_\pm^{i,k}) = L_\pm^{i-1,k} \text{ and } S_\mp(L_\pm^{i,k}) \text{ is loose.}$$

(3) *In (S^3, ξ_1), there are non-loose Legendrian knots*

$$\begin{aligned} &L_\pm^i, \quad \text{for } i > 2n+1, \\ &L_{2,\pm}^i, \quad \text{for } 2n+4 \leq i \leq 4n+2, \\ &L^{2n+1}, \text{ and } L_2^{2n+3} \end{aligned}$$

with

$$\begin{aligned} \mathrm{tb}(L_\pm^i) = i, \text{ and } \mathrm{rot}(L_\pm^i) &= \mp(i - 2n - 1), \\ \mathrm{tb}(L^{2n+1}) = 2n+1, \text{ and } \mathrm{rot}(L^{2n+1}) &= 0, \\ \mathrm{tb}(L_{2,\pm}^i) = i, \text{ and } \mathrm{rot}(L_{2,\pm}^i) &= \mp(i - 2n - 3), \\ \mathrm{tb}(L_2^{2n+3}) = 2n+3, \text{ and } \mathrm{rot}(L_2^{2n+3}) &= 0 \end{aligned}$$

such that

$$\begin{aligned} S_\pm(L_\pm^i) = L_\pm^{i-1}, \text{ for } i \geq 2n+3, \text{ and } S_\pm(L_\pm^{2n+2}) = L^{2n+1}, \\ S_\pm(L_{2,\pm}^i) = L_{2,\pm}^{i-1}, \text{ for } i \geq 2n+5, \text{ and } S_\pm(L_{2,\pm}^{2n+4}) = L_2^{2n+3}, \end{aligned}$$

$$S_{\mp}(L^{i}_{2,\pm}) = L^{i-1}_{\pm}, \text{ for } i \geq 2n+4, S_{\mp}(L^{2n+3}_{2}) = L^{2n+2}_{\pm}$$

and $S_{\mp}(L^{i}_{\pm})$ *and* $S_{\pm}(L^{2n+1})$ *are loose. All these Legendrian knots have* tor $= 0$.

See Figure 5 for the mountain ranges of non-loose Legendrian right-handed trefoils.

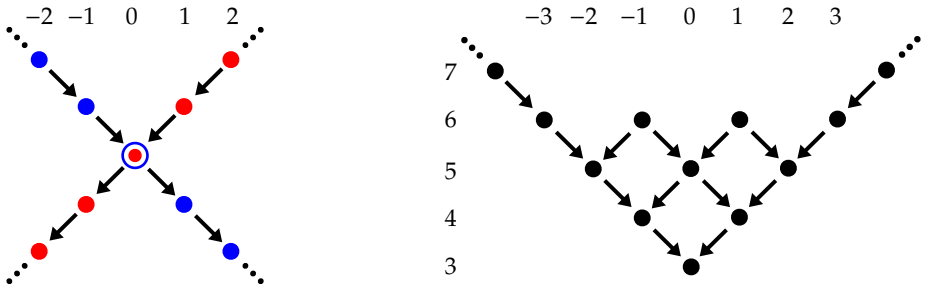

FIGURE 5. The mountain ranges of non-loose Legendrian right-handed trefoils. On the left we see the mountain range in ξ_0 and ξ_{-1}. In ξ_0, the crossing point of the X is at tb $= 1$ while in ξ_{-1}, it is at tb $= -1$. Each dot represents an infinite family of Legendrian representatives distinguished by convex Giroux torsion, and at the cross we have two infinite families. On the right we see the mountain range in ξ_1. Each dot represents a unique non-loose Legendrian representative.

We not turn to Legendrian $(2, -(2n+1))$–torus knots.

Theorem 1.12. *The* $(2, -(2n+1))$*–torus knot has non-loose Legendrian representatives only in* ξ_{n+l+1} *and* ξ_{n-l} *for* $l \in \{-n+1, -n+3, \dots, n-3, n-1\}$. *The classification in each of these contact structures is as follows.*

(1) *In* (S^3, ξ_{2n})*, there are non-loose Legendrian* $(2, 2n+1)$*–torus knots* $L^{i,k}_{n-1,\pm}$ *for* $i \in \mathbb{Z}, k \in \mathbb{N} \cup \{0\}$*, and* L_e *with*

$$\text{tb}(L^{i,k}_{n-1,\pm}) = i, \ \text{rot}(L^{i,k}_{n-1,\pm}) = \mp(i-2n+1), \text{ and } \ \text{tor}(L^{i,k}_{n-1,\pm}) = k,$$
$$\text{tb}(L_e) = 2n-1, \ \text{rot}(L_e) = 0, \text{ and } \ \text{tor}(L_e) = 0,$$

such that

$$L^{i,k}_{n-1,\pm} = S_{\pm}(L^{i-1,k}_{n-1,\pm}) \text{ and } S_{\pm}(L_e) = L^{2n-2,0}_{n-1,\pm},$$

and

$$S_{\mp}(L^{i,k}_{n-1,\pm}) \text{ is loose.}$$

(2) *In* (S^3, ξ_{n+l+1}) *for* $l \in \{-n+1, -n+3, \dots, n-3\}$*, there are non-loose Legendrian* $(2, 2n+1)$*–torus knots* $L^{i,k}_{l,\pm}$ *having*

$$\text{tb}(L^{i,k}_{l,\pm}) = i, \ \text{rot}(L^{i,k}_{l,\pm}) = \mp(i-2l-1), \text{ and } \ \text{tor}(L^{i,k}_{l,\pm}) = k$$

such that

$$S_{\pm}(L^{i,k}_{l,\pm}) = L^{i-1,k}_{l,\pm} \text{ and } S_{\mp}(L^{i,k}_{l,\pm}) \text{ loose.}$$

(3) *In* (S^3, ξ_{n-l}) *for* $l \in \{-n+1, -n+3, \dots, n-3, n-1\}$, *there are non-loose Legendrian* $(2, 2n+1)$*–torus knots* $L_{l,\pm}^{i,k+\frac{1}{2}}$ *having*

$$\mathrm{tb}(L_{l,\pm}^{i,k+\frac{1}{2}}) = i, \ \mathrm{rot}(L_{l,\pm}^{i,k+\frac{1}{2}}) = \mp(i+2l+1), \text{ and } \mathrm{tor}(L_{l,\pm}^{i,k+\frac{1}{2}}) = k + \frac{1}{2}$$

such that

$$S_{\pm}(L_{l,\pm}^{i,k+\frac{1}{2}}) = L_{l,\pm}^{i-1,k+\frac{1}{2}} \text{ and } S_{\mp}(L_{l,\pm}^{i,k+\frac{1}{2}}) \text{ loose.}$$

See Figure 6 for the mountain ranges of non-loose Legendrian left-handed trefoils.

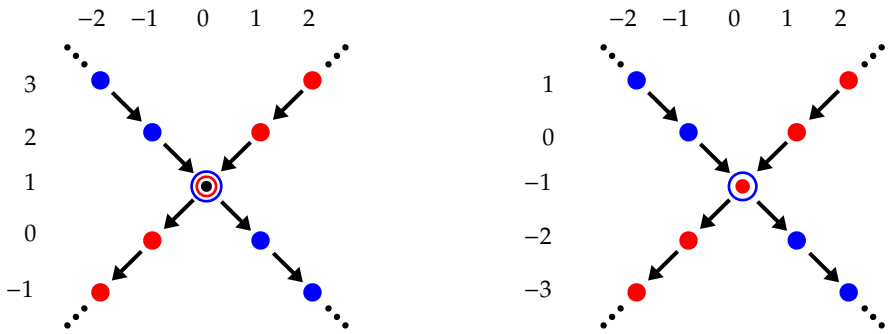

FIGURE 6. The mountain ranges of non-loose Legendrian left-handed trefoils. On the left we see the mountain range in ξ_2. Each dot not at the cross represents an infinite family of Legendrian representatives distinguished by convex Giroux torsion. At the cross the black dot represents the extra Legendrian L_e and each ring represents an infinite family of Legendrian representatives. On the right we see the mountain range in ξ_1. Each dot represents an infinite family of Legendrian representatives distinguished by convex Giroux torsion and at the cross we have two infinite families.

We now consider the classification of non-loose transverse $(2, 2n+1)$–torus knots.

Theorem 1.13. *The* $(2, 2n+1)$*–torus knot has non-loose transverse representatives only in* ξ_0, *and* ξ_{1-2n}. *The classification in each of these structures is as follows.*

(1) *In* (S^3, ξ_0), *there is a family of non-loose transverse* $(2, 2n+1)$*–torus knots* T^k *for* $k \geq 1$ *with*

$$\mathrm{sl}(T^k) = 2n-1 \text{ and } \mathrm{tor}(T^k) = k$$

and when stabilized T^k *becomes loose. Moreover,* T^{k+1} *is obtained from a Lutz twist on* T^k *for* $i > i$ *and* T^1 *is obtained from a Lutz twist on the maximal self-linking transverse representative of the* $(2, 2n+1)$*–torus knot in* (S^3, ξ_{std}).

(2) *In* (S^3, ξ_{1-2n}), *there is a family of non-loose transverse* $(2, 2n+1)$*–torus knots* $T^{k+\frac{1}{2}}$ *for* $i \geq 0$ *with*

$$\mathrm{sl}(T^{k+\frac{1}{2}}) = -2n+1 \text{ and } \mathrm{tor}(T^{k+\frac{1}{2}}) = k + \frac{1}{2}$$

any when stabilized $T^{k+\frac{1}{2}}$ becomes loose. Moreover, $T^{k+\frac{1}{2}}$ is obtained by the half Lutz twist of T^k.

Finally we discuss non-loose transverse $(2,-(2n+1))$–torus knots.

Theorem 1.14. *The $(2,-(2n+1))$–torus knot has non-loose transverse representatives only in ξ_{n+l+1} and ξ_{n-l} for $l \in \{-n+1,-n+3,\dots,n-3,n-1\}$. The classification in each of these structures is as follows.*

(1) *In (S^3,ξ_{n+l+1}), for $l \in \{-n+1,-n+3,\dots,n-3,n-1\}$ there are non-loose transverse $(2,-(2n+1))$–torus knots T_l^k for $k \geq 0$ with*

$$\mathrm{sl}(T_l^k) = 2l+1 \text{ and } \mathrm{tor}(T_l^k) = k$$

and when stabilized T_l^k becomes loose. Moreover, T_l^{k+1} is obtained from a Lutz twist on T_l^k for $k \geq 0$.

(2) *In (S^3,ξ_{n-l}) for $l \in \{-n+1,-n+3,\dots,n-3,n-1\}$, there are non-loose transverse $(2,-(2n+1))$–torus knots $T_l^{k+\frac{1}{2}}$ for $k \geq 0$ with*

$$\mathrm{sl}(T_l^{k+\frac{1}{2}}) = -2l-1 \text{ and } \mathrm{tor}(T_l^{k+\frac{1}{2}}) = k+\frac{1}{2}$$

and when stabilized $T_l^{k+\frac{1}{2}}$ becomes loose. Moreover, $T_l^{k+\frac{1}{2}}$ is obtained from the half Lutz twist on T_l^k.

1.4. **Non-loose $(5,\pm 8)$–torus knots.** In this section we give a complete classification of non-loose Legendrian and transverse $(5,\pm 8)$–torus knots as their classification show some features not seen in the non-loose $(2,\pm(2n+1))$–torus knots. We note that these knots are part of the family of $(5,5n+3)$–torus knots. Their classification is quite similar and is left as an exercise for the reader. We begin with the non-loose Legendrian knots.

Theorem 1.15. *The $(5,8)$–torus knot has non-loose Legendrian representatives only in ξ_1, ξ_0, ξ_{-1}, ξ_{-2}, ξ_{-3}, ξ_{-4}, ξ_{-7}, ξ_{-8}, ξ_{-9} ξ_{-15}, ξ_{-19}, and ξ_{-27}. The classification in each of these contact structures is as follows. See Figures 7 and 8.*

(1) *in (S^3,ξ_1) we have non-loose Legendrian knots $L_\pm^i$ for $i > 29$ and L^{29} such that $\mathrm{tb}(L_\pm^i) = i$, $\mathrm{tb}(L^{29}) = 29$ and*

$$\mathrm{rot}(L_\pm^i) = \mp(i-29) \text{ and } \mathrm{rot}(L^{29}) = 0$$

that satisfy

$$S_\pm(L_\pm^i) = L_\pm^{i-1}, \text{ for } i > 30\ , S_\pm(L_\pm^{20}) = L^{29}, \text{ and } S \mp (L_\pm^i) \text{ and } S \pm (L^{29}) \text{ are loose.}$$

In addition, there are Legendrian knots $L_{k,\pm}^{40}$, $k = 2,3,4$, with Thurston-Bennequin invariant 40 and

$$\mathrm{rot}(L_{2,\pm}^{40}) = \mp 9, \mathrm{rot}(L_{3,\pm}^{40}) = \mp 7, \text{ and } \mathrm{rot}(L_{4,\pm}^{40}) = \mp 3.$$

When these knots are stabilized to have the same invariants (or the invariants of the $L_\pm^i$ or L^{29}) they become equivalent and they are non-loose until stabilized outside the V defined by the $L_\pm^i$ and L^{29}. None of these Legendrian knots have convex Giroux torsion in their complement.

(2) *In* (S^3, ξ_{-1}) *there are Legendrian knots* $L^i_\pm$ *for* $i \in \mathbb{Z}$ *and* $L^i_{2,\pm}$ *for* $i \leq 40$ *such that*

$$\mathrm{tb}(L^i_\pm) = \mathrm{tb}(L^i_{2,\pm}) = i, \mathrm{rot}(L^i_\pm) = \mp(i-21), \text{ and } \mathrm{rot}(L^i_{2,\pm}) = \mp(i-19).$$

Moreover, $S_\pm(L^i_\pm) = L^{i-1}_\pm, S_\pm(L^i_{2,\pm}) = L^{i-1}_{2,\pm}, S_\mp(L^i_{2,\pm}) = L^{i-1}_\pm$, *and* $S_\mp(L^i_\pm)$ *is loose. No stabilization of* L^i_+ *or* $L^i_{2,+}$ *is equivalent to a stabilization of* L^i_i *or* $L^i_{2,-}$. *All these Legendrian knots have no convex Giroux torsion in their complement.*

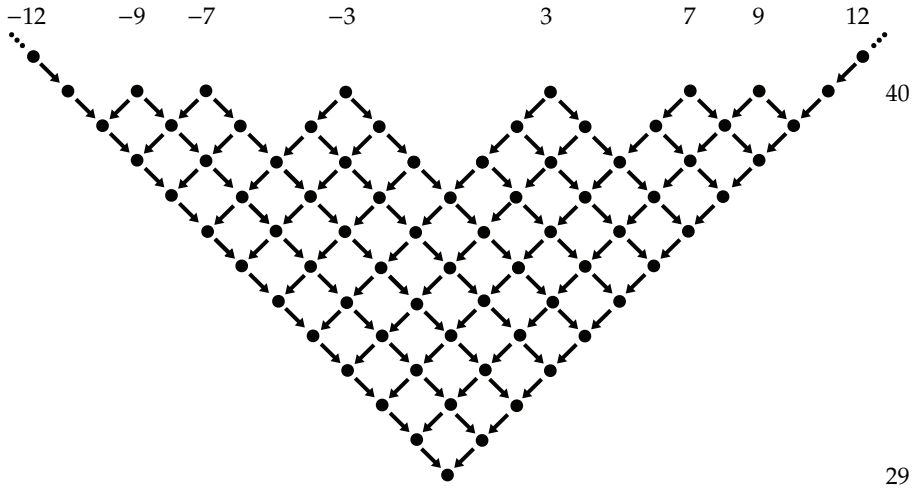

FIGURE 7. The mountain range for the non-loose Legendrian $(5, 8)$–torus knots in ξ_1. Each dot or circle represents a unique non-loose Legendrian knot.

(3) *In* (S^3, ξ_{-3}) *and* (S^3, ξ_{-7}) *we have Legendrian knots* $L^i_\pm$ *with* $\mathrm{tb}(L^i_\pm) = i$ *and* $\mathrm{tor}(L^i_\pm) = 0$ *such that*

$$\mathrm{rot}(L^i_\pm) = \begin{cases} \mp(i-13) & \text{in } \xi_{-3} \\ \mp(i-3) & \text{in } \xi_{-7} \end{cases}$$

and

$$S_\pm(L^i_\pm) = L^{i-1}_\pm \text{ and } S_\mp(L^i_\pm) \text{ is loose.}$$

(4) *In* S^3 *with the contact structures* $\xi_{-9}.\xi_{-15}, \xi_{-19}, \xi_{-27}$ *we have the Legendrian knots* $L^{i,k}_\pm$ *where* $\mathrm{tb}(L^{i,k}_\pm) = i$ *and*

$$\mathrm{rot}(L^{i,k}_\pm) = \begin{cases} \mp(i+1) & \text{in } \xi_{-9} \\ \mp(i+11) & \text{in } \xi_{-15} \\ \mp(i+17) & \text{in } \xi_{-19} \\ \mp(i+27) & \text{in } \xi_{-27} \end{cases}$$

that satisfy

$$S_\pm(L^{i,k}_\pm) = L^{i-1,k}_\pm \text{ and } S \mp (L^{i,k}_\pm) \text{ is loose.}$$

Moreover, $\mathrm{tor}(L^{i,k}_\pm) = k + 1/2$ *if it is in* ξ_{-27} *and* $i \leq 27$. *Otherwise,* $\mathrm{tor}(L^{i,k}_\pm) = k$.

(5) *In S^3 with the contact structures ξ_{-8}, ξ_{-4}, ξ_{-2}, and ξ_0 we have the Legendrian knots $L_\pm^{i,k+\frac{1}{2}}$ where $\mathrm{tb}(L_\pm^{i,k+\frac{1}{2}}) = i$ and*

$$\mathrm{rot}(L_\pm^{i,k+\frac{1}{2}}) = \begin{cases} \mp(-1+i) & \text{in } \xi_{-8} \\ \mp(-11+i) & \text{in } \xi_{-4} \\ \mp(-17+i) & \text{in } \xi_{-2} \\ \mp(-27+i) & \text{in } \xi_{-0} \end{cases}$$

that satisfy

$$S_\pm(L_\pm^{i,k+\frac{1}{2}}) = L_\pm^{i-1,k+\frac{1}{2}} \text{ and } S_\mp(L_\pm^{i,k+\frac{1}{2}}) \text{ is loose.}$$

Moreover, $\mathrm{tor}(L_\pm^{i,k+\frac{1}{2}}) = k+1$ *if it is in ξ_0 and $i \le 27$. Otherwise,* $\mathrm{tor}(L_\pm^{i,k+\frac{1}{2}}) = k + 1/2$.

We not turn to the Legendrian $(5,-8)$–torus knots.

Theorem 1.16. *The $(5,-8)$–torus knots has non-loose Legendrian representatives only in ξ_1, ξ_2, ξ_7, ξ_8, ξ_{14}, and ξ_{28}. The classification in each of these contact structures is as follows. See Figure 9.*

(1) *In (S^3, ξ_{28}), there are non-loose Legendrian $(5,-8)$–torus knots $L_\pm^{i,k}$, $i \in \mathbb{Z}, k \in \mathbb{N} \cup \{0\}$ and L_e with*

$$\mathrm{tb}(L_\pm^{i,k}) = i,\ \mathrm{rot}(L_\pm^{i,k}) = \mp(i-27), \text{ and } \mathrm{tor}(L_\pm^{i,k}) = k$$

$$\mathrm{tb}(L_e) = 27,\ \mathrm{rot}(L_e) = 0, \text{ and } \mathrm{tor}(L_e) = 0$$

such that

$$S_\pm(L_\pm^{i,k}) = L_\pm^{i-1,k},\ S_\pm(L_e) = L_\pm^{2n-2,0} \text{ and } S_\mp(L_\pm^{i,k}) \text{ is loose.}$$

(2) *In (S^3, ξ_2), there are non-loose Legendrian $(5,-8)$–torus knots $L_\pm^i$ for $i \in \mathbb{Z}$ and $L_{2,\pm}^i$ for $i \le -40$ having*

$$\mathrm{tb}(L_\pm^i) = \mathrm{tb}(L_{2,\pm}^i) = i, \text{ and } \mathrm{tor}(L_\pm^i) = \mathrm{tor}(L_{2,\pm}^i) = 0,$$

and

$$\mathrm{rot}(L_\pm^i) = \mp(i+25), \text{ and } \mathrm{rot}(L_{2,\pm}^i) = \mp(i+23)$$

such that

$$S_\pm(L_\pm^i) = L_\pm^{i-1}, \text{ and } S_\pm(L_{2,\pm}^i) = L_{2,\pm}^{i-1},$$

and

$$S_\mp(L_{2,\pm}^i) = L_\pm^{i-1}, \text{ and } S_\mp(L_\pm^i) \text{ is loose.}$$

(3) *In (S^3, ξ_8) there are non-loose Legendrian $(5,-8)$–torus knots $L_\pm^i$ for $i \in \mathbb{Z}$ with*

$$\mathrm{tb}(L_\pm^i) = i,\ \mathrm{rot}(L_\pm^i) = \mp(i+5), \text{ and } \mathrm{tor}(L_\pm^i) = 0$$

satisfying

$$S_\pm(L_\pm^i) = L_\pm^{i-1} \text{ and } S_\mp(L_\pm^i) \text{ is loose.}$$

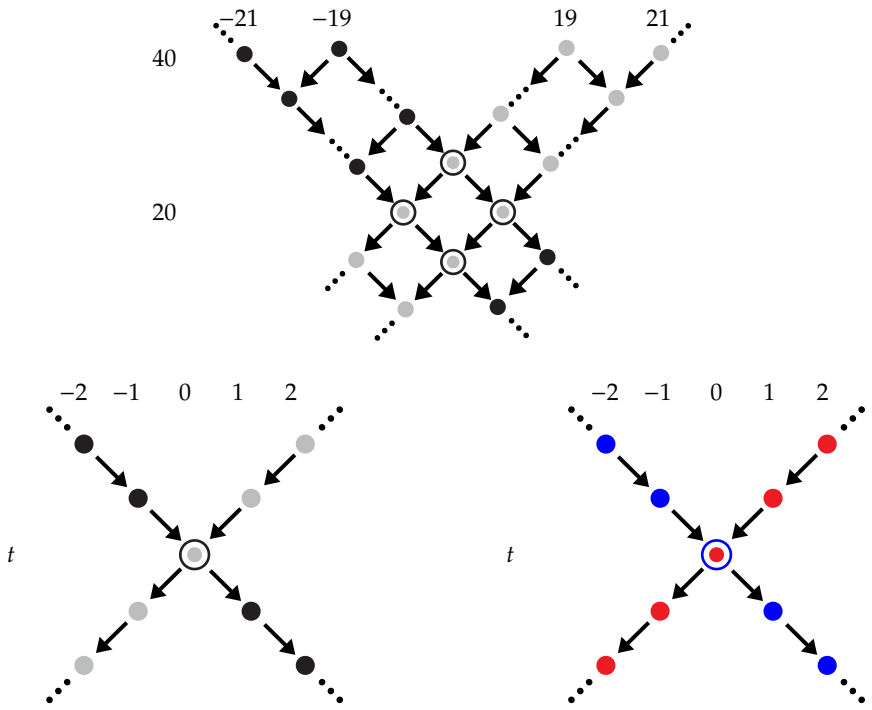

FIGURE 8. On the top is the mountain range for the non-loose Legendrian $(5,8)$–torus knots in ξ_{-1}. Each dot or circle represents a unique non-loose representative. The bottom left shows the mountain range for the non-loose Legendrian knots in ξ_{-3} and ξ_{-7}. In the first case $t = 13$ and in the second it is 3. Each dot or circle represents a unique non-loose representative. On the bottom right we see the mountain range for non-loose Legendrian knots in $\xi_{-9}, \xi_{-15}, \xi_{-19}, \xi_{-27}, \xi_{-8}, \xi_{-4}, \xi_{-2}$, and ξ_0. The values of t in those cases are $-1, -11, -17, -27, 1, 11, 17$, and 27, respectively, and each dot or circle represents infinitely many non-loose Legendrian knots.

(4) *In* (S^3, ξ_{14}) *there are non-loose Legendrian* $(5,-8)$*–torus knots* $L_{\pm}^{i,k}$ *for* $i \in \mathbb{Z}$ *and* $k \in \mathbb{N} \cup \{0\}$ *satisfying*

$$\mathrm{tb}(L_{\pm}^{i,k}) = i, \ \mathrm{rot}(L_{\pm}^{i,k}) = \mp(i-7), \text{ and } \mathrm{tor}(L_{\pm}^{i,k}) = k$$

such that

$$S_{\pm}(L_{\pm}^{i,k}) = L_{\pm}^{i-1,k} \text{ and } S_{\mp}(L_{\pm}^{i,k}) \text{ is loose.}$$

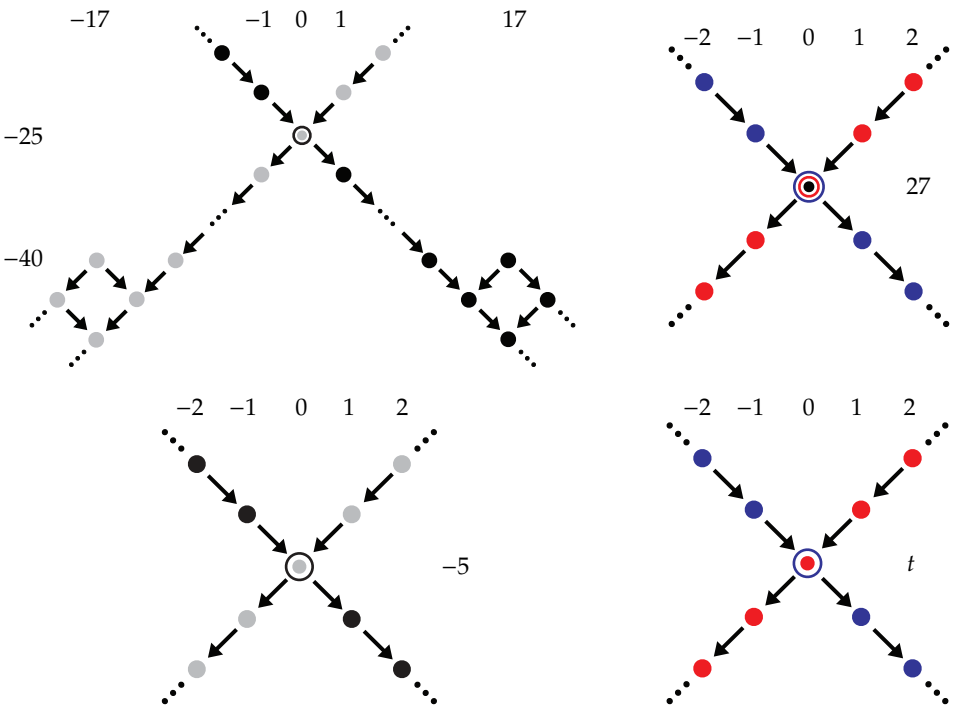

FIGURE 9. In the upper left we see the mountain range for non-loose $(5,-8)$–torus knots in ξ_2 and on the upper left we see the mountain range in ξ_{28}. On the bottom left is the mountain range in ξ_8 and on the bottom right in ξ_1 and ξ_7 and ξ_{14} where t is 27, 7, and -7, respectively. In the diagrams on the left each dot or circle represents a unique non-loose Legendrian knot while on the right each dot represents infinitely many distinct Legendrian knots.

(5) *In S^3 with the contact structures ξ_1 and ξ_7 there are non-loose Legendrian $(5,-8)$–torus knots $L_\pm^{i,k+\frac{1}{2}}$ satisfying* $\operatorname{tb}(L_\pm^{i,k+\frac{1}{2}}) = i$, $\operatorname{tor}(L_\pm^{i,k+\frac{1}{2}}) = k+1/2$,

$$\operatorname{rot}(L_\pm^{i,k+\frac{1}{2}}) = \begin{cases} \mp(i+27) & \text{in } \xi_1, \\ \mp(i+7) & \text{and } \xi_7, \end{cases}$$

and

$$S_\pm(L_\pm^{i,k+\frac{1}{2}}) = L_\pm^{i-1,k+\frac{1}{2}} \text{ and } S_\mp(L_\pm^{i,k+\frac{1}{2}}) \text{ is loose.}$$

With the classification of non-loose Legendrian $(5,\pm 8)$–torus knots, one may easily classify non-loose transverse knots.

Theorem 1.17. *The $(5,8)$–torus knot has non-loose transverse representatives only in ξ_{-1}, ξ_{-3}, ξ_{-7}, ξ_{-9}, ξ_{-15}, ξ_{-19}, ξ_{-27}, ξ_{-8}, ξ_{-4}, ξ_{-2}, and ξ_0. The classification in each of these contact structures is as follows.*

(1) *In* (S^3, ξ_{-1}) *there are two non-loose transverse knots* T *and* T' *with* $sl(T) = -19$, $sl(T') = -21$, *and the stabilization of* T *is contactomorphic to* T'. *Neither knot has Giroux torsion in its complement.*
(2) *In* S^3 *with the contact structure* ξ_{-3} *or* ξ_{-7} *there is exactly one non-loose transverse knot* T *and it has* $sl(T) = 13$ *in* ξ_{-3} *and* -3 *in* ξ_{-7}. *Neither knot has Giroux torsion in its complement.*
(3) *In* S^3 *with the contact structure* $\xi_{-7}, \xi_{-9}, \xi_{-15}, \xi_{-19}$ *or* ξ_{-27} *there is a family of non-loose transverse knots* T^k *for* $k \geq 1$ *with* $\mathrm{tor}(T^k) = k$ *and*

$$sl(T^k) = \begin{cases} -1 & \text{in } \xi_{-9} \\ -11 & \text{in } \xi_{-15} \\ -17 & \text{in } \xi_{-19} \\ -27 & \text{in } \xi_{-27}. \end{cases}$$

(4) *In* S^3 *with the contact structures* $\xi_{-8}, \xi_{-4}, \xi_{-2}$, *or* ξ_0 *there is a family of non-loose transverse knots* $T^{k+\frac{1}{2}}$ *for* $k \geq 0$ *with* $\mathrm{tor}(T^{k+\frac{1}{2}}) = k + 1/2$ *and*

$$sl(T^{k+\frac{1}{2}}) = \begin{cases} 1 & \text{in } \xi_{-8} \\ 11 & \text{in } \xi_{-4} \\ 17 & \text{in } \xi_{-2} \\ 27 & \text{in } \xi_0. \end{cases}$$

Finally we can consider the transverse $(5, -8)$–torus knots.

Theorem 1.18. *The* $(5, -8)$*–torus knot has non-loose transverse representatives only in* $\xi_1, \xi_2, \xi_7, \xi_8, \xi_{14}$, *and* ξ_{28}. *The classification in each of these contact structures is as follows.*

(1) *In* (S^3, ξ_2) *there are two non-loose transverse knots* T *and* T' *with* $sl(T) = 27$, $sl(T') = 25$, *and the stabilization of* T *is contactomorphic to* T'. *Neither knot has Giroux torsion in its complement.*
(2) *In* (S^3, ξ_8) *there is exactly one non-loose transverse knot* T *and it has* $sl(T) = -7$ *and* $\mathrm{tor}(T) = 0$.
(3) *In* S^3 *with the contact structure* ξ_{14} *and* ξ_{28} *there is a family of non-loose transverse knots* T^k *for* $k \geq 0$ *with* $\mathrm{tor}(T^k) = k$ *and*

$$sl(T^k) = \begin{cases} -7 & \text{in } \xi_{14} \\ 27 & \text{in } \xi_{28} \end{cases}$$

(4) *In* S^3 *with the contact structures* ξ_1 *or* ξ_7 *there is a family of non-loose transverse knots* $T^{k+\frac{1}{2}}$ *for* $k \geq 0$ *with* $\mathrm{tor}(T^{k+\frac{1}{2}}) = k + 1/2$ *and*

$$sl(T^{k+\frac{1}{2}}) = \begin{cases} 27 & \text{in } \xi_1 \\ 7 & \text{in } \xi_7 \end{cases}$$

1.5. **Qualitative features of non-loose Legendrian knots: known and new results.** Very little was known about the qualitative behavior of non-loose Legendrian knots, but we greatly illuminate their nature in this paper. The first most basic result about non-loose

Legendrian and transverse knots is a Bennequin type inequality concerning their classical invariants.

Theorem 1.19 (Świątkowski, see [12, 15])**.** *Let (M, ξ) be an overtwisted contact 3–manifold and L a non-loose Legendrian knot in ξ. Then*

$$-|\operatorname{tb}(L)| + |\operatorname{rot}(L)| \leq -\chi(\Sigma)$$

for any Seifert surface Σ for L. For non-loose transverse knots we have

$$sl(T) \leq -\chi(\Sigma).$$

The theorem above gives restrictions on the mountain range for non-loose representatives of K, see Figure 10.

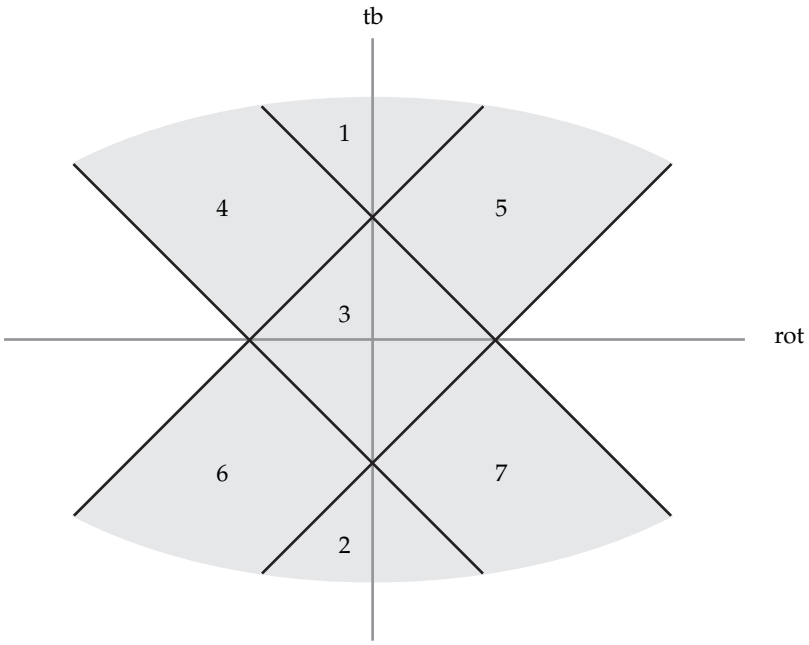

FIGURE 10. The mountain range of non-loose Legendrian representatives of a knot type K is contained in the shaded region defined by the four lines l_1, l_2, l_3, and l_4. The lines divide the shaded region into the 7 parts shown.

Recall that $\Phi : \mathcal{L}(K) \to \mathbb{Z}^2$ is a map that sends $L \in \mathcal{L}(K)$ to $(\operatorname{rot}(L), \operatorname{tb}(L))$. If one considers the non-loose unknots discussed in Section 1.1, we see that their image under Φ is an infinite V with vertex at $(0, 1)$. Our classification of non-loose torus knots and [15, Theorem 1.12 and 1.13] shows that the non-loose mountain range frequently *contains an X*, that is Legendrian knots whose invariants fill the integer points on a line of slope 1 and a line of slope -1. Given our current knowledge it is reasonable to ask if all mountain ranges have such a feature.

Question 1.20. *If ξ admits non-loose representatives of a knot type K, then does the mountain range of non-loose Legendrian knots of the knot type K in ξ always contain a V or X? Does it always contain an X if ξ is not ξ_1?*

Looking back at [15, Theorem 1.13], a reasonable place to start looking for a knot where the answer was NO, would be to consider a knot type K for which $-K$ is not smoothly isotopic to K.

In [15], there were many questions asked as to what the mountain ranges of non-loose Legendrian knots could look like. At the time the only known examples showed you could have Xs and Vs and that was all. In particular it was asked if there could ever be any non-loose Legendrian knots in Regions 1 or 2 in Figure 10, and if so could there be multiple (maybe infinitely many) representatives mapping to a fixed point in one of those regions. If one considers, for example, the $(n-1,n)$–torus knot in ξ_1 we can see that there are indeed non-loose Legendrian knots with invariants in Region 1, but at most one Legendrian representative can map to any point there. We do not know if Region 2 can be populated. So we reiterate, are refine the questions and ask

Question 1.21. *Are there any non-loose Legendrian knots with invariants in R_2? Is the cardinality of the pre-image of any point in R_1 under the geography map Φ on non-loose Legendrian knots bounded by 1?*

It was also asked in [15] if for any knot K, there are at most finitely many contact structures in which it could have non-loose representatives and if there were finitely many contact structures in which there could be infinitely many Legendrian representatives mapping to a fixed point (rot, tb). (It was suggested that there might just be two such contact structures.) All our examples point to the answer being YES to both these questions, but our examples of the $(2,-(2n+1))$–torus knots show that this finite number of contact structures can be arbitrarily large.

In [2], Baker and Onaran defined three invariants that quantify "how tight" are the complement of non-loose Legendrian knots. Our results given quite a bit of new information about two of them, so we discuss those. Given a non-loose knot L, they were the *depth of* L, $d(L)$, defined to be the minimal number of times an overtwisted disk intersects L and the *tension of* L, $t(L)$, defined to be the minimal number of stabilizations needed to make L loose. In [2, Problem 6.1], they asked for constructions of non-loose Legendrian knots with arbitrarily large tension. We can easily construct such examples by finding torus knots with arbitrarily large wings, as is guaranteed by Theorem 1.6 (and we can similarly find such examples for positive torus knots in ξ_1).

Baker and Onaran also noted that tension can be refined to consider only positive or negative stabilizations, so we set $t_\pm(L)$ to be the minimal number of $\pm$ stabilizations that are required to make L loose. From prior work, *e.g.* [15], it is clear that $t_\pm(L)$ can be infinite. In [2, Question 6.7] it was asked if there was an L such that both $t_+(L)$ and $t_-(L)$ can be infinite. The "extra" Legendrian L_e for negative torus knots given in Theorem 1.3 is an example of such a non-loose Legendrian knot. Similarly, Baker and Onaran [2, Question 6.7] asked if one could have both $t_\pm(L)$ larger than $t(L)$. Again, our extra Legendrian has $t_\pm(L_e)=\infty$ and $t(L_e)=2$, so the answer is YES.

It was shown in [2] that $t(L) \leq d(L)$, so the examples above (ones with arbitrarily large wings) show that $d(L)$ can be arbitrarily large.

Acknowledgements. The authors thank Rima Chatterjee for reminding us of interesting questions on non-loose knots, and Irena Matkovič for a helpful discussion, in particular the idea of Theorem 1.2. We also thank Bülent Tosun for a useful conversation. The first and third authors were partially supported by NSF grant DMS-1906414.

2. Background and preliminary observations

We assume the reader is familiar with basic Legendrian and transverse knot theory as discussed in [16] and the convex surface theory in [34]. In Section 2.2 we review the classification of contact structures on simple manifolds that will be needed in the remainder of the paper. Before that, we recall the definition of the Farey graph and some important properties that are needed in those classifications. Then in Section 2.3 we discuss the construction of contact structures on S^3 using pairs of decorated paths in the Farey graph. We then show how to translate this description of the contact structure into a contact surgery diagram in (S^3, ξ_{std}). Then in Section 2.5, we see how to compute the d_3-invariant of these contact structures as well as the rotation numbers of some Legendrian knots in them. We end this section by classifying contact structures, with certain boundary conditions, on $P \times S^1$ where P is a pair of pants (that is, a disk with two disjoint sub-disks removed).

2.1. **The Farey graph.** We will keep track of curves on a torus using the Farey graph. The Farey graph is constructed as follows. Consider the unit disk in the xy-plane. Label the point $(0,1)$ with $0 = 0/1$ and $(0,-1)$ with $\infty = 1/0$. Connect 0 and ∞ with a straight line. Now if a point on the boundary of this disk with positive x-coordinate lies half way between two points labeled a/b and c/d, then label it $(a+c)/(b+d)$ and connect this point to each of the other two by a hyperbolic geodesic (put the hyperbolic metric on the interior of the unit disk). We call this the "Farey sum" of a/b and c/d, and denote it by $\frac{a}{b} \oplus \frac{c}{d}$. (We will also use $\frac{a}{b} \ominus \frac{c}{d}$ to represent $(a-c)/(b-d)$.) If we iterate this construction, then all the positive rational numbers will appear. We can repeat this construction for points on the boundary with negative x-coordinate, but when we do we let $\infty = -1/0$, so we will get all the negative rational numbers.

Recall that if one fixes a basis λ, μ for $H_1(T^2)$, then embedded curves on T^2 are in one-to-one correspondence with $\mathbb{Q} \cup \{\infty\}$, where a/b is associated to the embedded curve on T^2 in the homology class $a\mu + b\lambda$. One may easily check that two curves associated to the numbers r and s form a basis for $H_1(T^2)$ if and only if there is an edge between r and s in the Farey graph.

We also introduce the dot product of two rational numbers: $\frac{a}{b} \bullet \frac{c}{d} = ad - bc$ and note that $\left|\frac{a}{b} \bullet \frac{c}{d}\right|$ is the minimal number of times curves associated to $\frac{a}{b}$ and $\frac{c}{d}$ can intersect.

We end this section by setting up some notation that will be used frequently in the rest of the paper. Given two numbers r and s in $\mathbb{Q} \cup \{\infty\}$ we let $[r,s]$ denote the elements in $\mathbb{Q} \cup \{\infty\}$ that are clockwise of r in the Farey graph and anti-clockwise of s.

We have the following well-known lemma, see for example [18].

Lemma 2.1. *Suppose $q/p < -1$. Given $q/p = [a_1, \dots, a_n]$, let $(q/p)^c = [a_1, \dots, a_n + 1]$ and $(q/p)^a = [a_1, \dots, a_{n-1}]$. There will be an edge in the Farey graph between each pair of numbers q/p, $(q/p)^c$, and $(q/p)^a$. Moreover $(q/p)^c$ will be farthest clockwise point from q/p that is larger than q/p with an edge to q/p, while $(q/p)^a$ will be the farthest anti-clockwise point from q/p that is less than q/p with an edge to q/p.*

In the lemma, if $a_n + 1 = -1$, then $[a_1, \dots, a_n + 1]$ is considered to be $[a_1, \dots, a_{n-1} + 1]$.

A path in the Farey graph is a sequence of elements $p_1, \dots, p_k$ in $\mathbb{Q} \cup \{\infty\}$ such that each p_i is connected to p_{i+1} by an edge in the Farey graph, for $i < k$. From the above lemma we see that given $q/p < -1$ with $q/p = [a_1, \dots, a_n]$ the minimal path from q/p clockwise to -1 in the Farey graph is $p_1, \dots, p_k$ such that if p_i is given by $[b_1, \dots, b_l]$ then p_{i+1} is given by $[b_1, \dots, b_l + 1]$.

The rational numbers $[a_1, \dots, a_n], [a_1, \dots, a_n + 1], \dots, [a_1, \dots, a_{n-1}, -1]$ are said to form a *continued fraction block*.

2.2. **Contact structures on $T^2 \times [0, 1]$, solid tori, and lens spaces.** Both Giroux [31] and Honda [34] classified tight contact structures on $T^2 \times [0, 1]$, solid tori, and lens spaces. Below we discuss the classification along the lines of Honda.

2.2.1. *Contact structures on $T^2 \times [0, 1]$.* Suppose ξ is a tight contact structure on $T^2 \times [0, 1]$ with convex boundary and the dividing slope on $T^2 \times \{i\}$ is s_i for $i = 0, 1$. We say that ξ is *minimally twisting* if any convex torus in $(T^2 \times [0, 1], \xi)$ that is parallel the the boundary has dividing slope in $[s_0, s_1]$.

We denote by $\text{Tight}^{min}(T^2 \times [0, 1]; s_0, s_1)$ the minimally twisting tight contact structures, up to isotopy, on $T^2 \times [0, 1]$ with convex boundary having two dividing curves of slope s_0 and s_1 on $T^2 \times \{0\}$ and $T^2 \times \{1\}$, respectively. Let P be a minimal path in the Farey graph that starts at s_0 and goes clockwise to s_1. We say P is a *decorated path* if its edges have each been labeled with a $+$ or a $-$. We say two decorated paths are *equivalent* if the number of $+$ signs in each continued fraction block is the same.

Theorem 2.2. *The contact structures on $\text{Tight}^{min}(T^2 \times [0, 1]; s_0, s_1)$ are in one-to-one correspondence with equivalence classes of decorations on P.*

Notice that if s_0 and s_1 share an edge in the Farey graph, then there are exactly two tight contact structures in $\text{Tight}^{min}(T^2 \times [0, 1]; s_0, s_1)$. These are called *basic slices* and the correspondence in the theorem can be understood in terms of stacking basic slices according to the decorated path.

Consider $\text{Tight}^{min}(T^2 \times [0, 1]; q/p, -1)$ with $q/p < -1$ (note that given any s_0 and s_1 there is a diffeomorphism of the torus taking s_1 to -1 and s_0 such a q/p). Let $q/p = [a_1, \dots, a_n]$, and recall $a_i \leq -2$. According to the discussion in the previous subsection, we know the number of edges in the continued fraction blocks in the minimal path from q/p to -1 is $|a_n + 1|, |a_{n-1} + 2|, \dots, |a_1 + 2|$. So according to the theorem above the number of contact structures on $\text{Tight}^{min}(T^2 \times [0, 1]; q/p, -1)$ is

$$|(a_1 + 1) \cdots (a_{n-1} + 1)a_n|.$$

Suppose P is a non-minimal path in the Farey graph, then there will be a vertex v in P such that there is an edge between its neighboring vertices. Let P' be the path obtained by removing v and the edges coming into v and adding the edge between v's neighbors. We say P' is obtained from P by shortening at v. Given any decorated path in the Farey graph, even a non-minimal one, one can construct a contact structure on $T^2 \times [0,1]$ by stacking basic slices. It will be important to know when this contact structure is tight. To this end, we have the following result.

Theorem 2.3. *Let ξ be a contact structure on $T^2 \times [0,1]$ described by a non-minimal decorated path P in the Farey graph. Then ξ is tight if and only if one may construct a shortest path from P by shortening at vertices with edges labeled with the same sign. When ξ is tight, it will be minimally twisting and is described by the decorated shortest path between the endpoints of P obtained by labeling the added edges in the shortening process with the label of the two replaced edges.*

We now turn to convex Giroux torsion. Consider the contact structure $\xi = \ker(\sin 2\pi z\, dx + \cos 2\pi z\, dy)$ on $T^2 \times \mathbb{R}$, where (x, y) are the coordinates on T^2 and z is the coordinate on $\mathbb{R}$. Consider the region $T^2 \times [0,k]$ for $k \in \frac{1}{2}\mathbb{N}$ and notice that the contact planes twist k times as z goes from 0 to k. We can now perturb $T^2 \times \{0\}$ and $T^2 \times \{k\}$ so that they become convex with two dividing curves of slope 0. Let ξ^k be the resulting contact structure on $T^2 \times [0,1]$ (after $T^2 \times [0,k]$ has been identified with $T^2 \times [0,1]$ in the obvious way). Notice that inside of $(T^2 \times [0,1], \xi^k)$ there is a basic slice with one boundary component agreeing with $T^2 \times \{0\}$ and having boundary slope 0 and ∞. This will either be a positive or a negative basic slice. By reversing the orientation of ξ_k, if necessary, we can assume it is positive.

We call $(T^2 \times [0,1], \xi^k)$ a *convex k Giroux torsion layer* and if we have a contact structure (M, ξ) into which $(T^2 \times [0,1], \xi^k)$ embeds, we say (M, ξ) has *convex k Giroux torsion*. We will use the phrase (M, ξ) has *exactly convex k Giroux torsion* to the situation where one can embed $(T^2 \times [0,1], \xi^k)$ into (M, ξ) but not $(T^2 \times [0,1], \xi^{k+\frac{1}{2}})$. We say (M, ξ) has no convex Giroux torsion, or convex 0 Giroux torsion, if $(T^2 \times [0,1], \xi^k)$ does not embed in (M, ξ) for any $k \in \frac{1}{2}\mathbb{N}$.

Theorem 2.4. *For $k \in \frac{1}{2}\mathbb{N}$, there are exactly two contact structures $\pm\xi^k$, up to isotopy, on $T^2 \times [0,1]$ with convex boundary having two dividing curves, both of slope 0, and exactly convex k Giroux torsion. The two contact structures are contactomorphic.*

Lastly, we define a new invariant tor for Legendrian and transverse knots. For a Legendrian knot L, $\mathrm{tor}(L) = k$ if the complement of the standard neighborhood of L contains exactly convex k Giroux torsion in a neighborhood of the boundary but not convex $k + 1/2$ Giroux torsion. For a transverse knot T, $\mathrm{tor}(T) = k$ if $(T^2 \times [0,k], \xi)$ embeds in the complement of T in a neighborhood of the boundary, but $(T^2 \times [0, k + 1/2], \xi)$ does not. If L and T are loose, we define $\mathrm{tor}(L) = \mathrm{tor}(T) = \infty$.

2.2.2. *Contact structures on solid tori.* Notice we can construct a solid torus from $T^2 \times [0,1]$ in two ways. If we choose a rational slope s on $T^2 \times \{0\}$ and collapse the linear curves of slope s on this torus we will get a solid torus S_s. We call this the solid torus with lower meridional slope s. Similarly we can collapse the linear curves of slope s on $T^2 \times \{1\}$ to get a solid torus S^s and we say it has upper meridian s.

We denote by $\text{Tight}(S_s; r)$ the isotopy classes of tight contact structures on the solid torus S_s with lower meridian s and convex boundary having two dividing curves of slope r. Similarly $\text{Tight}(S^s; r)$ is the isotopy classes of tight contact structures on the solid torus S^s with upper meridian s and convex boundary having two dividing curves of slope r.

Theorem 2.5. *Let P be a minimal path in the Farey graph from r clockwise to s. Then, the elements of* $\text{Tight}(S_r; s)$ *are in one-to-one correspondence with equivalence classes of decorations on the path P where the first edge is left undecorated. Similarly, the elements of* $\text{Tight}(S^s; r)$ *are in one-to-one correspondence with equivalence classes of decorations on the path P where the last edge is left undecorated.*

We now consider formulas for the number of tight contact structures on some solid tori. If $r < -1$ and $r = [a_1, \dots, a_n]$, then we see that

$$|\text{Tight}(S^0; r)| = |(a_1 + 1) \cdots (a_{n-1} + 1)a_n|, \tag{1}$$

this is because the minimal path from r to 0 is the same as the minimal path from r to -1 followed by the last edge to 0. Decorations on this first path from r to -1 also characterize $\text{Tight}^{min}(T^2 \times [0,1]; q/p, -1)$ discussed above.

Notice that there is an orientation preserving diffeomorphism from $T^2 \times [0,1]$ to itself that exchanges the two S^1 factors of T^2 and inverts $[0,1]$. This diffeomorphism identifies $\text{Tight}(S_\infty; r)$ with $\text{Tight}(S^0; r^{-1})$. So if $r \notin \mathbb{Z}$, then $r - \lceil r \rceil \in (-1, 0)$ and $\text{Tight}(S_\infty; r) = \text{Tight}(S_\infty; r - \lceil r \rceil)$ via the diffeomorphism that cuts the solid torus along the meridian disk and adds $-\lceil r \rceil$ twists before re-glueing. Thus if $(r - \lceil r \rceil)^{-1} = [b_1, \dots, b_n]$, then

$$|\text{Tight}(S_\infty; r)| = |(b_1 + 1) \cdots (b_{n-1} + 1)b_n|. \tag{2}$$

Now if $r > 1$, then as above we have

$$\text{Tight}(S^0; r) = \text{Tight}(S_\infty, r^{-1}) = \text{Tight}(S_\infty; r^{-1} - 1) = \text{Tight}(S^0; (r^{-1} - 1)^{-1}),$$

and $(r^{-1} - 1)^{-1} < -1$. So if $(r^{-1} - 1)^{-1} = [a_1, \dots, a_n]$, then the number of tight contact structures on $\text{Tight}(S^0; r)$ is also given by the formula on the right-hand side of Equation (1). Lastly, we note that when $r \in \mathbb{Z}$, there is a unique tight contact structure on $(S_\infty; r)$.

We end our discussion of contact structures on solid tori with a simple observation.

Lemma 2.6. *Let ξ be the unique tight contact structure on* $\text{Tight}(S_\infty; m)$*. Given any contact structure $\xi' \in \text{Tight}^{min}(T^2 \times [0,1]; n, m)$, for $m > n$ integers, there is an embedding of the unique tight contact structure $\xi'' \in \text{Tight}(S_\infty; n)$ into (S_∞, ξ) whose complement is $(T^2 \times [0,1], \xi')$. In particular, gluing (S_∞, ξ'') to $(T^2 \times [0,1], \xi')$ along $T^2 \times \{0\}$ is tight.*

Proof. Notice that (S_∞, ξ) is a standard neighborhood of a Legendrian knot L. Now inside S_∞ we can stabilize L. Let $N_\pm$ be the standard neighborhood of $S_\pm(L)$ in S_∞. Notice that the contact structure on $S_\infty \setminus N_\pm$ is a basic slice and the sign of the basic slice depends on the sign of the stabilization. This establishes the lemma for $m - n = 1$, in general the lemma follows by further stabilizing L. □

2.2.3. *Contact structures on lens spaces.* We can construct a lens space from $T^2 \times [0,1]$ as follows: choose a slope r on $T^2 \times \{0\}$ and a slope s on $T^2 \times \{1\}$ and let L^s_r be the result of collapsing the linear curves of the given slope on the boundary components. We say L^s_r is the lens space with upper meridian s and low meridian r. Note that the lens space $L(p,q)$, which is $-p/q$ surgery on the unknot, can also be described at $L^0_{-p/q}$ (this is essentially the definition of $-p/q$ surgery on the unknot) and similarly as $L^{-q/p}_\infty$. This latter expression is because there is an orientation preserving diffeomorphism of $T^2 \times [0,1]$ that exchanges the S^1 factors of T^2 and inverts the interval.

Let $\mathrm{Tight}(L^s_r)$ be the isotopy classes of tight contact structures on the lens space L^s_r.

Theorem 2.7. *Let P be a minimal path in the Farey graph from r clockwise to s. Then the elements of $\mathrm{Tight}(L^s_r)$ are in one-to-one correspondence with equivalence classes of decorations on the path P where the first and last edges are left undecorated.*

Arguing as above to count the number of minimally twisting contact structures on $T^2 \times [0,1]$ we can easily compute the well know formula that

$$\mathrm{Tight}(L^0_r) = |(a_1+1)\cdots(a_m+1)|$$

if $r < -1$ and $r = [a_1, \dots, a_m]$.

Remark 2.8. Given r and s rational numbers let r' be the rational number such that r' is clockwise of r in the Farey graph and as close to s as possible with an edge back to r. Similarly s' is the rational number such that s' is anti-clockwise of s in the Farey graph and the closest point to r with an edge to s. Then from the classification results above notice that

$$|\,\mathrm{Tight}(L^s_r)| = |\,\mathrm{Tight}(S_r; s')| = |\,\mathrm{Tight}(S^s; r')|.$$

Geometrically this can be seen by splitting L^s_r in to two solid tori $S_r \cup S^s$ along a convex torus of slope r' or s'. In the former case the contact structure on S_r will be unique so all the contact structures on L^s_r will come from $\mathrm{Tight}(S^s; r')$, and similarly in the other case.

2.3. **Paths in the Farey graph and continued fractions.** When studying non-loose torus knots in S^3, we will need to consider S^3 as L^0_∞ (that is a lens space with lower meridian ∞ and upper meridian 0, see Section 2.2.3). We will describe contact structures on L^0_∞ using paths in the Farey graph. More precisely, given a rational number q/p we will write L^0_∞ as the union of two solid tori: V_1 with lower meridian ∞ and convex boundary having slope q/p and V_2 with upper meridian 0 and convex boundary having slope q/p, where p, q are coprime integers and $|q| > p > 1$. According to Theorem 2.5, we will need two paths in the Farey graph to specify contact structures on these tori. Let P_1 be a path that describes a contact structure on $\mathrm{Tight}(S_\infty; q/p)$ and P_2 be a path describing a contact structure on $\mathrm{Tight}(S^0; q/p)$. Given these paths we get a contact structure ξ_{P_1,P_2} on S^3. In this section we will see when the contact structures associated to two different decorated pairs of paths correspond to the same contact structure. In [42], Matkovič has done the same things for some small Seifert fibered spaces in terms of her "characteristic vectors", and then in [43] used this to understand when negative (p,q)-torus knots with $\mathrm{tb} < pq$ are in the same overtwisted contact structure.

Recall that from Theorem 2.5 we know that P_1 is a path from q/p anti-clockwise to ∞ with all edges decorated by a sign except the last edge from $\lfloor q/p \rfloor$ to ∞ (this edge describes the unique tight contact structure on a solid torus with convex boundary having two longitudinal dividing curves), as such we will denote by P_1 the decorated path from q/p anti-clockwise to $\lfloor q/p \rfloor$ as it contains all the information describing the contact structure. We have a similar discussion for P_2. If $q/p < -1$, then we need to consider P_2 as a decorated path from q/p clockwise to -1 (the jump from -1 to 0 describes the unique tight solid torus with given dividing curves and meridian). If $q/p > 1$, then P_2 will be a decorated path from q/p clockwise to ∞ (the jump from ∞ to 0 describes the unique tight solid torus with given dividing curves and meridian).

We say the pair (P_1, P_2) is a *pair of paths representing* q/p.

Below, we will see that when $pq < 0$, the part of P_2 from $\lceil q/p \rceil$ to -1 plays a very different role in our analysis, and in Section 3, we mainly consider the part of P_2 from q/p to $\lceil q/p \rceil$. Thus we denote by $P_2^{\intercal}$ the truncated path from q/p to $\lceil q/p \rceil$.

Case 1: $q/p < -1$**.** To describe these paths, we consider the continued fraction expansion of q/p

$$\frac{q}{p} = a_1 - \frac{1}{a_2 - \frac{1}{\cdots - \frac{1}{a_n}}}$$

where $a_i \leq -2$. We denote this by $[a_1, \ldots, a_n]$.

An immediate corollary of Lemma 2.1 is the following result.

Lemma 2.9. *Let $p_1, \ldots, p_k$ be the points on the Farey graph in P_1, where $p_1 = q/p$ and $p_k = \lfloor q/p \rfloor$ and $q_1, \ldots q_l$ be the points on the Farey graph in P_2, where $q_1 = q/p$ and $q_l = -1$. If $p_i = [b_1, \ldots, b_j]$ then $p_{i+1} = [b_1, \ldots, b_{j-1}]$ and if $q_i = [c_1, \ldots, c_j]$ then $q_{i+1} = [c_1, \ldots, c_j + 1]$.*

Notice that this lemma allows us to inductively compute all the p_i and q_j. In particular, $k = n$ and $l = |a_n| - n - 1 + \sum_{i=1}^{n-1} |a_i + 1|$.

Let A be the continued fraction block in P_1 starting at q/p and let B be the continued fraction block in P_2 starting at q/p. The *legnth* of a continued fraction block C is the number of points in C minus 1, which is the number of edges in C. Denote the length of a continued fraction block C by $|C|$.

Lemma 2.10. *The length of either A or B is* 1.

Proof. In [21, Section 2.3], it was shown how to construct the path P_2 in the Farey graph from the continued fraction $q/p = [a_1, \ldots, a_n]$. In particular there are two cases to consider, when $a_n = -2$ and when it is not. We will consider the case when $a_n = -k < -2$ first. In this case, the continued fraction block B is

$$q_1 = q/p = [a_1, \ldots, a_n],\ q_2 = [a_1, \ldots, a_n + 1],\ \cdots,\ q_k = [a_1, \ldots, a_{n-1}, -1] = [a_1, \ldots, a_{n-1} + 1].$$

We also know that

$$p_1 = q/p = [a_1, \ldots, a_n] \text{ and } p_2 = [a_1, \ldots, a_{n-1}].$$

Note that p_2 and q_k have an edge between them in the Farey graph and that

$$q_i = (k - i)p_2 \oplus q_k$$

for $1 \leq i \leq k$, see Figure 11. Thus there is an edge in the Farey graph from p_2 to q_i for all $1 \leq i \leq k$. In particular, the points q/p, p_2 and q_2 all have edges between them. This says that the next vertex in a continued fraction block that starts with q/p and p_2 would be q_3, but as P_1 is a path anti-clockwise from q/p to ∞ we see that p_3 cannot be q_3 (which is clockwise of q/p), so $|A| = 1$.

Now suppose that $a_n = -2$, and furthermore suppose that $a_n = \cdots = a_{n-(k-1)} = -2$ and $a_{n-k} < -2$ for some $1 \leq k < n$. In this case, the continued fraction block A is

$$p_1 = q/p = [a_1, \dots, a_n],\ p_2 = [a_1, \dots, a_{n-1}],\ \cdots,\ p_{k+1} = [a_1, \dots, a_{n-k}].$$

We also have

$$q_1 = q/p = [a_1, \dots, a_n] \text{ and } q_2 = [a_1, \dots, a_n + 1] = [a_n, \dots, a_{n-k} + 1].$$

Note that p_{k+1} and q_2 have an edge between them in the Farey graph and that

$$p_i = p_{k+1} \oplus (k + 1 - i)q_2$$

for $1 \leq i \leq k + 1$. Thus there is an edge in the Farey graph between p_i and q_2 for all $1 \leq i \leq k + 1$. So we once again see that the points q/p, p_2 and q_2 all have edges between them. This says that the next vertex in a continued fraction block that starts with q/p and q_2 would be p_3 (note that this is true even if $k = 1$). Again, since P_2 is a path clockwise from q/p to 0, q_3 cannot equal to p_3 (which is anti-clockwise of q/p), so $|B| = 1$.

Finally, consider the case that $a_i = -2$ for $1 \leq i \leq n$. In this case, $q/p = -(n + 1)/n$ and $P_2 = \{-(n + 1)/n, -1\}$. It is clear that $|B| = 1$. □

Lemma 2.11. *A and B both have length 1 if and only if $q/p = -(2n + 1)/2$.*

Proof. One may readily check that for $-(2n + 1)/2$ both A and B have length 1. Now if $q/p \neq -(2n + 1)/2$ then let $n = \lfloor q/p \rfloor$, so $q/p \in [n, n + 1]$. Recall there is an edge in the Farey graph between n and $n+1$. Now the first edge in A is from q/p to $(q/p)^a$ and the first edge in B is from q/p to $(q/p)^c$. Recall there is an edge in the Farey graph from $(q/p)^a$ to $(q/p)^c$. Now as any two vertices in the Farey graph that share an edge, also both share an edge to exactly two other vertices, we know that $(q/p)^a$ and $(q/p)^c$ share an edge to q/p and another vertex v. Since $q/p \neq -2(n + 1)/2$, we can assume $(q/p)^a > n$ or $(q/p)^c < n + 1$. Since n and $n + 1$ have an edge, v must be in $[n, n + 1]$ and outside $[(q/p)^a, (q/p)^c]$. If $v > (q/p)^c$, then we see that v is a vertex in P_2 and since $\{q/p, (q/p)^c, v\}$ is a continued fraction block, we see that B has length greater than 1. Similarly if v is less than $(q/p)^a$ then A has length greater than 1. □

If $|A| = 1$ then we denote by $(A_1, A_3, \dots, A_{2n-1})$ the subdivision of P_1 such that each A_i is a continued fraction block and $A_1 = A$, and denote by $(B_2, B_4..., B_{2m})$ the subdivision of P_2^{T} such that each B_i is a continued fraction block and $B_2 = B$. If $|B| = 1$, then we denote the continued faction blocks by $(A_2, A_4, ..., A_{2n})$ and $(B_1, B_3, ..., B_{2m-1})$. (If $|A| = 1 = |B|$ then one may choose the either numbering convention and we know $q/p = -(2n + 1)/2$.)

Example 2.12. Consider the two paths for $-21/8 = [-3, -3, -3]$. In this case we have $P_1 = \{-21/8, -8/3, -3\}$ and $P_2^{\mathsf{T}} = \{-21/8, -13/5, -5/2, -2\}$, and the subdivisions $A_1 = \{-21/8, -8/3\}$, $A_3 = \{-8/3, -3\}$, $B_2 = \{-21/8, -13/5, -5/2\}$, $B_4 = \{-5/2, -2\}$.

Observation 2.13. It will be useful to notice that given the concatenated path $\overline{P_1} \cup P_2^{\intercal}$ (here $\overline{P_1}$ means P_1 run though backwards) there is a unique way to shorten this path to the one edge path from $\lfloor q/p \rfloor$ to $\lceil q/p \rceil$. See Figure 11. Let $(p_1, ..., p_k)$ be the points in P_1 where $p_1 = q/p$ and $(q_1, ..., q_l)$ be the points in P_2 where $q_1 = q/p$. Clearly the first point that can be removed is $p_1 = q_1 = q/p$. To continue we suppose we are in the case where the continued fraction blocks are labeled

$$(A_2, \dots, A_{2n}) \text{ and } (B_1, B_3, \dots, B_{2m-1}),$$

so B_1 has length one. The proof of Lemma 2.10 shows that there is an edge in the Farey graph between $q_2 = (q/p)^c$ and all the vertices in the continued fraction block $A_2 = \{p_1, \dots, p_i\}$. Thus we may first remove $p_1 = q/p$ from the path, then p_2 and continue until we have removed p_{i-1}. Notice that there is an edge from p_i to q_3 so the next vertex we can shorten is q_2. We now have two cases to consider, if B_3 has length 1 or greater. See Figure 11.

If B_3 has length 1, then there is an edge from p_{i+1} to q_3 and thus the edge from p_i to q_2 extends the continued fraction block A_4, i.e. $A_4' = \{q_2, p_i\} \cup A_4$ is a continued fraction block. Thus we have

$$P_1' = (A_4', A_6, \dots, A_{2n}) \text{ and } P_2' = (B_3, \dots, B_{2m-1})$$

and P_1' is a minimal path from q_2 anti-clockwise to $\lfloor q/p \rfloor$, and P_2' is is a minimal path from q_2 clockwise to $\lceil q/p \rceil$. Thus (P_1', P_2') are a pair of paths representing q_2 and each has one less continued fraction block than P_1 and P_2, respectively. We can now inductively continue to shorten the path until we have the path of length one from $\lfloor q/p \rfloor$ to $\lceil q/p \rceil$.

In the case when $|B_3| > 1$, $A_2' = \{q_2, p_i\}$ replaces A_2 and we have

$$P_1' = (A_2', A_4 \dots, A_{2n}) \text{ and } P_2' = (B_3, \dots, B_{2m-1})$$

and P_1' is still a minimal path from q_2 anti-clockwise to $\lfloor q/p \rfloor$, but now A_2' is its own continued fraction block with length 1. So the number of continued fraction blocks in P_1' is the same as for P_1 while the number in P_2' is one less than in P_2. Moreover, numbering the continued fraction block by our convention above will give P_1' the odd indices and P_2' the even. Once again we can inductively continue to shorten the paths until we have the path of length one from $\lfloor q/p \rfloor$ to $\lceil q/p \rceil$.

Notice that this observation implies that $|n - m| \leq 1$.

We will call a pair of decorated paths (P_1, P_2) *i-consistent* if the signs of the decorations on the paths A_j and B_j with $j \leq i$ in are all the same and we call the paths *i-inconsistent* if (P_1, P_2) is $(i-1)$-consistent but not i-consistent.

We now wish to consider when two pairs of paths give the same contact structure on S^3. We consider the breakdown of P_1 and P_2 as above (we will only discuss this case here, with the case of $(A_1, \dots, A_{2n-1})$ and $(B_2, \dots, B_{2m})$, and the case when the maximal odd index is smaller, being analogous). Let D_i denote A_i if i is even and B_i if i is odd. Suppose P_1 and P_2 are i-inconsistent for some $i > 2$, then of course the paths are $(i-1)$-consistent. From the discussion above we know that there is an edge in the Farey graph between the first vertex v_i of D_i and the last vertex v_i' in D_{i-1}. Moreover, if v_i'' is the second to last vertex in D_{i-1} then it is the Farey sum of v_i and v_i'; in particular it extends the continued fraction

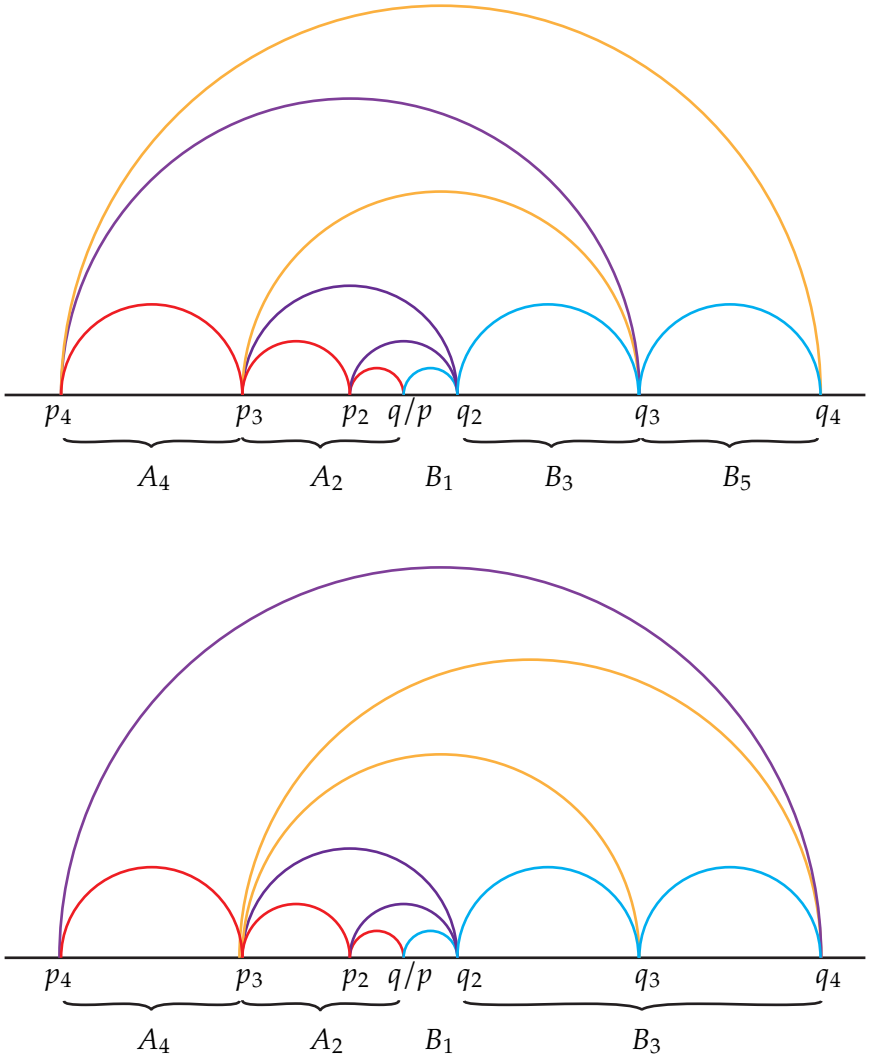

FIGURE 11. Two types of paths that behave differently when shortening. The difference is whether or not B_3 has length 1 or not. (The edges are not to scale to fit into the picture.)

block D_i by one extra jump. Since all the edges between v_i and v_i'' have the same sign, the contact structure described by the path between v_i and v_i'' is a basic slice with sign the common sign of the edges in the path. Now in D_i we know there is an edge with opposite sign and since D_i is a continued fraction block one may assume it is the edge adjacent to v_i. So we can exchange the sign on the edge between v_i'' and v_i and the first edge in D_i. This is equivalent to changing all the signs on the edges in of P_1 and P_2 between v_i and v_i'' as well as the sign of the first basic slice in D_i. After we have done this, we have a new pair of decorated paths P_1' and P_2'. We say that (P_1, P_2) is *i-compatible* with (P_1', P_2'). Notice, since one edge in D_{i-1} kept its same sign, that (P_1', P_2') is $(i-1)$-inconsistent.

Of course we can iterate and find decorated paths (P_1'', P_2'') that are $(i-1)$-compatible with (P_1', P_2') and continue until we have $(P_1^{(i-2)}, P_2^{(i-2)})$ which is 2-inconsistent. We say all these paths are *compatible*, see Figure 12.

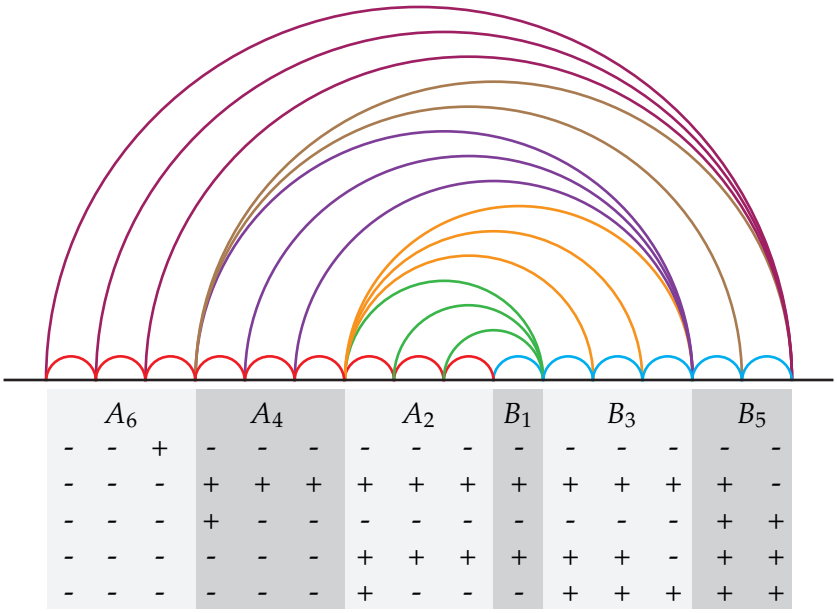

FIGURE 12. The signs in the top row give a 6-inconsistent pair of paths. In the next row we have shuffled sights in a continued fraction block to get a 5-inconsistent pair of paths. Each of the subsequent rows is obtained from the previous row by shuffling a basic slice in a continued fraction block to get a 4, then 3 and finally 2-inconsistent pair of paths.

Since ξ_{P_1,P_2} and $\xi_{P_1^{(j)},P_2^{(j)}}$ are build by gluing the same tight contact structures on solid tori together, the following lemma is self-evident.

Lemma 2.14. *Compatible pairs of decorated paths define the same contact structure on S^3.*

Remark 2.15. We can now see why it is important to consider the path $P_2^\intercal$ instead of the path from q/p to -1 as discussed at the beginning of this section. When all the edges in $P_1 \cup P_2^\intercal$ have the same sign but some edge in between $\lceil q/p \rceil$ and -1 has a different sign, we know that $\overline{P}_1 \cup P_2^\intercal$ describes a basic slice. One can see that performing the same "shuffling" discussed above will change the signs of all of the basic slices in $\overline{P}_1 \cup P_2^\intercal$ and so you will not get a pair of paths that is inconsistent at an earlier stage.

In addition, suppose P_1 and $P_2^\intercal$ are totally consistent (that is all their signs are the same) but some of the signs in the path from $\lceil q/p \rceil$ can be different. Then notice that by Theorem 2.3 the path $\overline{P}_1 \cup P_2^\intercal$ describes a basic slice and so the path from ∞ clockwise to $\lfloor q/p \rfloor$ followed by $\overline{P}_1 \cup P_2$ describes the unique tight contact structure on a solid torus and using Lemma 2.6 when one extends the path all the way to -1 we will have the unique tight contact structure on a solid torus with dividing slope -1. Notice that the complementary

solid torus in S^3 also has a unique tight contact structure and the union of these tori is the tight contact structure on S^3. In other words, such a path does not describe an overtwisted contact structure and is unrelated to non-loose Legendrian knots.

Case 2: $q/p > 1$**.** To describe these paths we consider the continued fraction expansion of q/p

$$\frac{q}{p} = a_1 - \cfrac{1}{a_2 - \cfrac{1}{\cdots - \cfrac{1}{a_n}}}$$

where $a_1 = \lfloor q/p \rfloor$ and $a_i \leq -2$ for $2 \leq i \leq n$. We, again, denote this $[a_1, \dots, a_n]$.

The same arguments as in Case 1 show the following lemmas.

Lemma 2.16. *Let $p_1 = q/p, p_2, \dots, p_{k-1} = \lceil q/p \rceil, p_k = \infty$ be the points on the Farey graph in P_2, and $q_1 = q/p, q_2, \dots, q_l = \lfloor q/p \rfloor$ be the points on the Farey graph in P_1. If $p_i = [b_1, \dots, b_j]$ then $p_{i+1} = [b_1, \dots, b_j + 1]$ for $1 \leq i < k-1$, and if $q_i = [c_1, \dots, c_j]$ then $q_{i+1} = [c_1, \dots, c_{j-1}]$ for $1 \leq i < l$.*

Lemma 2.17. *The first continued fraction block of P_1 or P_2 has length 1, and the other is bigger than 1.*

Remark 2.18. Recall when $q/p = -(2n+1)/2$ we saw in Lemma 2.11 that the leading continued fraction block of P_1 and P_2 both had length 1. However, when $q/p = (2n+1)/2$, we have $P_2 = \{(2n+1)/2, n, \infty\}$ which is a continued fraction block, so there are no $q/p > 1$ with both leading continued fraction blocks having length 1.

When $pq > 1$ we have one extra type of pair of decorated paths to consider. Suppose all the signs of P_1 and P_2 are the same, say negative. Let i be an integer such that $i < q/p < i+1$. As all the signs in all the paths are the same, we can shorten $\overline{P_1} \cup P_2$ to a path going from i to ∞ and describing a basic slice. Now split this path into P going from i to $i+1$ and P' going from $i+1$ to ∞ and decorate the paths with the common sign. Now the path P describes a contact structure on the solid torus S_∞ that is the unique solid torus with longitudinal divides and so may be split into a path going from ∞ to i and then to $i+1$ where the first jump corresponds to the unique contact structure on the solid torus with given slope and the second is a basic slice of either sign (see Lemma 2.6). We can choose the sign of the basic slice to be positive and then subdivide the path to $(\overline{P_1} \cup P_2) \cap [i, i+1]$ so that all the basic slices are positive. However, P_2 has one more edge going from $i+1$ to ∞ that is still negative. The paths with the new signs will be denoted (P_1^{2m-1}, P_2^{2m-1}) (here, we assume $2n > 2m-1$ without loss of generality). Clearly ξ_{P_1,P_2} and $\xi_{P_1^{2m-1},P_2^{2m-1}}$ are the same as they are described by gluing together the same contact structures on solid tori.

Notice that if the paths are broken into their continued fraction blocks

$$(A_2, \dots, A_{2n}) \text{ and } (B_1, B_3, \dots, B_{2m-1}),$$

as above, this new pair of paths (P_1^{2m-1}, P_2^{2m-1}) is $2m-1$-inconsistent. As we saw above we will now get k-inconsistent pairs of paths (P_1^k, P_2^k) for $k = 2, 3, \dots, 2m-1$ that are all compatible. Notice that all the signs of the basic slices in P_1^2 are of a fixed sign, say positive, except the first one which is negative and all the basic slices of P_2^2 are negative, except the first one which is positive.

2.4. **From decorated Farey graphs to contact surgery diagrams.** Let (P_1, P_2) be a pair of paths in the Farey graph representing q/p. As discussed in the previous section, once the paths are decorated they give a contact structure ξ_{P_1,P_2}; moreover, there is a convex torus T with two dividing curves of slope q/p that separates S^3 into two solid tori with contact structures described by P_1 and P_2. We will show in Lemma 6.8 that a Legendrian divide on this torus will be a non-loose (p,q)–torus knot L_{P_1,P_2} and all such torus knots with tb $= pq$ and tor $= 0$ will occur in this way, as we will show in Section 7.7. Here we would like to turn the Farey graph description of L_{P_1,P_2} into a contact surgery diagram in (S^3, ξ_{std}). The relation between the surgery construction and paths in the Farey graph was originally observed by Matkovič [42] in the case of small Seifert fibered spaces and then used to study negative torus knots in her paper [43].

We subdivide P_1 and P_2 as discussed in Section 2.3. We can convert this decorated Farey graph into a contact surgery diagram in (S^3, ξ_{std}) for the contact structure ξ_{P_1,P_2}. To this end, we first consider a smooth surgery diagram for S^3 shown in the left drawing of Figure 13.

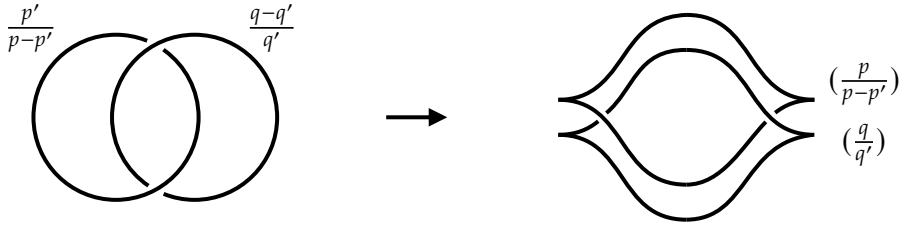

FIGURE 13. Left: smooth surgery diagram of S^3. Right: contact surgery diagram of (S^3, ξ)

Here, we denote $(q/p)^c$ by q'/p'. To see this manifold is S^3, think of this manifold as a result of Dehn filling $T^2 \times I$ along a curve on $-T^2 \times \{0\}$ of slope $p'/(p-p')$ and a curve on $T^2 \times \{1\}$ of slope $q'/(q-q')$. Let ϕ be a diffeomorphism of a torus whose matrix representation is

$$\phi = \begin{pmatrix} p' & p'-p \\ q' & q'-q \end{pmatrix}.$$

After change the coordinates of $T^2 \times I$ using ϕ, the meridional slope of two solid tori glued on $T^2 \times \{0\}$ and $T^2 \times \{1\}$ are ∞ and 0, respectively. Thus the surgered manifold is diffeomorphic to S^3. Next, convert this diagram into a contact surgery diagram as shown in the right drawing of Figure 13. Observe that the region between the two Legendrian unknots is a thickened torus $T^2 \times I$ with an I-invariant contact structure having dividing slope -1. After changing the coordinates using ϕ, we have

$$\begin{pmatrix} p' & p'-p \\ q' & q'-q \end{pmatrix} \begin{pmatrix} 1 \\ -1 \end{pmatrix} = \begin{pmatrix} p \\ q \end{pmatrix}.$$

Thus the dividing slope of the torus is q/p after change of the coordinates. Thus the two solid tori glued on $T^2 \times \{0\}$ and $T \times \{1\}$ are elements of Tight$(S_\infty; q/p)$ and Tight$(S^0; q/p)$

respectively. Recall that in [9], Ding, Geiges, and Stipsicz provided an algorithm to convert a general contact surgery diagram to a contact (± 1)–surgery diagram:

- contact (p/q)–surgery on a Legendrian knot L with $p/q < 0$:
  (1) Stabilize L, $|r_1 + 2|$ times, where
  $$\frac{p}{q} = r_1 + 1 - \cfrac{1}{r_2 - \cfrac{1}{r_3 \cdots - \cfrac{1}{r_n}}}$$
  for $r_i \leq -2$. Let the resulting Legendrian knot be L_1.
  (2) For $i = 2, \ldots, n$, let L_i be the Legendrian push-off of L_{i-1} and stabilize it $|r_i + 2|$ times.
  (3) Then a contact (p/q)–surgery on L corresponds to a contact (-1)–surgeries on a link $(L_1, \ldots, L_n)$.
- contact (p/q)–surgery on a Legendrian knot L with $p/q > 0$:
  (1) Choose a positive integer k such that $q - kp < 0$. Let $r' = p/(q - kp)$.
  (2) Let $L_1, \ldots, L_k$ be k successive Legendrian push-offs of L.
  (3) Then a contact (p/q)–surgery on L corresponds to $(+1)$–surgeries on $L_1, \ldots, L_k$ and a contact (r')–surgery on L.

Applying the second algorithm to the contact surgery diagram in Figure 13, we obtain the contact surgery diagram shown in Figure 2. To see this notice that since $q/p = (q/p)^a \oplus (q/p)^c$, see Lemma 2.1, we know that $p - p' > 0$ and $q - q' > 0$ and q and q' will both either be positive or both negative. Choosing $k = 1$ in the above algorithm will result in the surgery coefficients shown in Figure 2 which can easily be checked to be less than -1. Notice that the above algorithm actually produces Figure 2 with the second the third surgery coefficients interchanged; however, since the two negative surgery coefficients are less than -1 those Legendrian knots must be stabilized to perform Legendrian surgery and in [6] it was shown that stabilized components of a $(4, -4)$-torus link (that is, the surgery link in Figure 2) can be arbitrarily permuted amongst the other components.

In [8], Ding and Geiges showed that the choice of stabilizations on L_1 with contact surgery coefficient $(p/(p - p'))$ and L_2 with contact surgery coefficient (q/q') corresponds to the choice of signs on the basic slices of V_1 and V_2, respectively. To be more precise, suppose

$$-\frac{p}{p'} = r_1 + 1 - \cfrac{1}{r_2 - \cfrac{1}{r_3 \cdots - \cfrac{1}{r_u}}} \quad \text{and} \quad -\frac{q}{q - q'} = s_1 + 1 - \cfrac{1}{s_2 - \cfrac{1}{s_3 \cdots - \cfrac{1}{s_v}}}$$

for $r_i \leq -2$ and $s_i \leq -2$. Let $[r_{p_1}, \ldots, r_{p_n}]$ be the subsequence of $[r_1, \ldots, r_u]$ such that $r_{p_i} < -2$. Now the choice of stabilizations on L_{p_i} corresponds to the choice of signs on each basic slice in the continued fraction block A_{2i-1}. Similarly, let $[s_{q_1}, \ldots, s_{q_m}]$ be the subsequence of $[s_1, \ldots, s_v]$ such that $s_{q_i} < -2$. Now the choice of stabilizations on L_{q_i} corresponds to the choice of signs on each basic slice in the continued fraction blocks B_{2i}. Observe that since P_2 represents a contact structure on $Tight(S^0, q/p)$, the positive stabilization corresponds to the negative basic slice (respectively the negative stabilization corresponds to the positive basic slice). See Figure 17 for examples.

2.5. **Homotopy class of plane fields and rotation numbers.** Given a pair (P_1, P_2) of decorated paths in the Farey graph for the (p, q)–torus knot, we saw in Section 2.4 that we define a contact structure ξ_{P_1,P_2} on S^3 and a non-loose Legendrian (p, q)–torus knot $L_{P_1,P_2} \in (S^3, \xi_{P_1,P_2})$ with tor = 0. Moreover, Lemma 6.8 says that all such Legendrian knots come from this construction.

To calculate the d_3-invariant of ξ_{P_1,P_2}, we first convert the decorated Farey graph (P_1, P_2) for the (p, q)–torus knot into the corresponding contact (± 1)–surgery diagram as described in Section 2.4. See Figure 17 for examples. From the surgery diagram we can compute d_3-invariant of the contact structure on S^3 using the formula from [9, Corollary 3.6]:

$$d_3(\xi) = \frac{1}{4}(c^2 - 3\sigma(X) - 2(\chi(X) - 1)) + q, \tag{3}$$

where X is the 4–manifold obtained by attaching 2-handles to the 4-ball as indicated in the diagram, and q is the number of contact (+1)-surgery components. The quantity c^2 is $(\mathbf{rot})^\intercal M^{-1}\mathbf{rot}$, where M is the linking matrix of the surgery diagram and $\mathbf{rot}$ is a vector of rotation numbers of each surgery component. Since $\mathbf{rot}^\intercal M^{-1}\mathbf{rot} = (-\mathbf{rot}^\intercal)M^{-1}(-\mathbf{rot})$, we see that ξ_{P_1,P_2} is the same as $\xi_{-P_1,-P_2}$.

We give two methods to compute the rotation number of L_{P_1,P_2}. The first method for computing $\mathrm{rot}(L_{P_1,P_2})$ involves the surgery diagram used above. In particular, we have the formula from [11, Theorem 2.2]:

$$\mathrm{rot}(L) = \mathrm{rot}_0 - \mathbf{rot}^\intercal \cdot M^{-1} \cdot \mathbf{lk}, \tag{4}$$

where rot_0 is the rotation number of L in the surgery diagram before surgery and $\mathbf{lk}$ is the vector of linking numbers between each surgery component and L. In our surgery diagram, it is clear that

$$\mathbf{lk} = \begin{bmatrix} -1 \\ \vdots \\ -1 \end{bmatrix}.$$

In our examples $rot_0 = 0$, so we see that $\mathrm{rot}(L_{P_1,P_2}) = -\mathrm{rot}(L_{-P_1,-P_2})$.

The second method for computing the rotation number makes the computation directly from the Farey graph. Given a pair (P_1, P_2) of decorated paths in the Farey graph for the (p, q)–torus knot, let $p_1 = q/p, p_2, \ldots, p_k = \lfloor q/p \rfloor$ be the vertices in P_1 and $q_1 = q/p, q_2, \ldots, q_l$ be the vertices in P_2. Recall, when $pq < 0, q_l = -1$ and when $pq > 0, q_l = \infty$. Define

$$r_m = \sum_{i=1}^{k-1} \epsilon_i \left((p_{i+1} \ominus p_i) \bullet \frac{1}{0} \right)$$

and

$$r_n = \sum_{i=1}^{l-1} \epsilon'_i \left((q_{i+1} \ominus q_i) \bullet \frac{0}{1} \right)$$

where ϵ_i is the sign of the edge from p_i to p_{i+1} and ϵ'_i is the sign of the edge from q_i to q_{i+1}. Then define

$$R(P_1, P_2) = p\, r_n + q\, r_m$$

Lemma 2.19. *The Legendrian knot L_{P_1,P_2} has rotation number*

$$\mathrm{rot}(L_{P_1,P_2}) = R(P_1, P_2).$$

Notice that since $R(P_1, P_2)$ is simply the rotation number of L_{P_1,P_2} it can also be computed from the surgery formula above.

Proof. Suppose T is a convex torus. Let λ and μ be curves on the torus that form a basis for $H_1(T)$. If γ is a curve on T that in homology is $p\lambda + q\mu$, then when T is isotoped through convex tori so that γ is a Legendrian curve, it was shown in [16, discussion before Lemma 4.11] that

$$\mathrm{rot}(\gamma) = p\ \mathrm{rot}(\lambda) + q\ \mathrm{rot}(\mu),$$

where $\mathrm{rot}(\lambda)$, respectively $\mathrm{rot}(\mu)$, is computed by isotoping T through convex tori so that λ, respectively μ, is a Legendrian curve.

In our setting T is a Heegaard torus for S^3 thought of as a neighborhood of an unknot. The the standard longitude and meridian for the unknot are exactly λ and μ and one bounds a compressing disk in V_1 and the other bounds one in V_2. From this we see that the relative Euler class these two Heegaard tori are the rotation numbers of λ and μ. From [34, proof of Proposition 4.22] we can compute these relative Euler classes and see that $\mathrm{rot}(\lambda) = r_n$ and $\mathrm{rot}(\mu) = r_m$. The result follows. □

Using this lemma, we can show that $\mathrm{rot}(L_{P_1,P_2})$ differs by the choice of the decorated paths (P_1, P_2).

Lemma 2.20. *If $(P_1, P_2) \neq (P'_1, P'_2)$, then $\mathrm{rot}(L_{P_1,P_2}) \neq \mathrm{rot}(L_{P'_1,P'_2})$.*

Proof. We compute the rotation numbers using Lemma 2.19. That is $\mathrm{rot}(L_{P_1,P_2}) = pr_n + qr_m$ and $\mathrm{rot}(L_{P'_1,P'_2}) = pr'_n + qr'_m$ where r_m, r_n, r'_m and r'_n are computed in terms of the decorated paths as described in Section 2.5. The numbers r_m and r_n are the relative Euler numbers for the contact structures on V_1 and V_2, and similarly for r'_m and r'_n. In [34], Honda showed that tight contact structures on solid tori are determined by their relative Euler class. Since $(P_1, P_2) \neq (P'_1, P'_2)$, we know that either $r_m \neq r'_m$ or $r_n \neq r'_n$.

Arguing by contradiction we assume that $\mathrm{rot}(L_{P_1,P_2}) = \mathrm{rot}(L_{P'_1,P'_2})$, so we have that

$$p(r_n - r'_n) + q(r_m - r'_m) = 0.$$

We first notice that $r_m - r'_m$ and $r_n - r'_n$ are both even, since from the formula in Section 2.5 we see that

$$r_m - r'_m = \sum_{i=1}^{k-1} (\epsilon_i - \epsilon'_i) \left((p_{i+1} \ominus p_i) \bullet \frac{1}{0} \right),$$

where the ϵ_i are the signs in P_1 and the ϵ'_i are the signs in P'_1. Thus $(\epsilon_i - \epsilon'_i)$ is even for all i and we have a similar argument for $r_n - r'_n$. Moreover

$$|r_m| \leq \left| \left(\frac{q}{p} \ominus \left\lfloor \frac{q}{p} \right\rfloor \right) \bullet \frac{1}{0} \right| = p - 1$$

and similarly for $|r'_m|$. We also have

$$|r_n| \leq |q| - 1$$

since $|r_n| \leq |(\frac{q}{p} \ominus \frac{1}{0}) \bullet \frac{0}{1}|$ when $pq > 0$ and $|r_n| \leq |(\frac{q}{p} \ominus \frac{-1}{1}) \bullet \frac{0}{1}|$ when $pq < 0$, and similarly for r'_n.

Since $\gcd(p, q) = 1$, the only integer solutions to $pa + qb = 0$ are $a = nq$ and $b = -np$ for $n \in \mathbb{Z}$. But given the above, we see that

$$|r_m - r'_m| < 2p,$$
$$|r_n - r'_n| < 2|q|.$$

Thus, $p = |r_m - r'_m|$ and $|q| = |r_n - r'_n|$. However this implies that p and q are both even, contradicting the fact that $\gcd(p, q) = 1$. Thus we have $\text{rot}(L_{P_1,P_2}) \neq \text{rot}(L_{P'_1,P'_2})$ as claimed. □

2.6. **Contact structures on $S^1 \times P$.** Consider $S^1 \times P$ where P is a pair of pants (a disk with two disjoint open sub-disks removed). Label the boundary components T_1, T_2, and T_3 and consider the basis $S^1 \times \{pt\}$ and $\mu_i = T_i \cap (\{\theta\} \times P)$ for $H_1(T_i)$. Let $S^1 \times \{pt\}$ have slope 0 and μ_i have slope ∞. Let $\text{Tight}_0^{free}(S^1 \times P; r_1, r_2, r_3)$ be the set of tight contact structures, up to isotopy (not fixing the boundary point-wise, but preserving it set-wise), on $S^1 \times P$ with convex boundary such that T_i has two dividing curves of slope r_i and having no convex Giroux torsion.

Lemma 2.21. $|\text{Tight}_0^{free}(S^1 \times P; 0, 0, 0)| = 1$

This lemma follows from Lemmas 10 and 11 in [17], though we give the simple proof for completeness.

Proof. Any contact structure $\xi \in \text{Tight}_0^{free}(S^1 \times P; 0, 0, 0)$ has dividing curves parallel to the S^1–fibers on all boundary components. We can make the ruling curves have slope ∞ and then arrange for $P = \{\theta\} \times P$ to have its boundary be ruling curves and then make it convex. We need to consider two cases for the dividing curves on P.

Case 1. There is a boundary-parallel dividing curve on one of the tori T_i for $1 \leq i \leq 3$. See the right drawing of Figure 14 for example. Without loss of generality, we can assume that there is a boundary-parallel dividing curve on T_1. Then we can attach a bypass to T_1 to obtain a thickened torus N_1 with convex boundary where its back face has slope 0 and its front face (T_1) has slope ∞. Now take the 0 sloped annulus A from the back face of N_1 to T_3 and attach the neighborhood of A to thicken N_1 and obtain a thickened torus N'_1 with front and back face both having slope ∞. Moreover, since N'_1 contains convex tori parallel to the boundary with dividing slope different from ∞, we know it must contain convex half Giroux torsion. This contradiction shows there is no boundary-parallel dividing curves on any T_i.

Case 2. There is no boundary parallel dividing curves on any T_i. See the left drawing of Figure 14 for example. Honda showed in [35, Lemma 4.1], that the tight contact structures on $S^1 \times P$ with 0 slope dividing curves on every T_1, T_2 and T_3 are in one-to-one correspond with the choice of dividing set on P. There is a unique such configuration of dividing curves on P up to some number of half twists near each boundary component.

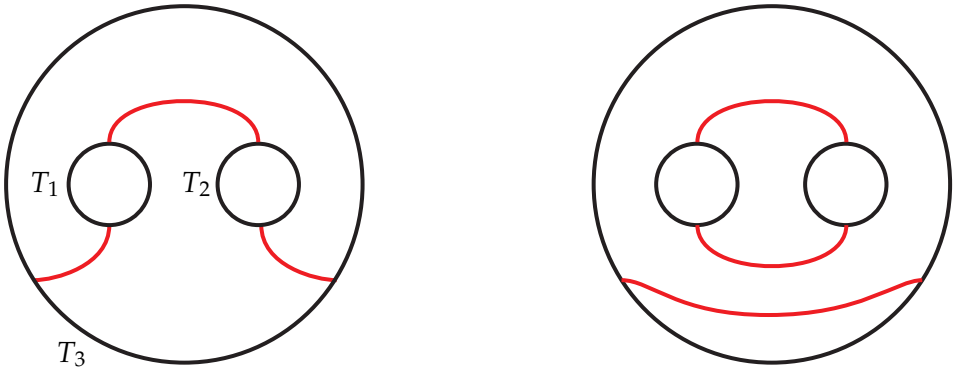

FIGURE 14. Some possible dividing sets on the pair of pants P.

As we are allowing the boundary components to rotate among themselves, these twists can be undone and we can assume the dividing curves are as given on the left-hand side of Figure 14. □

Given any contact structure on $\mathrm{Tight}_0^{free}(S^1 \times P; -1, \infty, 0)$ let T_3' be a copy of T_3 that is contact isotopic to T_3. We can take an annulus A_i from a slope 0 ruling curve on T_i to a Legendrian divide on T_3' and make it convex, for $i = 1, 2$. One may take a neighborhood N_i of $T_i \cup A_i$ to be a basic slice in $\mathrm{Tight}^{min}(T^2 \times [0,1]; r_i, 0)$ and the contact structure on the complement of the N_i is the unique contact structure on $\mathrm{Tight}_0^{free}(S^1 \times P; 0, 0, 0)$. Let s_i be the sign of the basic slice N_i and denote the contact structure by $\xi_{s_1 s_2}$.

Lemma 2.22. *We have*

$$\mathrm{Tight}_0^{free}(S^1 \times P; -1, \infty, 0) = \{\xi_{++}, \xi_{+-}, \xi_{-+}, \xi_{--}\}.$$

In $\xi_{\pm\pm}$ there is a convex annulus A with boundary slope 0 ruling curves on T_1 and T_2 that has two dividing curves each running from one boundary component to the other. In $\xi_{\pm\mp}$ the analogous annulus will always have boundary parallel dividing curves.

Let $\eta_\pm$ be the $\pm$ basic slice in $\mathrm{Tight}^{min}(T^2 \times [0,1]; -1, 0)$ and $\zeta_\pm$ be the $\pm$ basic slice in $\mathrm{Tight}^{min}(T^2 \times [0,1]; 0, \infty)$. Then $\xi_{\pm\mp}$ is obtained by gluing the front face of $\eta_\pm$ to the back face of $\zeta_\pm$ together and removing a standard neighborhood of a Legendrian divide on the convex torus of slope 0. Similarly $\xi_{\pm\pm}$ is obtained by gluing the front face of $\eta_\pm$ to the back face of $\zeta_\mp$ together and removing a standard neighborhood of a Legendrian divide on the convex torus of slope 0.

The construction of the contact structures $\xi_{\pm\pm}$ and the annulus in the lemma follows closely the construction in [30, Lemma 4.13], where as the classification itself follows from [29, Lemma 5.4]. We give the proof of the lemma here, as we will need all the properties of the contact structures described in the lemma.

Remark 2.23. Notice that given a contact structure in $\mathrm{Tight}_0^{free}(S^1 \times P; -1, \infty, 0)$ the 0 sloped ruling curves on T_1 and T_2 will be isotopic if and only if there is a convex annulus that they bound has dividing curves running from one boundary component to the other.

Proof. From the discussion before the lemma, it is clear that there are at most 4 contact structures, so we are left to see that the given contact structures are indeed tight and satisfy the required properties.

First consider the $\pm$ basic slice $\xi_\pm$ in $\text{Tight}(T^2 \times [0,1]; -1, \infty)$. We know there is a convex torus T inside of $T^2 \times [0,1]$ with dividing slope 0. Notice that T breaks $\xi_\pm$ into $\eta_\pm$ and $\zeta_\pm$. Remove a neighborhood of a dividing curve on T to get a contact structure on $S^1 \times P$. Clearly this contact structure contains no convex Giroux torsion and is in $\text{Tight}_0(S^1 \times P; -1, \infty, 0)$. Recall when considering $T^2 \times [0,1]$ we orient $T^2 \times \{0\}$ using the inward pointing normal vector and $T^2 \times \{1\}$ with the outward pointing vector. However, when factoring a contact structure in $\text{Tight}_0(S^1 \times P; -1, \infty, 0)$ as above both the basic slices with back face T_1 and T_2 are oriented with the inward pointing vector. Thus the sign of the bypass on T_2 is opposite to what one sees when concatenating $\eta_\pm$ and $\zeta_\pm$. Thus the contact structure on $S^1 \times P$ coming from $\xi_\pm$ is $\xi_{\pm\mp}$. Also, consider a convex annulus A from a slope 0 ruling curve on T_1 to a slope 0 ruling curve on T_2. This will also be an annulus in $(T^2 \times [0,1], \xi_\pm)$. We know the Poincare dual of the relative Euler class of this contact structure is $\pm(1,-2)$ and so evaluates to ± 2 on A. Since we know the relative Euler class evaluated on a convex surface is $\chi(A_+) - \chi(A_-)$, where $A_\pm$ is the $\pm$ regions of the convex surface A, we see that the dividing curves cannot run across A.

Now for the other two contact structures consider the $\pm$ basic slice $\xi'_\pm$ in $\text{Tight}(T^2 \times [0,1]; 0, \infty)$. Now let T be a convex torus contact isotopic to $T^2 \times \{1\}$ on the interior of $T^2 \times [0,1]$. Let L be a slope 0 ruling curve on T. Removing a standard neighborhood of L will result in a contact structure on $S^1 \times P$. It will again clearly have no convex Giroux torsion and be an element in $\text{Tight}_0(S^1 \times P; -1, \infty, 0)$. Moreover, by construction there is a convex annulus with boundary slope 0 ruling curves on the boundary components with dividing slope -1 and ∞ that has dividing curves going from one boundary component to the other. Thus the two contact structures on $S^1 \times P$ coming from $\xi'_\pm$ are different from the ones coming from $\xi_\pm$ by their relative Euler classes. Thus they must be $\xi_{\pm\pm}$. Notice that by construction $\xi_{\pm\pm}$ is a union of some contact structure on the thickened tori N_1 and N_2 and the unique contact structure on $S^1 \times P'$ (where $P' \subset P$) in $\text{Tight}_0^{free}(S^1 \times P; 0, 0, 0)$. Notice that if one glues a solid torus S to T_3 and extends the contact structure so that it is tight on the solid torus, then $(S^1 \times P') \cup S$ will be an I invariant contact structure on $T^2 \times I$. Thus $(S^1 \times P) \cup S$ will be the result of concatenating a basic slice in $\text{Tight}(T^2 \times [0,1]; -1, 0)$ and one in $\text{Tight}(T^2 \times [0,1]; 0, \infty)$. Since we have already identified $\eta_\pm \cup \zeta_\pm$ above, we see that the current contact structures must come from $\eta_\pm \cup \zeta_\mp$ by removing a 0 sloped dividing curves from a convex torus. This establishes all the claimed properties. □

Remark 2.24. Notice that in the local model for $\xi_{\pm\pm}$ we see that if we attach a $\pm$ basic slice from $\text{Tight}(T^2 \times [0,1]; 0, \infty)$ to $\xi_{\pm\pm}$ we will still have a tight contact manifold, but if we attach the $\mp$ basic slice then it will become overtwisted.

2.7. **Non-rotative layers and properties of bypasses.** To study convex Giroux torsion in the complement of non-loose Legendrian torus knots, we need to understand non-rotative $T^2 \times I$ layers. In this subsection, we will review basic definitions and properties of non-rotative layers. For more details, see [36]. After that, we will review some useful properties of bypasses which will be used to prove Lemma 6.15. For more details, see [5, 34, 37, 38].

A *non-rotative* $T^2 \times I$ *layer*, or a *non-rotative layer* in short, is a tight $T^2 \times I$ with convex boundary such that any convex torus parallel to the boundary has the same dividing slope. We will denote $T_i = T^2 \times \{i\}$ for $i = 0, 1$ and let n_0 and n_1 be the number of dividing curves on T_0 and T_1, respectively. Note that n_0 and n_1 are always even. We say a convex annulus A in a non-rotative layer is *horizontal* if it has Legendrian boundary and intersects each dividing curve on T_1 and T_2 exactly once. Let (M, ξ) be a tight contact 3–manifold with a torus boundary T. Then a *non-rotative outer layer for* T is a non-rotative layer $N = T^2 \times I$ in (M, ξ) such that $T_1 = T$, $n_0 = 2$ and $n_1 \geq 2$. Given two such non-rotative outer layers N_1 and N_2 for the boundary component T of (M, ξ), Let A_i be a horizontal annulus in N_i such that $A_1 \cap T = A_2 \cap T$ and denote this curve c. We say that N_1 and N_2 are *disk-equivalent* if there exist a disk D and embeddings $\phi_i : A_i \to D$ such that $\phi(c) = \phi(c) = \partial D$, $\phi|_c = \phi|_c$, and Γ_1 is isotopic to Γ_2 on D where Γ_i is obtained from $\phi_i(\Gamma_{A_i})$ by extending over $D - \phi_i(A_i)$ by a single arc (here Γ_S denotes the dividing curves on a convex surface S). See Figure 15 for example.

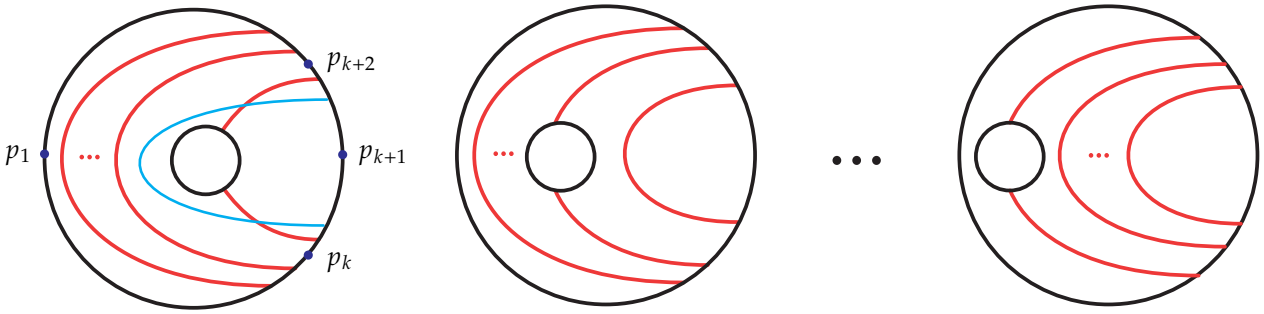

FIGURE 15. Disk-equivalent annuli (up to holonomy). The blue arc is a Legendrian arc.

Honda showed that some non-rotative layers are embedded in I-invariant neighborhoods.

Theorem 2.25 (Honda [36]). *Let $T^2 \times [0, 1]$ is a non-rotative layer with $n_0 = 2$. Then it can be embedded in an I-invariant neighborhood $T^2 \times [0, 2]$ where $n_0 = n_2 = 2$.*

One important property is that any two non-rotative outer layers for a fixed torus are disk-equivalent.

Theorem 2.26 (Honda [36]). *Let (M, ξ) be a tight contact 3–manifold with convex boundary and T be a torus boundary component. Then any two non-rotative outer layers for T are disk-equivalent.*

Even though (M, ξ) can contain two different (but disk-equivalent) non-rotative outer layers for a fixed torus, the complements of these layers are contactomorphic.

Theorem 2.27 (Honda [36]). *Let (M, ξ) be a tight contact 3–manifold with convex boundary and T be a torus boundary component. Suppose $(M, \xi) = (M_i, \xi_i) \cup N_i$ for $i = 0, 1$ where N_i is a non-rotative outer layers for T. Then there is a co-orientation preserving contactomorphism between (M_0, ξ_0) and (M_1, ξ_1).*

It is clear that any tight solid torus with convex boundary can be decomposed into a solid torus with two dividing curves and a non-rotative outer layer. Using Theorem 2.25, the following is also clear.

Theorem 2.28. *Let V be a tight solid torus having convex boundary T with two dividing curves of slope s. Let N be a non-rotative layer of slope s with $n_0 = 2$ and $n_1 > 2$. Then $V \cup N$ is tight.*

Consider a tight solid torus V with convex boundary T. Let n be the number of dividing curves on the boundary and q/p be the slope of the dividing curves. We can find (after perturbation) a Legendrian meridian c on T, which intersect the dividing curves in $2k$ points. Label these intersection points as $p_0, \dots, p_{2k-1}$ consecutively. Let D be a convex meridian disk in V bounded by c. Clearly, there exists $2k$ dividing curves on D. We say a bypass on D is a *bypass for* p_i if there exists a bypass with attaching arc containing p_{i-1}, p_i, p_{i+1} (indices are considered as an element in $\mathbb{Z}_{2k}$). We also say a bypass is *effective* if the attaching arc of the bypass passes three dividing curves and the center dividing curve is different from the others. Recall that Honda showed [34] attaching an effective bypass to a torus will decrease the number of dividing curves or change the dividing slope. Honda also showed that if a bypass in a tight solid torus is not effective, then it is contained in an I-invariant neighborhood of T (we note that when the bypass is not effective, it could still increase the number of dividing curves, but one can always find another torus that, with the original torus, co-bounds an I-invariant contact structure that contains the bypass).

Theorem 2.29 (Honda [34])**.** *Let V be a tight solid torus with convex boundary T. If a bypass in V whose attaching arc is on T is not effective, then the bypass is contained in an I-invariant neighborhood of T. In fact, it is either a trivial bypass, or a folding bypass which increases the number of dividing curves on T by 2.*

Here, we review Colin's isotopy discretization, which is the key idea of "state transition" (see [37, Section 2]).

Theorem 2.30 (Isotopy Discretization, Colins [4], see also Honda [37])**.** *Let Σ and Σ' be two convex surfaces with the same Legendrian boundary. If there is a smooth isotopy between them rel boundary, then there exists a sequence of surfaces $\Sigma_0 = \Sigma, \dots \Sigma_n = \Sigma'$ with the same boundary and Σ_{i+1} is obtained from a single bypass attachment to Σ_i.*

We say a bypass on a disk is *non-nested* if it is associated to a dividing curve that separates the disk into two components, one of which has no dividing curves. We say there are *nested bypasses* for a point p if there are consecutive dividing curves parallel to a non-nested bypass for p. The number of dividing curves for nested bypasses is called the *length of the nested bypasses*. See Figure 16 for example.

3. An algorithm to classify non-loose torus knots

In this section we give a user's guide to the complete classification of non-loose Legendrian (p, q)–torus knots. We prove that this algorithm really gives the complete classification in Section 7.7.

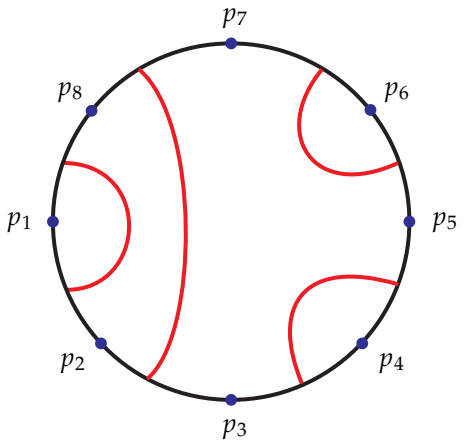

FIGURE 16. Nested bypasses for p_1 with length 2. There are three non-nested bypasses for p_1, p_4 and p_6.

3.1. **The classification of non-loose torus knots without convex Giroux torsion.** Below is an algorithm to classify non-loose (p,q)–torus knots with tor = 0.

Step 1. Determine the overtwisted contact structures that support non-loose (p,q)–torus knots. Find all 2-inconsistent pairs of decorated paths representing q/p:

$$\{(\pm P_1^1, \pm P_2^1), \dots, (\pm P_1^n, \pm P_2^n)\}.$$

For each $i \in \{1,\dots,n\}$ draw a contact surgery diagram for $L_{P_1^i,P_2^i}$ as described in Section 2.4, and then use the formula (3) in Section 2.5 to compute the d_3-invariant of the contact structure. These are the only contact structures supporting non-loose (p,q)–torus knots without convex Giroux torsion.

Step 2. Compute the non-loose Legendrian knots with "exceptional" mountain ranges. For any (p,q)–torus knot, there is an exceptional overtwisted contact structure where the classification is qualitatively different from all the others. These are shown in Figure 4 and described as follows. For $pq > 0$, this is the contact structure ξ_1 and for $pq < 0$, it is the contact structure $\xi_{|pq|-|p|-|q|+1}$. It is useful to note that for $pq > 0$ the contact structure ξ_1 is described by the pair of paths (P_1, P_2) with all signs the same and also by the 2-inconsistent pair of paths (P_1', P_2') where the signs of all the basic slices in P_1' are the same, say $\pm$, except for one edge in the first block that is $\mp$, while all blocks P_2' are labeled with $\mp$ except for one edge in the first block that is $\pm$. We also note that when $pq < 0$ the contact structure $\xi_{|pq|-|p|-|q|+1}$ is described by the 2-inconsistent pair of paths (P_1, P_2) where all the signs in P_1 are the same and opposite to all the signs in P_2.

We begin with the $pq > 0$ case. Let (P_1, P_2) be a pair of paths representing q/p. Recall that we can arrange the continued fraction blocks in P_1 and P_2 as follows.

$$(A_1, A_3, \dots, A_{m-1}) \text{ and } (B_2, B_4, \dots, B_m)$$

(notice that there are several other cases, but they can be dealt in the same way). Let s_k be the slope in the k^{th} continued fraction block that is farthest from q/p. Set $n_k = |s_k \bullet \frac{q}{p}|$ for $k = 2, \dots, m$.

In ξ_1, there is an infinite V with bottom vertex having $r = 0$ and $\mathrm{tb} = pq - p - q + 2$. That is, there are Legendrian knots $L^i_\pm$ for $i > pq - p - q + 2$ and $L^{pq-p-q+2}$ with

$$\mathrm{tb}(L^i_\pm) = i,\ \mathrm{rot}(L^i_\pm) = \mp(i - pq + p + q - 2),\ \text{and}\ \mathrm{tor}(L^i_\pm) = 0,$$

$$\mathrm{tb}(L^{pq-p-q+2}) = pq - p - q + 2,\ \mathrm{rot}(L^{pq-p-q+2}) = 0,\ \text{and}\ \mathrm{tor}(L^{pq-p-q+2}) = 0,$$

such that

$$S_\pm(L^i_\pm) = L^{i-1}_\pm,\ \text{for i} \geq pq - p - q + 4, \text{and } S_\pm(L^{pq-p-q+3}_\pm) = L^{pq-p-q+2},$$

and

$$S_\mp(L^i_\pm) \text{ and } S_\pm(L^{pq-p-q+2}) \text{ are loose.}$$

Moreover, there are Legendrian knots $L^{pq}_{k,\pm}$ with $k = 2, \ldots, m$ such that

$$\mathrm{tb}(L^{pq}_{k,\pm}) = pq,\ \mathrm{rot}(L^{pq}_{k,\pm}) = \mp\left(p + q - 2n_k\right),\ \text{and}\ \mathrm{tor}(L^{pq}_{k,\pm}) = 0$$

and a stabilization of $L^{pq}_{k,\pm}$ is non-loose if and only if it stays on or above the V described above. Lastly, the Legendrian knots described above are coarsely Legendrian simple, so if stabilizations of any two of them have the same Thurston-Bennequin invariant and rotation number, then they are equivalent.

We now consider the $pq < 0$ case. In $\xi_{|pq|-|p|-|q|+1}$, there are non-loose Legendrian knots $L^i_\pm, i \in \mathbb{Z}$ and L_e with

$$\mathrm{tb}(L^i_\pm) = i,\ \mathrm{rot}(L^i_\pm) = \mp(i - |pq| + |p| + |q|),\ \text{and}\ \mathrm{tor}(L^i_\pm) = 0,$$

$$\mathrm{tb}(L_e) = |pq| - |p| - |q|,\ \mathrm{rot}(L_e) = 0,\ \text{and}\ \mathrm{tor}(L_e) = 0,$$

such that

$$S_\pm(L^i_\pm) = L^{i-1}_\pm \text{ and } S_\pm(L_e) = L^{|pq|-|p|-|q|-1}_\pm$$

and

$$S_\mp(L^i_\pm) \text{ is loose.}$$

Notice that all these Legendrian knots are determined by the Thurston-Bennequin invariants and the rotation numbers, except when $\mathrm{tb} = |pq| - |p| - |q|$, there are 3 distinct Legendrian knots all with the rotation number 0.

Step 3. Compute the non-loose Legendrian knots with "generic" mountain ranges. All other mountain ranges are as shown in Figure 3 and described as follows. Consider any 2-inconsistent pair of paths (P_1, P_2) representing q/p that is not compatible with the ones discussed in Step 2, it may be compatible with other decorated pairs of paths as discussed in Section 2.3. Let $\{(P^i_1, P^i_2)\}_{i=2}^n$ be the collection of all pairs of paths compatible with (P_1, P_2) where (P^i_1, P^i_2) is i-inconsistent and $(P^2_1, P^2_2) = (P_1, P_2)$.

Recall the truncated path $P_2^\intercal = P_2 \cap \left[q/p, \lceil q/p \rceil\right]$. Let s_k be the slope in the k^{th} continued fraction block of $P_1 \cup P_2^\intercal$ that is farthest from q/p. Set $n_k = |s_k \bullet \frac{q}{p}|$ for $k = 2, \ldots, n$.

In the contact structure ξ_{P_1,P_2} there are non-loose Legendrian knots L^i_+ and L^i_- for $i \in \mathbb{Z}$ with invariants

$$\mathrm{tb}(L^i_\pm) = i,\ \text{and}\ \mathrm{rot}(L^i_\pm) = \begin{cases} \mp(i - pq + |R(P_1, P_2)|) & pq > 0, \\ \mp(i - pq - |R(P_1, P_2)|) & pq < 0, \end{cases}$$

where $R(P_1, P_2)$ is defined in Section 2.5, such that

$$S_\pm(L^i_\pm) = L^{i-1}_\pm \text{ and } S_\mp(L^i_\pm) \text{ is loose.}$$

Moreover, if $n \geq 3$, there are Legendrian knots $L^{pq}_{k,\pm}$ with $k = 2, \dots, n-1$ such that

$$\mathrm{tb}(L^{pq}_{k,\pm}) = pq, \text{ and } \mathrm{tor}(L^{pq}_{k,\pm}) = 0$$

and

$$\mathrm{rot}(L^{pq}_{k,\pm}) = \begin{cases} \mp(|R(P_1,P_2)| - 2(n_k - 1)) & pq > 0, \\ \mp(-|R(P_1,P_2)| - 2(n_k - 1)) & pq < 0. \end{cases}$$

and $S^i_\pm S^j_\mp(L^{pq}_{k,\pm})$ is non-loose if and only if $j \leq n_k - 1$. Lastly, if stabilizations of the $L^{pq}_{k,\pm}$ and $L^{pq}_{l,\pm}$ have the same invariants, then they are equivalent, while non-loose stabilizations of $L^{pq}_{k,\pm}$ and $L^{pq}_{l,\mp}$ are never equivalent. Notice that when $pq < 0$ then non-loose stabilizations of $L^{pq}_{k,\pm}$ and $L^{pq}_{l,\mp}$ will never share the same invariants but when $pq > 0$ they will. See Figure 3.

One subtlety arises when $pq > 0$ and all blocks in P_1 have the same sign and all blocks P_2 have the opposite sign. In this case, we will see in Lemma 7.1 that ξ_{P_1,P_2} is simply $\xi_{-pq+p+q}$ which is obtained from ξ_{std} by a half Lutz twist on the unique maximal self-linking number transverse representative of the (p, q)–torus knot. In this case, the knots $L^i_\pm$ will have $\mathrm{tor}(L^i_\pm) = 1/2$ when $i \leq pq - p - q$ and otherwise have $\mathrm{tor}(L^i_\pm) = 0$.

3.2. **The classification of non-loose torus knots with convex Giroux torsion.** We now consider non-loose Legendrian knots with tor $= n$ for $n \in \mathbb{N} \cup \{0\}$. For any pair of paths (P_1, P_2) representing q/p that is totally 2-inconsistent, the classification of non-loose Legendrian knots in ξ_{P_1,P_2} is as follows.

First, assume that when $pq > 0$ and (P_1, P_2) is not the pair of paths such that P_1 has only one sign while P_2 has only the other sign. There are non-loose Legendrian knots $L^{i,n}_\pm$ in ξ_{P_1,P_2} for $i \in \mathbb{Z}$ with invariants

$$\mathrm{tb}(L^{i,n}_\pm) = i \text{ and } \mathrm{tor}(L^{i,n}_\pm) = n,$$

and

$$\mathrm{rot}(L^{i,n}_\pm) = \begin{cases} \mp(i - pq + |R(P_1,P_2)|) & pq > 0, \\ \mp(i - pq - |R(P_1,P_2)|) & pq < 0, \end{cases}$$

where $R(P_1, P_2)$ is defined in Section 2.5. We also have

$$S_\pm(L^{i,n}_\pm) = L^{i-1,n}_\pm \text{ and } S_\mp(L^{i,n}_\pm) \text{ is loose.}$$

Moreover, $L^{i,0}_\pm$ corresponds to $L^i_\pm$ in the previous section. Notice that the mountain range for non-loose Legendrian knots in ξ_{P_1,P_2} does not contain any extra "wings" as seen for some contact structures on the previous section.

We now turn to non-loose Legendrian knots with tor $= n + 1/2$ for $n \in \mathbb{N} \cup \{0\}$. Let (P_1, P_2) be a pair of paths representing q/p that is totally 2-inconsistent and let L^i_- be the family of Legendrian knots in ξ_{P_1,P_2} described in the previous section. Let T the transverse push-off of L^i_- (notice L^i_- has the same transverse push-off for any $i \in \mathbb{Z}$). Finally set ξ'_{P_1,P_2} to be the result of a half Lutz twist applied to T in ξ_{P_1,P_2}.

In [10], Ding, Geiges and Stipsicz showed that if we perform the half Lutz twist on a transverse knot T in (S^3, ξ) and obtain a new contact structure (S^3, ξ'), then the relative d_3-invariant is

$$d_3(\xi', \xi) = d_3(\xi) - d_3(\xi') = \mathrm{sl}(T).$$

In [10], this was only verified when ξ was the standard tight contact structure on S^3, but it is true in general, see [23, Proof of Theorem 4.3.1]. Thus we see that

$$d_3(\xi'_{P_1,P_2}) = \begin{cases} d_3(\xi_{P_1,P_2}) + |R(P_1,P_2)| - pq & pq > 0, \\ d_3(\xi_{P_1,P_2}) - |R(P_1,P_2)| - pq & pq < 0. \end{cases}$$

There are non-loose Legendrian knots $L_{\pm}^{i,n+\frac{1}{2}}$ in ξ'_{P_1,P_2} for $i \in \mathbb{Z}$ with invariants

$$\mathrm{tb}(L_{\pm}^{i,n+\frac{1}{2}}) = i, \text{ and } \mathrm{tor}(L_{\pm}^{i,n+\frac{1}{2}}) = n + \frac{1}{2}$$

and

$$\mathrm{rot}(L_{\pm}^{i,n+\frac{1}{2}}) = \begin{cases} \mp(i + pq - |R(P_1,P_2)|) & pq > 0, \\ \mp(i + pq + |R(P_1,P_2)|) & pq < 0. \end{cases}$$

We also have

$$S_{\pm}^{j}(L_{\pm}^{i,n+\frac{1}{2}}) = L_{\pm}^{i-j,n+\frac{1}{2}} \text{ and } S_{\mp}(L_{\pm}^{i,n+\frac{1}{2}}) \text{ is loose.}$$

Notice that the mountain range for non-loose Legendrian knots in ξ_{P_1,P_2} does not contain any extra "wings" as seen for some contact structures on the previous section.

Now suppose that $pq > 0$, P_1 has all one sign and P_2 has only the other sign, as noted above, ξ_{P_1,P_2} is $\xi_{-pq+p+q}$. In this case the classification of contact structures on $\xi_{-pq+p+q}$ is as stated above except

$$\mathrm{tor}(L_{\pm}^{i,n}) = \begin{cases} n & i > pq - p - q, \\ n + 1/2 & i \leq pq - p - q. \end{cases}$$

Similarly, in $\xi_0 = \xi'_{P_1,P_2}$ the classification is as stated above except

$$\mathrm{tor}(L_{\pm}^{i,n+\frac{1}{2}}) = \begin{cases} n + 1/2 & i > pq - p - q, \\ n + 1 & i \leq pq - p - q. \end{cases}$$

When $pq < 0$ the classification in all cases is as in the case for $pq > 0$ and (P_1, P_2) is not the pair of paths such that P_1 has only one sign while P_2 has only the other sign.

4. Classification of non-loose $(2, \pm(2n+1))$–torus knots

In this section, we apply the algorithm in Section 3 to classify non-loose $(2, \pm(2n+1))$–torus knots and prove Theorem 1.11, Theorem 1.12, Theorem 1.13, and Theorem 1.14. We note that the classification of the $(2, 2n+1)$-torus knots is quite straight forwards and many steps in the algorithm described above are not necessary. To see the algorithm carried out in its full generality, please see Sections 4.2, 5.1, and 5.2

4.1. **Non-loose $(2, 2n+1)$–torus knots.** We begin by classifying non-loose Legendrian $(2, 2n+1)$–torus knots.

Proof of Theorem 1.11. First, we apply Step 1 of the algorithm. The pair of path representing $(2n+1)/2$ is

$$P_1 = \left\{\frac{2n+1}{2}, n\right\}, \text{ and } P_2 = \left\{\frac{2n+1}{2}, n+1, \infty\right\},$$

and the continued fraction blocks in P_1 and P_2 are

$$A_1 = \left\{\frac{2n+1}{2}, n\right\}, \text{ and } B_2 = \left\{\frac{2n+1}{2}, n+1, \infty\right\}.$$

Now we can list all non-loose decorations of $(\overline{P_1}, P_2)$ as follows:

$$\pm(+,+,+),\ \pm(-,+,-),\ \pm(-,+,+)$$

(Since P_2 is a continued fraction block, $\pm(-,-,+)$ and $\pm(-,+,-)$ are the same). As stated in the algorithm, we know that when all the signs are the same, the contact structure will be ξ_1. We also know that the sign choices $\pm(-)$ on P_1 and $\pm(+,-)$ on P_2 will also give ξ_1 since they are compatible with $\pm(+,+,+)$, see the last two paragraphs of Section 2.3. Thus we only need to compute d_3-invariant of $\pm(-,+,+)$, which is $-pq+p+q = 1-2n$ by Lemma 7.1.

Now applying Step 2 of the algorithm, we have the Legendrian knots in ξ_1 as follows:

$$L^i_\pm \text{ for } i > 2n+1,$$
$$L^{2n+1},$$
$$L^i_{2,\pm} \text{ for } 2n+4 \le i \le 4n+2,$$
$$L^{2n+3}_2$$

with

$$\mathrm{tb}(L^i_\pm) = i, \text{ and } \mathrm{rot}(L^i_\pm) = \mp(i-2n-1),$$
$$\mathrm{tb}(L^{2n+1}) = 2n+1, \text{ and } \mathrm{rot}(L^{pq-p-q+2}) = 0,$$
$$\mathrm{tb}(L^i_{2,\pm}) = i, \text{ and } \mathrm{rot}(L^i_{2,\pm}) = \mp(i-2n-3),$$
$$\mathrm{tb}(L^{2n+3}_2) = 2n+3, \text{ and } \mathrm{rot}(L^{2n+3}_2) = 0$$

such that

$$S_\pm(L^i_\pm) = L^{i-1}_\pm, \text{ for } i \ge 2n+3, \text{ and } S_\pm(L^{2n+2}_\pm) = L^{2n+1},$$
$$S_\pm(L^i_{2,\pm}) = L^{i-1}_{2,\pm}, \text{ for } i \ge 2n+5, \text{ and } S_\pm(L^{2n+4}_{2,\pm}) = L^{2n+3}_2,$$
$$S_\mp(L^i_{2,\pm}) = L^{i-1}_\pm, \text{ for } i \ge 2n+4, S_\mp(L^{2n+3}_2) = L^{2n+2}_\pm,$$

and $S_\mp(L^i_\pm)$ and $S_\pm(L^{2n+1})$ are loose. All these Legendrian knots have tor $= 0$. See Figure 5.

Applying Step 3 of the algorithm, we obtain the classification of non-loose Legendrian knots in ξ_{1-2n} as follows. Note that the decoration $\pm(-,+,+)$ are totally 2-inconsistent, so we do not have to consider the "wings". We must first compute $R(P_1, P_2)$. One many easily check that $r_m = 1$ and $r_n = 2n$ and hence

$$R(P_1, P_2) = (2n+1)\cdot 1 + 2\cdot(2n) = 6n+1.$$

Step 3 of the algorithm now gives non-loose Legendrian knots $L_{\pm}^{i,k}$ for $i \in \mathbb{Z}$ and $k \in \mathbb{N} \cup \{0\}$ such that

$$\mathrm{tb}(L_{\pm}^{i,k}) = i, \text{ and } \mathrm{rot}(L_{\pm}^{i,k}) = \mp(i + 2n - 1)$$

and

$$\mathrm{tor}(L_{\pm}^{i,k}) = \begin{cases} k & i > 2n-1, \\ k + \frac{1}{2} & i \leq 2n-1. \end{cases}$$

We also have

$$S_{\pm}(L_{\pm}^{i,k}) = L_{\pm}^{i-1,k}$$

and $S_{\mp}(L_{\pm}^{i,k})$ is loose. See Figure 5.

Finally we consider the non-loose Legendrian knots coming from adding convex half Giroux torsion to the complements of $L_{-}^{i,0}$. This will give the contact structure obtained from ξ_{1-2n} by a half Lutz twist on the transverse push-off of $L_{-}^{i,0}$, which is ξ_0. So in ξ_0, we have non-loose Legendrian knots $L_{\pm}^{i,k+\frac{1}{2}}$ for $i \in \mathbb{Z}$ and $k \in \mathbb{N} \cup \{0\}$ such that

$$\mathrm{tb}(L_{\pm}^{i,k+\frac{1}{2}}) = i \text{ and } \mathrm{rot}(L_{\pm}^{i,k+\frac{1}{2}}) = \mp(i - 2n + 1)$$

and

$$\mathrm{tor}(L_{\pm}^{i,k+\frac{1}{2}}) = \begin{cases} k + \frac{1}{2} & i > 2n-1, \\ k + 1 & i \leq 2n-1. \end{cases}$$

We also have

$$S_{\pm}(L_{\pm}^{i,k+\frac{1}{2}}) = L_{\pm}^{i-1,k+\frac{1}{2}}$$

and $S_{\mp}(L_{\pm}^{i,k+\frac{1}{2}})$ is loose. See Figure 5. □

We now turn to the classification of non-loose transverse $(2, 2n+1)$–torus knots.

Proof of Theorem 1.13. Since the classification of transverse knots is equivalent to the classification of Legendrian knots up to negative stabilization [16, Proof of Theorem 2.10], the theorem follows immediately from Theorem 1.11. In particular, then T^k and the $T^{k+\frac{1}{2}}$ are transverse push-offs of $L_{-}^{0,k}$ and $L_{-}^{0,k+\frac{1}{2}}$, respectively. □

4.2. **Non-loose $(2, -(2n+1))$–torus knots.** We begin with the classification of non-loose Legendrian $(2, -(2n+1))$–torus knots.

Proof of Theorem 1.12. According to Step 1 of the algorithm in the previous section, we first find all decorated pair paths (P_1, P_2) representing $-(2n+1)/2$. We have

$$P_1 = \{-\frac{2n+1}{2}, -n-1\}, \text{ and } P_2 = \{-\frac{2n+1}{2}, -n, -n+1, \ldots, -1\}.$$

Moreover, the breakdown into continued fraction blocks is

$$A_2 = \{-\frac{2n+1}{2}, -n-1\}, \text{ and } B_1 = \{-\frac{2n+1}{2}, -n\},\ B_3 = \{-n, \ldots -1\}.$$

Now we will list all non-loose decorations for $(\overline{P_1}, P_2)$. Since $(\pm, \pm, \dots)$ describes ξ_{std} by Remark 2.15, we have $2n$ non-loose decorations

$$\pm(-, +, \overbrace{+, \dots, +}^{k}, \overbrace{-, \dots, -}^{n-1-k})$$

for $0 \le k \le n-1$. See the top drawing of Figure 17 (notice that we can shuffle the signs in B_3). We now convert these pairs of decorated paths into contact surgery diagrams as discussed in Section 2.4. To this end notice that

$$-\frac{p}{p'} = -2 = [-2], \text{ and } -\frac{q}{q-q'} = -\frac{2n+1}{n+1} = [-2, -n-1].$$

We thus obtain the diagrams in Figure 17.

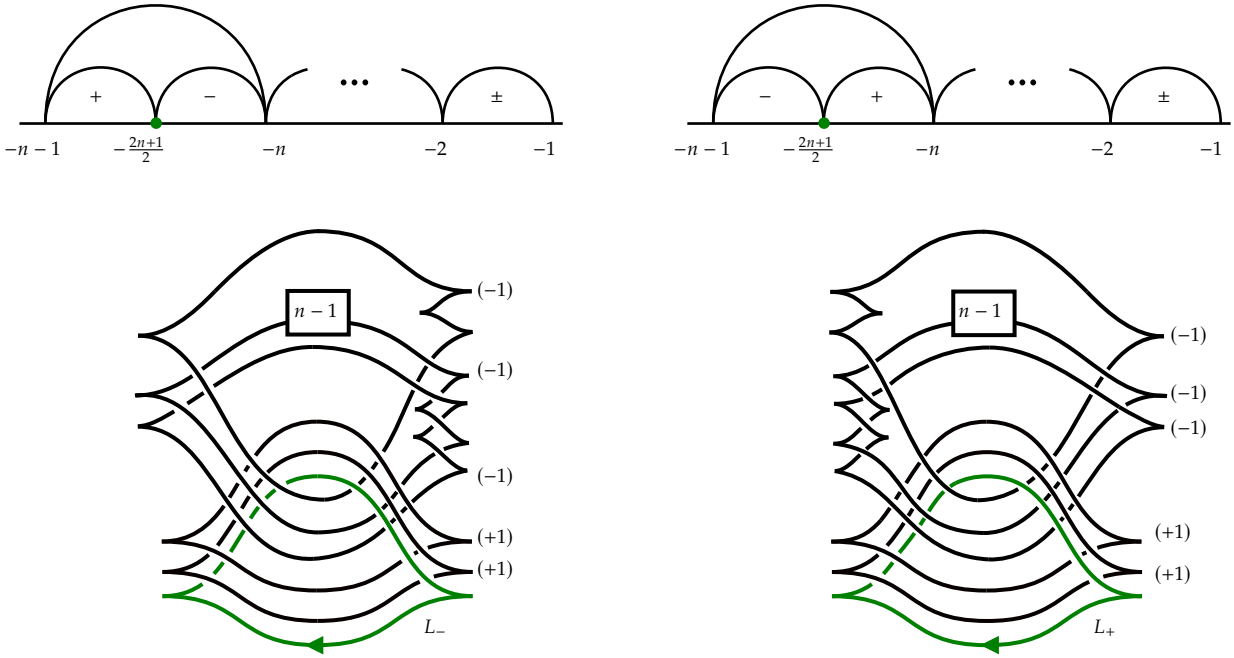

FIGURE 17. Surgery diagrams for the non-loose $(2, -(2n+1))$ torus knots with $\mathrm{tb} = -4n-2$. In the upper box there are $n-1$ stabilizations. The signs of the stabilizations depend on the signs in the continued fraction block A_2.

We now use the formula (3) in Section 2.5 to compute d_3-invariants. In particular, we have the linking matrix M for the diagram

$$M = \begin{bmatrix} -3 & -1 & -1 & -1 & -1 \\ -1 & -n-2 & -2 & -1 & -1 \\ -1 & -2 & -3 & -1 & -1 \\ -1 & -1 & -1 & 0 & -1 \\ -1 & -1 & -1 & -1 & 0 \end{bmatrix},$$

from which we can compute that $\sigma(X) = -1$ and $\chi(X) = 6$. There exist $2n$ rotation vectors:

$$\pm\mathbf{rot} = \begin{bmatrix} -1 \\ -(l+1) \\ -1 \\ 0 \\ 0 \end{bmatrix},$$

for $l \in \{-n+1, -n+3, ..., n-3, n-1\}$. From these, we can compute

$$d_3(\xi) = n + l + 1.$$

One may also use the surgery diagram to compute

$$|R(P_1, P_2)| = 4n + 2l + 3.$$

In Section 2.5 we also gave a formula for $R(P_1, P_2)$ in terms of the decorated pair of paths, since relating this computation to the one done in terms of the surgery diagram is a little involved, we give details. First, notice that

$$p_1 = -\frac{2n+1}{2},\ p_2 = -n-1,$$
$$q_1 = -\frac{2n+1}{2},$$
$$q_i = -n + i - 2 \ \text{ for } \ 2 \le i \le n+1.$$

In P_1, the signs of blocks are all negative. In P_2, there exist $k+1$ positive blocks, which are exactly $[q_1, q_2], \ldots, [q_{k+1}, q_{k+2}]$. Thus we can calculate r_m and r_n as follows:

$$r_m = (-1)\left((p_2 \ominus p_1) \bullet \frac{1}{0}\right) = -1,$$
$$r_n = (q_{k+2} \ominus q_1) \bullet \frac{0}{1} + (-1)\left((q_{n+1} \ominus q_{k+2}) \bullet \frac{0}{1}\right) = 2k + 2.$$

We could now easily compute $R(P_1, P_2)$ in terms of k, but we would like to make the computation in terms of the rotation numbers in the surgery diagram. The rotation number of the second link component of the surgery diagram in Figure 17 is equal to the difference between the number of negative blocks and positive blocks (notice that P_2 corresponds to the solid torus with the upper meridian). Thus we have

$$\begin{aligned} -(l+1) &= (n-k-1) - (k+1) \\ &= n - 2k - 2, \end{aligned}$$

and this implies that

$$k = (n + l - 1)/2.$$

Finally, we have

$$\begin{aligned} R(P_1, P_2) &= 2r_n + (-2n-1)r_m \\ &= 4n + 2l + 3. \end{aligned}$$

Now we will apply Step 2 of the algorithm and consider the exceptional contact structure corresponding to the decoration $(\pm, \mp, \ldots, \mp)$ such that P_1 having all one sign and P_2

having the other. This is the contact structure ξ_{2n} (since P_1 and P_2 are totally 2-inconsistent we also obtain non-loose knots with convex Giroux torsion and we list them now). According to the algorithm in Section 3, in this contact structure, we have the following non-loose Legendrian knots $L^{i,k}_{n-1,\pm}$ for $i \in \mathbb{Z}, k \in \mathbb{N} \cup \{0\}$ and L_e such that

$$\mathrm{tb}(L^{i,k}_{n-1,\pm}) = i,\ \mathrm{rot}(L^{i,k}_{n-1,\pm}) = \mp(i-2n+1) \text{ and } \mathrm{tor}(L^{i,k}_{n-1,\pm}) = k$$
$$\mathrm{tb}(L_e) = 2n-1,\ \mathrm{rot}(L_e) = 0 \text{ and } \mathrm{tor}(L_e) = 0.$$

We also have

$$L^{i,k}_{n-1,\pm} = S_{\pm}(L^{i-1,k}_{n-1,\pm}) \text{ and } S_{\pm}(L_e) = L^{2n-2,0}_{n-1,\pm}$$

and

$$S_{\mp}(L^{i,k}_{n-1,\pm}) \text{ is loose.}$$

See Figure 6.

Now we apply Step 3 of the algorithm and consider the other decorations. Since all these decorated paths are totally 2-inconsistent, they will also contribute to non-loose Legendrian knots with tor > 0.

Now in ξ_{n+l+1}, except for $l \neq n-1$ which was handled above, we have non-loose Legendrian knots $L^{i,k}_{l,\pm}$ with

$$\mathrm{tb}(L^{i,k}_{l,\pm}) = i,\ \mathrm{rot}(L^{i,k}_{l,\pm}) = \mp(i-2l-1) \text{ and } \mathrm{tor}(L^{i,k}_{l,\pm}) = k$$

and

$$S_{\pm}(L^{i,k}_{l,\pm}) = L^{i-1,k}_{l,\pm} \text{ and } S_{\mp}(L^{i,k}_{l,\pm}) \text{ is loose.}$$

See Figure 6.

In addition, when attaching convex half Giroux torsion to the complements of standard neighborhoods of the Legendrian knots above, we get non-loose Legendrian knots in the contact structures on ξ_{n-l} for $l \in \{-n+1, -n+3, \dots, n-3, n-1\}$. In ξ_{n-l}, we have the non-loose Legendrian knots $L^{i,k+\frac{1}{2}}_{l,\pm}$ for $i \in \mathbb{Z}, k \in \mathbb{N} \cup \{0\}$ with

$$\mathrm{tb}(L^{i,k+\frac{1}{2}}_{l,\pm}) = i,\ \mathrm{rot}(L^{i,k+\frac{1}{2}}_{l,\pm}) = \mp(i+2l+1) \text{ and } \mathrm{tor}(L^{i,k+\frac{1}{2}}_{l,\pm}) = k+\frac{1}{2}$$

and

$$S_{\pm}(L^{i,k+\frac{1}{2}}_{l,\pm}) = L^{i-1,k+\frac{1}{2}}_{l,\pm} \text{ and } S_{\mp}(L^{i,k+\frac{1}{2}}_{l,\pm}) \text{ is loose.}$$

See Figure 6. □

The classification of transverse $(2, -(2n+1))$–tours knots now follows.

Proof of Theorem 1.14. Since the classification of transverse knots is equivalent to the classification of Legendrian knots up to negative stabilization [16, Proof of Theorem 2.10], the theorem follows immediately from Theorem 1.12. In particular, T^k_l is the transverse push-off of $L^{0,k}_{l,-}$ in ξ_{n+l+1} and $T^{k+\frac{1}{2}}_l$ are transverse push-offs of $L^{0,k+\frac{1}{2}}_{l,-}$ in ξ_{n-l}. □

5. Classification of non-loose $(5, \pm 8)$–torus knots

In this section, we apply the algorithm in Section 3 and classify non-loose $(5, \pm 8)$–torus knots and prove Theorem 1.15, Theorem 1.16, Theorem 1.17 and Theorem 1.18. This will demonstrate the use of our algorithm in a more complicated setting than considered in the previous section.

5.1. **Non-loose $(5, 8)$–torus knots.** In this section we will classify non-loose Legendrian and transverse $(5, 8)$–torus knots. We begin with the Legendrian representatives.

Proof of Theorem 1.15. The pair of paths representing $8/5$ are

$$P_1 = \left\{\frac{8}{5}, \frac{3}{2}, 1\right\}, \text{ and } P_2 = \left\{\frac{8}{5}, \frac{5}{3}, 2, \infty\right\},$$

and the continued fraction blocks in P_1 and P_2 are

$$A_1 = \left\{\frac{8}{5}, \frac{3}{2}\right\}, A_3 = \left\{\frac{3}{2}, 1\right\}, \text{ and } B_2 = \left\{\frac{8}{5}, \frac{5}{3}, 2\right\}, B_4 = \{2, \infty\}.$$

Since we have

$$-\frac{p}{p'} = -\frac{5}{3} = [-2, -3] \text{ and } -\frac{q}{q - q'} = -\frac{8}{3} = [-3, -3],$$

the linking matrix M of the surgery diagram is

$$M = \begin{bmatrix} -4 & -2 & -1 & -1 & -1 & -1 \\ -2 & -3 & -1 & -1 & -1 & -1 \\ -1 & -1 & -5 & -3 & -1 & -1 \\ -1 & -1 & -3 & -4 & -1 & -1 \\ -1 & -1 & -1 & -1 & 0 & -1 \\ -1 & -1 & -1 & -1 & -1 & 0 \end{bmatrix}$$

and from this we can compute $\sigma(X) = -4$ and $\chi(X) = 7$. The rotation vectors $\pm$**rot** gotten by different choices of stabilizations are

$$\begin{bmatrix} 0 \\ -1 \\ 1 \\ 0 \\ 0 \\ 0 \end{bmatrix}, \begin{bmatrix} 0 \\ 1 \\ -1 \\ -2 \\ 0 \\ 0 \end{bmatrix}, \begin{bmatrix} -2 \\ -1 \\ 1 \\ 2 \\ 0 \\ 0 \end{bmatrix}, \begin{bmatrix} 2 \\ 1 \\ -3 \\ -2 \\ 0 \\ 0 \end{bmatrix}, \begin{bmatrix} 0 \\ -1 \\ -1 \\ 0 \\ 0 \\ 0 \end{bmatrix}, \begin{bmatrix} 0 \\ 1 \\ -3 \\ -2 \\ 0 \\ 0 \end{bmatrix}, \begin{bmatrix} -2 \\ -1 \\ 1 \\ 0 \\ 0 \\ 0 \end{bmatrix}, \begin{bmatrix} -2 \\ -1 \\ -1 \\ 0 \\ 0 \\ 0 \end{bmatrix}, \begin{bmatrix} 0 \\ -1 \\ -1 \\ -2 \\ 0 \\ 0 \end{bmatrix}, \begin{bmatrix} 0 \\ -1 \\ -3 \\ -2 \\ 0 \\ 0 \end{bmatrix}, \begin{bmatrix} -2 \\ -1 \\ -1 \\ -2 \\ 0 \\ 0 \end{bmatrix}, \begin{bmatrix} -2 \\ -1 \\ -3 \\ -2 \\ 0 \\ 0 \end{bmatrix}.$$

We can compute the d_3-invariant of each decoration of $(\overline{P_1}, P_2)$. The first 4 rotation vectors give ξ_1 and correspond to the decorations on the path $(\overline{P_1}, P_2)$

$$\pm(+,-,+,-,-),\ \pm(-,+,+,+,-),\ \pm(-,-,-,-,+),\ \pm(+,+,+,+,+)$$

(note that $\pm(+,-,-,+,-)$ and $\pm(+,-,+,-,-)$ are the same). These decorations are, respectively, 2, 3, 4-inconsistent and the last is totally consistent. The next two rotation vectors give ξ_{-1} and correspond to the decorations

$$\pm(+,-,+,-,+) \text{ and } \pm(-,+,+,+,+)$$

(note that $\pm(+,-,+,-,+)$ and $\pm(+,-,-,+,+)$ are the same). The first being 2-inconsistent while the second is 3-inconsistent. The remaining 6 rotation vectors give distinct d_3-invariants and correspond to 2-inconsistent pairs of decorated paths. In particular, in the order of the rotation vectors above we have the decorations for ξ_{-3} are

$$\pm(-,-,+,-,-)$$

(note that $\pm(-,-,-,+,-)$ and $\pm(-,-,+,-,-)$ are the same). The decorations for ξ_{-7} are

$$\pm(-,-,+,-,+)$$

(note that $\pm(-,-,-,+,+)$ and $\pm(-,-,+,-,+)$ are the same). The decorations for ξ_{-9} are

$$\pm(+,-,+,+,-).$$

The decorations for ξ_{-15} are

$$\pm(+,-,+,+,+).$$

The decorations for ξ_{-19} are

$$\pm(-,-,+,+,-).$$

The decorations for ξ_{-27} are

$$\pm(-,-,+,+,+).$$

We begin with the exceptional contact structure ξ_1. According to Step 2 of the algorithm in Section 3, there are non-loose Legendrian knots $L^i_\pm$ for $i > 29$ and L^{29} such that

$$\mathrm{tb}(L^i_\pm) = i, \mathrm{rot}(L^i_\pm) = \mp(i-29), \mathrm{tb}(L^{29}) = 29, \mathrm{rot}(L^{29}) = 0$$

and

$$S_\pm(L^i_\pm) = L^{i-1}_\pm \text{ for } i > 30, \text{ and } S_\pm(L^{30}_\pm) = L^{29}$$

and

$$S_\mp(L^i_\pm) \text{ and } S_\pm(L^{29}) \text{ are loose.}$$

To determine the other non-loose Legendrian $(5,8)$–torus knots in ξ_1, we note that $s_2 = 2$, $s_3 = 1$, $s_4 = \infty$ and that $n_2 = 2$, $n_3 = 3$, $n_4 = 5$. Thus we have Legendrian knots $L^{40}_{k,\pm}$ for $k = 2,3,4$ with tb $= 40$ and

$$\mathrm{rot}(L^{40}_{2,\pm}) = \mp 9, \mathrm{rot}(L^{40}_{3,\pm}) = \mp 7, \text{ and } \mathrm{rot}(L^{40}_{4,\pm}) = \mp 3.$$

Stabilizations of these Legendrian knots and the $L^i_\pm$ and L^{29} with the same invariants will be equivalent and they will remain non-loose until they are stabilized outside the V defined by the $L^i_\pm$ and L^{29}. All these knots have no convex Giroux torsion.

Now we consider the contact structure ξ_{-1}. First, notice that $\pm(+,-,+,-,+)$ are 2 inconsistent and $\pm(-,+,+,+,+)$ are 3-inconsistent, and they are compatible. Moreover, one easily computes that for the first decorations that $|R(P_1,P_2)| = 19$ and for the second decorations that $|R(P_1,P_2)| = 21$. Thus Step 3 of the algorithm gives us non-loose Legendrian knots $L^i_\pm$ for $i \in \mathbb{Z}$ and $L^i_{2,\pm}$ for $i \le 40$ such that

$$\mathrm{tb}(L^i_\pm) = \mathrm{tb}(L^i_{2,\pm}) = i, \ \mathrm{rot}(L^i_\pm) = \mp(i-21), \ \mathrm{rot}(L^i_{2,\pm}) = \mp(i-19)$$

and

$$S_\pm(L^i_\pm) = L^{i-1}_\pm, \text{ and } S_\pm(L^i_{2,\pm}) = L^{i-1}_{2,\pm},$$

and

$$S_{\mp}(L^i_{2,\pm}) = L^{i-1}_{\pm}, \text{ and } S_{\mp}(L^i_{\pm}) \text{ is loose.}$$

None of L^i_+ or $L^i_{2,+}$ is equivalent to L^j_- or $L^j_{2,-}$ for any $i, j \in \mathbb{Z}$. All these Legendrian knots have no convex Giroux torsion.

In ξ_{-3} and ξ_{-7}, we have following classification. First, notice that $\pm(-,-,+,-,-)$ and $\pm(-,-,+,-,+)$ are 2-inconsistent, so in each contact structure the mountain range is an infinite X. Since they are not totally 2-inconsistent, there are no non-loose Legendrian knots with tor > 0 in these contact structures. One can also check that $|R(P_1, P_2)| = 27$ and $|R(P_1, P_2)| = 37$, respectively. Thus there are Legendrian knots $L^i_\pm$ with $\mathrm{tb}(L^i_\pm) = i$ and $\mathrm{tor}(L^i_\pm) = 0$ in each contact structure and

$$\mathrm{rot}(L^i_\pm) = \begin{cases} \mp(i-13) & \text{in } \xi_{-3} \\ \mp(i-3) & \text{in } \xi_{-7} \end{cases}$$

that satisfy

$$S_{\pm}(L^i_{\pm}) = L^{i-1}_{\pm} \text{ and } S_{\mp}(L^i_{\pm}) \text{ is loose.}$$

All the decorations in ξ_{-9}, ξ_{-15}, ξ_{-19} and ξ_{-27} are totally 2-inconsistent, so these contact structures can have non-loose Legendrian representatives with convex Giroux torsion. One may compute that $|R(P_1, P_2)|$ for these four pairs of paths is $41, 51, 57$, and 67, respectively. So in each contact structure we have $L^{i,k}_\pm$ where $\mathrm{tb}(L^{i,k}_\pm) = i$ and

$$\mathrm{rot}(L^{i,k}_\pm) = \begin{cases} \mp(i+1) & \text{in } \xi_{-9} \\ \mp(i+11) & \text{in } \xi_{-15} \\ \mp(i+17) & \text{in } \xi_{-19} \\ \mp(i+27) & \text{in } \xi_{-27} \end{cases}$$

that satisfies

$$S_{\pm}(L^{i,k}_{\pm}) = L^{i-1,k}_{\pm} \text{ and } S_{\mp}(L^{i,k}_{\pm}) \text{ is loose.}$$

Moreover, $\mathrm{tor}(L^{i,k}_\pm) = k$ if it is not in ξ_{-27}, in that case we have

$$\mathrm{tor}(L^{i,k}_\pm) = \begin{cases} k & i > 27, \\ k + \frac{1}{2} & i \leq 27. \end{cases}$$

Finally we can add convex half Giroux torsion to these latter four contact structures. This results in the contact structures ξ_{-8}, ξ_{-4}, ξ_{-2}, and ξ_0, and we have non-loose Legendrian $(5, 8)$–torus knots $L^{i,k+\frac{1}{2}}_\pm$ where $\mathrm{tb}(L^{i,k+\frac{1}{2}}_\pm) = i$ and

$$\mathrm{rot}(L^{i,k+\frac{1}{2}}_\pm) = \begin{cases} \mp(i-1) & \text{in } \xi_{-8} \\ \mp(i-11) & \text{in } \xi_{-4} \\ \mp(i-17) & \text{in } \xi_{-2} \\ \mp(i-27) & \text{in } \xi_0 \end{cases}$$

that satisfy

$$S_{\pm}(L^{i,k+\frac{1}{2}}_{\pm}) = L^{i-1,k+\frac{1}{2}}_{\pm} \text{ and } S_{\mp}(L^{i,k+\frac{1}{2}}_{\pm}) \text{ is loose.}$$

Moreover, $\mathrm{tor}(L_{\pm}^{i,k+\frac{1}{2}}) = k + 1/2$ if it is not in ξ_0, and in that case we have

$$\mathrm{tor}(L_{\pm}^{i,k+\frac{1}{2}}) = \begin{cases} k+\frac{1}{2} & i > 27, \\ k+1 & i \leq 27. \end{cases}$$

□

We now turn to the transverse $(5,8)$–torus knots.

Proof of Theorem 1.17. This theorem follows directly from Theorem 1.15 given that the classification of transverse knots is the same as the classification of Legendrian knots up to negative stabilization [16, Proof of Theorem 2.10]. □

5.2. **Non-loose $(5,-8)$–torus knots.** In this section we will classify non-loose Legendrian and transverse $(5,-8)$–torus knots. We begin with the Legendrian representatives.

Proof of Theorem 1.16. The pair of paths representing $-8/5$ is

$$P_1 = \left\{-\frac{8}{5}, -\frac{5}{3}, -2\right\}, \text{ and } P_2 = \left\{-\frac{8}{5}, -\frac{3}{2}, -1\right\}$$

and the continued fraction blocks in P_1 and P_2 are

$$A_2 = \left\{-\frac{8}{5}, -\frac{5}{3}, -2\right\}, \text{ and } B_1 = \left\{-\frac{8}{5}, -\frac{3}{2}\right\}, B_3 = \left\{-\frac{3}{2}, -1\right\}.$$

Since we have

$$-\frac{p}{p'} = -\frac{5}{2} = [-3,-2], \text{ and } -\frac{q}{q-q'} = -\frac{8}{5} = [-2,-3,-2].$$

the linking matrix M of the surgery diagram is

$$M = \begin{bmatrix} -4 & -3 & -1 & -1 & -1 & -1 & -1 \\ -3 & -4 & -1 & -1 & -1 & -1 & -1 \\ -1 & -1 & -4 & -3 & -2 & -1 & -1 \\ -1 & -1 & -3 & -4 & -2 & -1 & -1 \\ -1 & -1 & -2 & -2 & -3 & -1 & -1 \\ -1 & -1 & -1 & -1 & -1 & 0 & -1 \\ -1 & -1 & -1 & -1 & -1 & -1 & 0 \end{bmatrix}$$

and from this we can compute $\sigma(X) = -3$ and $\chi(X) = 8$. Here, we list all rotation vectors depending on the choice of stabilizations:

$$\pm\mathbf{rot} = \begin{bmatrix} 0 \\ 0 \\ 0 \\ 0 \\ -1 \\ 0 \\ 0 \end{bmatrix}, \begin{bmatrix} -2 \\ -2 \\ 0 \\ 0 \\ 1 \\ 0 \\ 0 \end{bmatrix}, \begin{bmatrix} 0 \\ 0 \\ -2 \\ -2 \\ -1 \\ 0 \\ 0 \end{bmatrix}, \begin{bmatrix} -2 \\ -2 \\ 0 \\ 0 \\ -1 \\ 0 \\ 0 \end{bmatrix}, \begin{bmatrix} -2 \\ -2 \\ -2 \\ -2 \\ -1 \\ 0 \\ 0 \end{bmatrix}.$$

We can compute the d_3-invariant of each decoration of $(\overline{P_1}, P_2)$. The first 2 rotation vectors above give ξ_2 and correspond to the decorations on the paths $(\overline{P_1}, P_2)$ given by

$$\pm(+,-.+,-) \text{ and } \pm(-,-,-,+)$$

(note that $\pm(-,+,+,-)$ and $\pm(+,-,+,-)$ are the same). The decorations are, respectively, 2 and 3-inconsistent. The remaining rotation vectors give distinct d_3-invariants and correspond to 2-inconsistent pairs of paths. The third rotation vector gives ξ_8 and corresponds to the decorations

$$\pm(+,-,+,+)$$

(note that $\pm(-,+,+,+)$ and $\pm(+,-,+,+)$ are the same). The fourth rotation vector gives ξ_{14} and corresponds to the decorations

$$\pm(-,-,+,-).$$

The last rotation vector gives ξ_{28} and corresponds to the decorations

$$\pm(-,-,+,+).$$

We begin with the exceptional contact structure corresponding to the path P_1 having all one sign and P_2 having the other. This is the contact structure ξ_{28}. In this contact structure, we have the following non-loose Legendrian knots $L_\pm^{i,k}$, $i \in \mathbb{Z}, k \in \mathbb{N} \cup \{0\}$ and L_e such that

$$\text{tb}(L_\pm^{i,k}) = i, \ \text{rot}(L_\pm^{i,k}) = \mp(i-27) \text{ and } \ \text{tor}(L_\pm^{i,k}) = k,$$

and

$$\text{tb}(L_e) = 27 \text{ and } \ \text{rot}(L_e) = 0,$$

such that

$$L_\pm^{i,k} = S_\pm(L_\pm^{i-1,k}), \ S_\pm(L_e) = L_\pm^{26,0} \text{ and } \ \text{tor}(L_\pm^{i-1,k}) = k.$$

We also have

$$S_\mp(L_\pm^{i,k}) \text{ is loose.}$$

Now we consider ξ_2. First, notice that the decorations $\pm(+,-.+,-)$ are 2-inconsistent and $\pm(-,-,-,+)$ are 3-inconsistent, and they are compatible. Also, $|R(P_1,P_2)| = 15$ and 17 for each decoration, respectively. In addition, the 2-inconsistent decorations are not totally 2-inconsistent, and so none of the non-loose knots in ξ_2 will have convex Giroux torsion. Thus the algorithm yields the following non-loose Legendrian knots $L_\pm^i$ for $i \in \mathbb{Z}$ and $L_{2,\pm}^i$ for $i \leq -40$ such that

$$\text{tb}(L_\pm^i) = \text{tb}(L_{2,\pm}^i) = i, \text{ and } \ \text{tor}(L_\pm^i) = \text{tor}(L_{2,\pm}^i) = 0,$$

and

$$\text{rot}(L_\pm^i) = \mp(i+25), \text{ and } \ \text{rot}(L_{2,\pm}^i) = \mp(i+23).$$

We also have

$$S_\pm(L_\pm^i) = L_\pm^{i-1}, \text{ and } S_\pm(L_{2,\pm}^i) = L_{2,\pm}^{i-1},$$

and

$$S_\mp(L_{2,\pm}^i) = L_\pm^{i-1}, \text{ and } S_\mp(L_\pm^i) \text{ is loose.}$$

Next, we consider ξ_8. Because the decorations for ξ_8 is not totally 2-inconsistent and $|R(P_1, P_2)| = 35$, we have non-loose Legendrian knots $L^i_\pm$ with

$$\mathrm{tb}(L^i_\pm) = i,\ \mathrm{rot}(L^i_\pm) = \mp(i+5) \text{ and } \mathrm{tor}(L^i_\pm) = 0$$

satisfying

$$S_\pm(L^i_\pm) = L^{i-1}_\pm \text{ and } S_\mp(L^i_\pm) \text{ is loose.}$$

The decorations for ξ_{14} are totally 2-inconsistent and $|R(P_1, P_2)| = 47$, so ξ_{14} contains the non-loose Legendrian knots $L^{i,k}_\pm$ for $i \in \mathbb{Z}$ and $k \in \mathbb{N} \cup \{0\}$ satisfying

$$\mathrm{tb}(L^{i,k}_\pm) = i,\ \mathrm{rot}(L^{i,k}_\pm) = \mp(i-7) \text{ and } \mathrm{tor}(L^{i,k}_\pm) = k$$

satisfying

$$S_\pm(L^{i,k}_\pm) = L^{i-1,k}_\pm \text{ and } S_\mp(L^{i,k}_\pm) \text{ is loose.}$$

Finally, to the totally 2-inconsistent pairs of paths (that are the ones for ξ_{28} and ξ_{14}), we can also add convex half Giroux torsion. As described in Section 3.2, this yields the contact structures ξ_1 and ξ_7. In each of these contact structures we have non-loose Legendrian knots $L^{i,k+\frac{1}{2}}_\pm$ satisfying

$$\mathrm{tb}(L^{i,k+\frac{1}{2}}_\pm) = i \text{ and } \mathrm{tor}(L^{i,k+\frac{1}{2}}_\pm) = k + \frac{1}{2}$$

and

$$\mathrm{rot}(L^{i,k+\frac{1}{2}}_\pm) = \begin{cases} \mp(i+27) & \text{in } \xi_1 \\ \mp(i+7) & \text{in } \xi_7 \end{cases}$$

satisfying

$$S_\pm(L^{i,k+\frac{1}{2}}_\pm) = L^{i-1,k+\frac{1}{2}}_\pm \text{ and } S_\mp(L^{i,k+\frac{1}{2}}_\pm) \text{ is loose.}$$

□

We end with the classification of non-loose transverse $(5,-8)$–torus knots.

Proof of Theorem 1.18. This theorem follows directly from Theorem 1.16 given that the classification of transverse knots is the same as the classification of Legendrian knots up to negative stabilization [16, Proof of Theorem 2.10]. □

6. Tight contact structures on torus knot complements

In this section, we investigate the tight contact structures on the complements of torus knots. These are Seifert fibered spaces of the disk with two singular fibers. The first classification results on such spaces were obtained in [7] and used in [25] to give their classification results for non-loose torus knots and expanded upon in [43]. So several of the classification results below were already know, but as observed in [25, Section 4.2] most non-loose torus knot complements are not covered by the results of [7]. We also note that in [27] tight contact structures on these spaces were also constructed.

6.1. **Torus knot complements.** We start by building a topological model of the complement of a torus knot by following [18, Section 3.1]. Let $F_1 \sqcup F_2$ be the Hopf link in S^3 and V_1 and V_2 neighborhoods of F_1 and F_2, respectively. Then there is a torus T in the complement of the Hopf link that separates S^3 such that $S^3 = V_1 \cup (T \times [0,1]) \cup V_2$. We may take the (p,q)–torus knot $T_{p,q}$ to sit on $T \times \{1/2\}$. Let N be a neighborhood of $T_{p,q}$ in $T \times [0,1]$ and $C = S^3 \setminus N$. If we set $A' = (T \times \{1/2\}) \cap C$, then we can consider $T \times [0,1]$ as the union of N and $N(A')$, a neighborhood of the annulus A' in C. See the left drawing of Figure 18. In $N(A')$, we can find an annulus A for which each of the boundary component is a (p,q)–curve, one on ∂V_1 and the other on ∂V_2. See the right drawing of Figure 18. Here we use the coordinate system on any torus parallel to T coming from the Seifert framing of V_1 (so the meridian of V_1 has slope ∞ and the meridian of V_2 has slope 0). We denote this coordinate system $\mathcal{F}_1$. Since we can also think $N(A')$ as a neighborhood of A, we have the following model for C,

$$C = V_1 \cup N(A) \cup V_2.$$

We notice that C is a Seifert fibered space over a disk with two singular fibers. The regular fiber is a (p,q)–torus knot in $S^3 = C \cup N$ and this will be called a *vertical curve*.

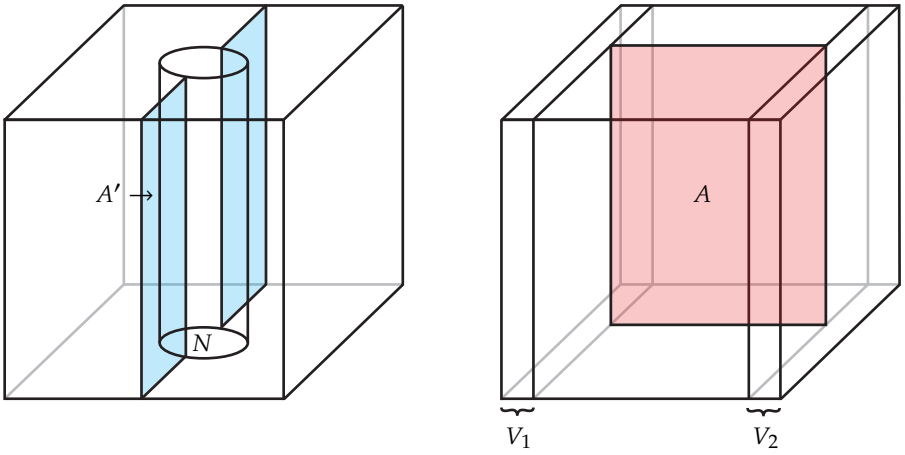

FIGURE 18. The complement of a neighborhood of a (p,q)–torus knot. Each cube is $T^2 \times [0,1]$ (so the top and bottom are identified as are the front and back) with curves on the right and left collapsed to give S^3. On the left we see that annulus A' in the C that separates C into two solid tori. On the right is the annulus A going from ∂V_1 to ∂V_2.

We will use two different framing conventions for the torus $-\partial C (= \partial N)$. One, which we denote $\mathcal{C}_1$, is the Seifert framing of $T_{p,q}$, and the other one, which we denote $\mathcal{C}_2$, comes from the torus T on which $T_{p,q}$ sits. We can convert from the first framing to the second framing by using the coordinate change map

$$\psi = \begin{pmatrix} 1 & 0 \\ -pq & 1 \end{pmatrix},$$

where $(a,b)^\intercal = a\lambda + b\mu$ and λ is a longitude from the given framing and μ is a meridian of N. There is another convenient topological model for C. Notice that if we take the neighborhood N of $T_{p,q}$ to be contained in the interior of $T^2\times[0,1]$, then $(T^2\times[0,1])\setminus N$ is $S^1\times P$ where P is D^2 with two disjoint open disks removed. Now $C = V_1\cup(S^1\times P)\cup V_2$. We have $\partial(S^1\times P) = T_1\cup T_2\cup T_3$ where T_i is identified with ∂V_i for $i=1,2$ and $T_3=\partial C$. For each T_i, we can take coordinates so that $S^1\times\{pt\}$ has slope 0 and $(\{\theta\}\times P)\cap T_i$ has slope ∞. Notice that on T_3 this framing agrees with the framing $\mathcal{C}_2$ that comes from the torus T. On the other T_i, this gives a coordinate system $\mathcal{F}_2$, and one can convert from the Seifert coordinates, $\mathcal{F}_1$, to this one by the map

$$\phi = \begin{pmatrix} q' & -p' \\ -q & p \end{pmatrix}$$

where $q'/p' = (q/p)^c$, the largest rational number satisfying $pq' - p'q = 1$. See Section 2.1 for this notation.

6.2. **Contact structures on C.** To classify non-loose torus knots, we will first classify tight contact structures on C having convex boundary with dividing slope $n\in\mathbb{N}$ (here we use the Seifert coordinates $\mathcal{C}_1$ on $-\partial C = \partial N$) and without convex Giroux torsion. See Section 2.2 for the definition of convex Giroux torsion. We note that as we are thinking of C as the complement of a knot we will orient its boundary as $-\partial C$, in particular the slopes of dividing curves of tori parallel to $-\partial C$ will change in a clockwise direction as they move into C. We will always assume that $|q|>p>0$. Also recall that we use the notation $\frac{a}{b}\bullet\frac{c}{d}$ to denote the quantity $ad-bc$ (which can be thought of as the intersection between a slope a/b curve and a slope c/d curve on T^2).

Given the complement C of a (p,q)–torus knot $T_{p,q}$ and a slope s on the boundary of C, we denote by

$$\begin{aligned}\mathrm{Tight}_i(C;s) =\{&\text{Tight contact structures on } C \text{ up to isotopy, with convex boundary having}\\ &\text{two dividing curves of slope } s \text{ and convex } i \text{ Giroux torsion for } i\in\tfrac{1}{2}\mathbb{N}\cup\{0\}\}.\end{aligned}$$

We begin with positive torus knots.

Lemma 6.1. *Consider the complement C of a positive (p,q)–torus knot. For any rational number s with $s>pq$ and any contact structure $\xi\in\mathrm{Tight}_0(C;s)$, there is a contact structure $\xi'\in\mathrm{Tight}_0(C;\infty)$ and a contact structure $\xi''\in\mathrm{Tight}^{min}(T^2\times[0,1];s,\infty)$ such that ξ is isotopic to $\xi'\cup\xi''$ under the natural identification $C\cong C\cup(T^2\times[0,1])$.*

Proof. If (C,ξ) contains 0-twisting vertical Legendrian curve, we can use this to find a convex torus T parallel to the boundary of C with dividing slope pq. Thus T cuts C into two pieces, one being $T^2\times[0,1]$ with dividing slopes s and pq. Inside of $T^2\times[0,1]$ there will be a convex torus T' with dividing slope ∞. This torus gives the claimed splitting of the contact structure ξ.

Thus we will consider the case when (C,ξ) does not contain 0-twisting vertical Legendrian curve. This implies that the dividing slope of V_1 is less than q/p and the dividing slope of V_2 is bigger than q/p or negative. Here, we are using $\mathcal{F}_1$, the Seifert coordinates of V_1.

Now we perturb ∂V_1 and ∂V_2 so that the ruling curves become (p,q)–curves, and perturb A so that it becomes convex and one boundary component is a ruling curve of ∂V_1 and the other a ruling curve of ∂V_2. We change the coordinate system of ∂V_1 from $\mathcal{F}_1$ to $\mathcal{F}_2$ using ϕ from the previous section. Suppose that the dividing slope of V_1 and V_2 are n_1/m_1 and n_2/m_2 respectively. Then ϕ maps $(m_i, n_i) \mapsto (q'm_i - p'n_i, -qm_i + pn_i)$ for $i = 1, 2$. If $|qm_1 - pn_1| \neq |qm_2 - pn_2|$, then the twisting numbers of the boundary components of A are different. Thus by the Imbalance Principle [34], there is a bypass on A along one of the boundary components, and we can thicken V_1 or V_2 using this bypass. Thus we can keep thickening the V_i until $|qm_1 - pn_1| = |qm_2 - pn_2|$.

Recall if the dividing slope of V_1 is s, then when a bypass is attached to ∂V_1 the dividing curves of the resulting torus will have slope s' which is clockwise of s and the closest point to q/p with an edge to s. Since we can start with V_1 as a standard neighborhood of a Legendrian knot with very negative Thurston-Bennequin invariant, the the possible dividing will be slopes on ∂V_1 will be

- $(1, n)$ for $n \leq \lfloor q/p \rfloor$,
- (m_1, n_1) in the shortest path from $\lfloor q/p \rfloor$ clockwise to q/p in the Farey graph.

Similarly, if ∂V_2 has dividing slope s, then when a bypass is attached to ∂V_2 the dividing curves will have slope s' which is anti-clockwise of s and the closest point to q/p with an edge to s. So if we start with V_2 being a standard neighborhood of a Legendrian knot with very negative tb, the the possible dividing will be slopes on ∂V_2 will be

- $(m, 1)$ for $m \leq 0$,
- (m_2, n_2) in the shortest path from q/p clockwise to ∞ in the Farey graph.

We denote $(q/p)^c$ by q'/p' and $(q/p)^a$ by q''/p'' and recall that there is an edge in the Farey graph between all three points (p,q), (p',q'), and (p'',q'') (See Section 2.1). There are three cases to consider when the dividing curves on A run from one boundary component to the other.

Case 1: $|\mathbf{q - pn}| = |\mathbf{p - qm}|$. We begin by assuming that $q - pn = p - qm$. In [18], the first author, LaFountain, and Tosun considered this case when $m, n \leq -1$ and $q - pn = p - qm$, and showed that the solutions are $m = pk - 1$ and $n = qk - 1$ for $k \leq 0$. They determined in these cases that the dividing curves on the boundary of $C' = V_1 \cup N(A) \cup V_2$ had slope $s_k = (pq - p - q)/(1 - k)$ (please note that the slope convention in [18] is the reciprocal of the one used here). Thus $C \setminus C'$ is a thickened torus $T^2 \times [0,1]$ with a contact structure that rotates from s clockwise to s_k. In particular, there will be a torus in $T^2 \times [0,1]$ with dividing slope ∞, and this torus provides the desired decomposition of C. Notice that when $k > 0$ then m is positive, the formula for s_k still holds and we can still find a torus of slope ∞ in $C \setminus C'$.

Now in the case that $q - pn = qm - p$, one can show that n and m will not satisfy the conditions in the bullet point above.

Case 2: $|\mathbf{qm_1 - pn_1}| = |\mathbf{p - qm}|$ or $|\mathbf{q - pn}| = |\mathbf{pn_2 - qm_2}|$. We will show that there is no solution to these equations. Consider the first equation and the case when $qm_1 - pn_1 = p - qm$. Let $a_0 = \lfloor q/p \rfloor, a_1, \ldots, a_k = q/p$ be a shortest path in the Farey graph from $\lfloor q/p \rfloor$, clockwise to q/p. As discussed in [3, Remark 2.13] we see that $|\frac{q}{p} \bullet a_i| < |\frac{q}{p} \bullet a_{i-1}|$, and hence the maximum value for $qm_1 - pn_1$ is $q - a_0 p$. If $m \leq -1$, we have $q - a_0 p \geq qm_1 - pn_1 =$

$p - qm \geq p + q$, but we are taking $p > 0$ and so there is no solution to this equation. We will deal with the case $m = 0$ in Case 3. Now consider the case that $pn_1 - qm_1 = p - qm$. One may check that the left-hand side is negative, while the right-hand side is positive when $m \leq -1$ and again the case of $m = 0$ will be handled in Case 3.

For the second equation in the case that $q - pn = pn_2 - qm_2$, we can similarly argue that the maximal value of $pn_2 - qm_2$ is p and so for $n < \lfloor q/p \rfloor$ we have $p \geq pn_2 - qm_2 = q - pn > p$; and this contradiction shows that there is no solution to the second equation. We will deal with the case of $n = \lfloor q/p \rfloor$ in Case 3. We may dispense with the case $q - pn = qm_2 - pn_2$ as above.

Case 3. $|\mathbf{qm_1 - pn_1}| = |\mathbf{pn_2 - qm_2}|$**.** We must have that $qm_1 - pn_1 = pn_2 - qm_2$, since both the right and left-hand sides are positive. We will show that the only solution is $(m_1, n_1) = (p'', q'')$ and $(m_2, n_2) = (p', q')$. Observe that if $qm_1 - pn_1 = pn_2 - qm_2$, then $(n_1 + n_2)/(m_1 + m_2) = q/p$. We know from our choice of (p', q') and (p'', q'') that $q = q' + q''$ and $p = p' + p''$, so $qp'' - pq'' = pq' - qp'$.

As above let $a_1 = \lfloor q/p \rfloor, a_1, \ldots, a_k = q/p$ be a shortest path in the Farey graph from $\lfloor q/p \rfloor$ clockwise to q/p and similarly $b_0 = q/p, \ldots b_l = \infty$ be the shortest path from q/p clockwise to ∞. Notice that $q''/p'' = a_{k-1}$ and $q'/p' = b_1$. The path $a_0, \ldots, a_{k-1}, a_k = b_0, b_1, \ldots, b_l$ can be shortened to a single jump from $\lfloor q/p \rfloor$ to ∞. In the process of shortening the path we first remove $q/p = a_k = b_0$ and the edges adjacent to it, and add the edge from a_{k-1} to b_1, we will then remove one of a_{k-1} or b_1, the edges adjacent to the removed vertex and add another edge in the Farey graph. Notice each vertex removed is the Farey sum of the two adjacent vertices. Thus the size of the numerator and denominator of the vertices a_i and b_j get smaller as we move out from q/p. Thus we see that if $(m_1, n_1) \neq (p'', q'')$ or $(m_2, n_2) \neq (p', q')$, then $m_1 < p''$ and $n_1 < q''$ or $m_2 < p'$ and $n_2 < q'$. Thus $m_1 + m_2 < p$ and $n_1 + n_2 < q$. But we observed above that $(n_1 + n_2)/(m_1 + m_2) = q/p$ which contradicts the fact that $\gcd(p, q) = 1$, so we must have that $(m_1, n_1) = (p'', q'')$ and $(m_2, n_2) = (p', q')$.

When the dividing slopes of V_1 and V_2 are q''/p'' and q'/p', there are two dividing curves on A, running from one boundary component to the other since we assume that there is no 0-twisting vertical Legendrian curve in C.

Since ϕ maps $(p', q') \mapsto (0, 1)$ and $(p'', q'') \mapsto (1, -1)$, we can compute the boundary slope of C under the coordinates C_2 after rounding the edges of $\partial V_1 \cup \partial N(A) \cup \partial V_2$ to be

$$\frac{1}{0 - 1 + 1} = \frac{1}{0}.$$

Now we use the coordinate change map ψ to compute the slope using Seifert coordinates C_1 of $T_{p,q}$. Since ψ^{-1} maps $(0, 1) \mapsto (0, 1)$, the slope of $\partial V_1 \cup \partial N(A) \cup \partial V_2$ is ∞ and we have our desired splitting of the contact structure on C. □

Now we will consider negative (p, q)–torus knot with $-q > p > 1$.

Lemma 6.2. *Consider the complement C of a negative (p, q)–torus knot. Consider the slopes $s_k = (|pq| - |p| - |q|)/k$ with $k \geq 1$ and $\gcd(|pq| - |p| - |q|, k) = 1$. For any $s > pq$ and $\xi \in \mathrm{Tight}_0(C; s)$ with $s \notin (s_k^a, s_k]$, there is a contact structure $\xi' \in \mathrm{Tight}_0(C; \infty)$ and a contact*

structure $\xi'' \in \text{Tight}^{min}(T^2 \times [0,1]; s, \infty)$ *such that* ξ *is isotopic to* $\xi' \cup \xi''$ *under the natural identification* $C \cong C \cup (T^2 \times [0,1])$.

If $s \in (s_k^a, s_k]$, *then either* ξ *is as above or there is a contact structure* $\xi_k' \in \text{Tight}_0(C; s_k)$ *and a contact structure* $\xi_k'' \in \text{Tight}^{min}(T^2 \times [0,1]; s, s_k)$ *such that* ξ *is isotopic to* $\xi_k' \cup \xi_k''$ *under the natural identification* $C \cong C \cup (T^2 \times [0,1])$. *Also, the contact structures* ξ_k' *have the property that any convex torus in* C *parallel to the boundary has dividing slope* s_k.

Remark 6.3. Notice that if s is an integer larger than pq then $s \notin (s_k^a, s_k]$ for any k unless $s = |pq| - |p| - |q|$. Thus all such integer values of $s \neq |pq| - |p| - |q|$ are in the first case of the lemma.

Proof. As in the positive case, if there is a 0-twisting vertical Legendrian in (C, ξ), then we have the desired splitting. So we assume there is no 0-twisting vertical Legendrian in (C, ξ). As in the proof of Lemma 6.1 we can take V_1 and V_2 to be neighborhoods of Legendrian knots with very negative Thurston-Bennequin invariant and then consider the annulus A in C between V_1 and V_2. We can make A convex and if the dividing curves on A do not all run from one boundary component to the other, we may attach a bypass to ∂V_1 or ∂V_2. As argued in Lemma 6.1, we know that the dividing slope of ∂V_1 is less than q/p and of the form

- $(1, n)$ for $n \leq \lfloor q/p \rfloor$,
- (m_1, n_1) where (m_1, n_1) is in the shortest path from $\lfloor q/p \rfloor$ clockwise to q/p in the Farey graph.

The dividing curves of ∂V_2 are greater than q/p but less than zero and of the form

- $(m, 1)$ for $m \leq -1$,
- (m_2, n_2) where (m_2, n_2) is in the shortest path from q/p clockwise to -1 in the Farey graph.

When the dividing curves on A all run from one boundary component to the other, we have three cases to consider.

Case 1. $|\mathbf{pn - q}| = |\mathbf{p - qm}|$**.** We must have that $pn - q = p - qm$, since both the right and left-hand sides are negative. The solutions are $m = -pk + 1$ and $n = qk + 1$ for $k \geq 1$. Now change the coordinates using ϕ and we have $(m, 1) \mapsto (-pq'k - p' + q', pqk + p - q)$ and $(1, n) \mapsto (-p'qk - p' + q', pqk + p - q)$. Now we round the edges of $C' = V_1 \cup N(A) \cup V_2$ and its dividing slope will be

$$\frac{pqk + p - q}{(-pq'k - p' + q') - (-p'qk - p' + q') + 1} = \frac{pqk + p - q}{-k + 1}$$

and there will be $2\gcd(pqk + p - q, k - 1)$ dividing curves. Now using ψ^{-1} we can express the slope under the Seifert coordinates C_1; $(-k + 1, pqk + p - q) \mapsto (-k + 1, pq + p - q)$. Relabel $k - 1$ as k, we have

$$\frac{-pq - p + q}{k} = \frac{|pq| - |p| - |q|}{k}$$

for $k \geq 0$. If $\gcd(|pq| - |p| - |q|, k) = 1$, we can identify $\xi|_{C'}$ with an element of $\text{Tight}_0(C; s_k)$. The argument in of [18, Lemma 3.3] shows that any convex torus in C' that is parallel to $\partial C'$ is contact isotopic to $\partial C'$ when $\gcd(|pq| - |p| - |q|, k) = 1$. Now $C \setminus C'$ is $T^2 \times [0,1]$ and

ξ on this thickened torus is an element of $\mathrm{Tight}^{min}(T^2\times[0,1];s,s_k)$. If $s\notin(s_k^a,s_k]$, then as shown in [18, Proposition 3.10], we may find bypasses for ∂V_1 or ∂V_2. We can continue to thicken these tori until we again have the annulus A having no bypasses. In which case we will be in Case 1, 2, or 3 again, but if in Case 1, the new dividing slope $s_{k'}$ on $\partial C'$ will be larger than s_k. We may continue as above, until either $s\in(s_k^a,s_k]$, and we have a splitting as in the theorem, or we are in Case 2 or 3.

If $\gcd(|pq|-|p|-|q|,k)>1$, $\partial C'$ will have more than two dividing curves. Then as indicated in [18, Remark 3.8] and since ∂C has less dividing curves, we can thicken V_1 and V_2 and as above come back to Case 1, 2, or 3 and eventually find the desired splitting.

We note that the contact structure on C obtained from taking a standard neighborhoods V_1 and V_2 of knots with Thurston-Bennequin invariants $-pk-1$ and $-qk-1$ by attaching an I invariant neighborhood $N(A)$ of A will be a tight contact structure ξ_k' such that any convex torus in C parallel to the boundary has dividing slope s_k. This follows an argument identical to that of the proof of [18, Lemma 3.3].

Case 2. $|\mathbf{q}-\mathbf{pn}|=|\mathbf{pn_2}-\mathbf{qm_2}|$ **or** $|\mathbf{qm_1}-\mathbf{pn_1}|=|\mathbf{p}-\mathbf{qm}|$**.** As in the proof of Lemma 6.1, we can see there are no solutions to these equations.

Case 3. $|\mathbf{qm_1}-\mathbf{pn_1}|=|-\mathbf{qm_2}+\mathbf{pn_2}|$**.** As in the proof of Lemma 6.1, we can see that the only solution is $(m_1,n_1)=(p'',q'')$ and $(m_2,n_2)=(p',q')$ and the boundary of $V_1\cup N(A)\cup V_2$ has 2 dividing curves with slope ∞ after edge rounding. □

We will need to know more about the exceptional contact structures $\xi_k'\in\mathrm{Tight}_0(C,s_k)$ from Lemma 6.2.

Lemma 6.4. *The contact structures $\xi_k'\in\mathrm{Tight}_0(C,s_k)$ from Lemma 6.2 are universally tight and remain so after gluing any amount of convex Giroux torsion on $T^2\times[0,1]$ to (C,ξ_k').*

Proof. To prove ξ_k' is universally tight, we recall the proof of [18, Lemma 3.3]. This lemma is about positive torus knots, but the same argument works for negative torus knots. First, C has a $|pq|$-fold cover $\widetilde{C}$ unwrapping the meridian $|pq|$-times which is diffeomorphic to $S^1\times\Sigma$ where Σ is a Seifert surface for the (p,q)–torus knot. Using the similar argument in [18, Lemma 3.3], one can show that the pullback contact structure $\widetilde{\xi}_k$ on $\widetilde{C}$ can be isotoped so that the S^1–fibers are all Legendrian with the twisting number $(pq(k+1)+p-q)$ (relative to the framing on the fibers coming from the product structure $S^1\times\Sigma$).

Now one can show that any Legendrian knot in $(\widetilde{C},\widetilde{\xi}_k)$ which is smoothly isotopic to a S^1–fiber of $S^1\times\Sigma$ must have the twisting number less than or equal to $(pq(k+1)+p-q)$. This of course implies that the contact structure on $\widetilde{C}$ is tight (recall if a contact structure is overtwisted, there is no upper bound on the twisting number of any smooth knot type). Any further finite cover of $\widetilde{C}$ will be diffeomorphic to $S^1\times\Sigma'$ for some surface Σ' and the S^1–fibers can all be made to be Legendrian with some fixed twisting number. Thus we see that they will also have to be tight. Since any finite cover of $(\widetilde{C},\widetilde{\xi}_k)$ is tight, we see that (C,ξ_k') must be universally tight.

We now show that (C,ξ_k') remains tight after one adds convex Giroux torsion. To this end, let (C_+,ξ) be the contact structure on the complement of the maximal Thurston-Bennequin invariant representative of Legendrian $(p,|q|)$–torus knot in (S^3,ξ_{std}). Then (C_+,ξ) is universally tight and it remains tight after convex Giroux torsion is added, see

[22]. Moreover, its $|pq|$-fold cover $\widetilde{C}_+ \cong S^1 \times \Sigma$ is also foliated by Legendrian curves with twisting $-(p + |q|)$. There is a further cover of $\widetilde{C}_+$ and $\widetilde{C}$ such that they are both $S^1 \times \Sigma$ and both foliated by Legendrian curves with the same twisting number. This implies that the contact structures on this common cover are isotopic (notice that one may cut $S^1 \times \Sigma$ open along some annuli to get a contact structure on a solid torus with a unique contact structure, see the proof of [18, Lemma 3.3]). Now if one adds a basic slice to (C, ξ'_k) and an appropriate contact structure on $T^2 \times [0,1]$ to (C_+, ξ), then when pulled back to the common cover, the contact structures will again be the same and hence (C, ξ'_k) with a basic slice attached will be universally tight. Since a basic slice is rotative, we can apply [38, Theorem 4.7]) and say that adding convex Giroux torsion to (C, ξ'_k) results in a universally tight contact structure. □

Lemma 6.5. *If L is a non-loose Legendrian (p, q)–torus knot in an overtwisted contact structure on S^3 with $\mathrm{tb}(L) < pq$ then L destabilizes.*

Proof. The contact structure on the complement $C = S^3 \setminus N(L)$ will be in $\mathrm{Tight}_i(C; \mathrm{tb}(L))$ for $i \geq 0$. If $i > 0$, we can clearly destabilize L. (Recall, from the point of view of the knot complement, a Legendrian knot destabilizes if you can find a convex torus parallel to the boundary of the knot complement with dividing slope one larger than the tb of the knot that separates off a basic slice from the complement.) If $i = 0$, a destabilization of L would correspond to finding $C' \subset C$, which is diffeomorphic to C such that $\partial C'$ is convex with dividing slope $\mathrm{tb}(L) + 1$. If there is a 0-twisting vertical Legendrian in C, we can clearly find such C'. Assume there is no 0-twisting vertical Legendrian in C. For negative torus knots, the argument in the proof of Lemmas 6.2 shows that all contact structures in $\mathrm{Tight}_0(C; \mathrm{tb}(L))$ contain (C', ξ') or (C', ξ'_k), and the dividing slope of $\partial C'$ is ∞ or $s_k > pq$. For positive torus knots, the same argument in the proof of Lemma 6.1 works and all contact structures in $\mathrm{Tight}_0(C; \mathrm{tb}(L))$ contains some C', whose boundary slope is ∞ or $s_k < pq$. It is known that all of these contact structures with boundary slope s_k exist in (S^3, ξ_{std}), see [18, Section 3.1], and hence are not of concern. □

Lemma 6.6. *Let $n(p, q)$ be the number of tight contact structures on $L(p, -q)\#L(q, -p)$ and C the complement of the (p, q)–torus knot. Then we have*

$$\left|\mathrm{Tight}_0(C; \infty)\right| = n(p, q).$$

Proof. Recall that our model for C from Section 6.1 is $V_1 \cup N(A) \cup V_2$, that is the union of two solid tori V_1 and V_2 and a neighborhood $N(A) = A \times [-1, 1]$ of an annulus. In the proofs of Lemmas 6.1 and 6.2, we saw that any contact structure $\xi \in \mathrm{Tight}_0(C, \infty)$ either

(1) contains a 0-twisting vertical Legendrian curve, or
(2) $pq > 0$ and there is a subset C' of C diffeomorphic to C such that $C \setminus C'$ is $T^2 \times [0,1]$, $\xi|_{C'}$ is in $\mathrm{Tight}_0(C, s_k)$ and $\xi|_{T^2 \times [0,1]}$ is in $\mathrm{Tight}^{min}(T^2 \times [0,1]; \infty, s_k)$ where $s_k = (pq - p - q)/k$ and $\gcd(k, pq - p - q) = 1$, and similarly for $pq < 0$, or
(3) $\xi|_{V_1} \in \mathrm{Tight}(V_1, (q/p)^a)$, $\xi|_{V_2} \in \mathrm{Tight}(V_2, (q/p)^c)$, and on $N(A)$ is an I-invariant neighborhood of a convex annulus A with two dividing curves.

Given $\xi \in \mathrm{Tight}_0(C; \infty)$, suppose that there exists a 0-twisting vertical Legendrian curve in C. Then there is a copy C' of C sitting inside C such that $C \setminus C' = T^2 \times [0,1]$, $\xi|_{C'} \in$

$\mathrm{Tight}_0(C;pq)$, and $\xi_{T^2\times[0,1]} \in \mathrm{Tight}^{min}(T^2\times[0,1];\infty,pq)$. If all convex tori in C' parallel to the boundary have dividing slope pq, then ξ is overtwisted by Remark 6.14 below. If $\xi|_{C'}$ contains tori parallel to the boundary with slopes different from pq, then by Lemmas 6.1 and 6.2, it contains C'' with $\partial C''$ having dividing slope ∞. Thus $C \setminus C''$ will be a convex Giroux torsion layer. That is ξ is not in $\mathrm{Tight}_0(C;\infty)$. So we know that (C,ξ) does not contain a 0-twisting vertical Legendrian curve.

Now suppose that ξ is of the form given in Item (2), we will show that it is also of the form given in Item (3) so that we will know that all $\xi \in \mathrm{Tight}_0(C;\infty)$ are of the form given in Item (3). To this end we recall that there is an annulus A' in C with boundary slope pq curves on ∂C, such that if we remove a neighborhood of A' from C we are left with V_1 and V_2, see Section 6.1. We can assume the ruling curves on ∂C are pq curves and $\partial A'$ consists of two ruling curves. Since the dividing slope of ∂C is ∞ we know that each component of $\partial A'$ intersects the dividing set twice. Note that when we make A' convex it must have two dividing curves that each run from one boundary component to the other, since if not we could Legendrian realize the core curve of A' giving a 0-twisting vertical Legendrian curve in C but we have already ruled this out above. Now consider cutting C along A' and rounding corners. The result will be the solid tori V_1 and V_2. Notice that the pq curve on ∂C with respect to the coordinate system $\mathcal{C}_1$ will become the q/p curve on V_1 and V_2 with respect to the coordinate system $\mathcal{F}_1$; moreover, we know the dividing curves will intersect the q/p curves at most two times. In fact, it must be two times, since if not we again could Legendrian realize a 0-twisting vertical Legendrian curve in C. Thus we know that the slope of the dividing curves has an edge in the Farey graph to the (p,q)-curve. We claim that we can assume that the slope on ∂V_1 is $(q/p)^a$ and on ∂V_2 is $(q/p)^c$. To see this suppose that the slope is r on ∂V_1, then inside of V_1 we can realize tori with dividing slopes larger than $-\infty$ and less than r. Thus there is a torus in V_1 parallel to the boundary with dividing slope $(q/p)^a$. Similarly we can take the dividing slope on ∂V_2 to be $(q/p)^c$. Now consider the convex annulus A used in the proof of Lemma 6.1 that connects ∂V_1 to ∂V_2. We know that the dividing curves on A must run from one boundary component to the other or else we could Legendrian realized the core curve of A giving a 0-twisting vertical Legendrian curve in C which we have ruled out above. Thus as in the proof of Case 3 in the proof of Lemma 6.1 we see that the boundary of $C' = V_1 \cup N(A) \cup V_2$ is convex with dividing slope ∞ and $C \setminus C'$ must be an I invariant contact structure on $T^2 \times I$.

So all the contact structures $\xi \in \mathrm{Tight}_0(C;\infty)$ are as described in Item (3). Thus the number of contact structures on $\mathrm{Tight}_0(C;\infty)$ is bounded above by the number of tight contact structures on $(V_1;(q/p)^a)$ times the number of tight contact structures on $(V_2;(q/p)^c)$. Recall that when discussing slopes on ∂V_1 or ∂V_2 we are using longitude-meridian coordinates coming from V_1 and as such V_1 has lower meridian $-\infty$ and V_2 has upper meridian 0 (see Section 2.2 for terminology). Thus as noted in Remark 2.8 we know

$$|\,\mathrm{Tight}(L_\infty^{q/p})| = |\,\mathrm{Tight}(S_\infty;(q/p)^a)| \text{ and } |\,\mathrm{Tight}(L^0_{q/p})| = |\,\mathrm{Tight}(S^0;(q/p)^c)|.$$

From Section 2.2 we also know that $L^0_{q/p} = L(q,-p)$ and $L_\infty^{q/p} = L(p,-q)$. Thus we see that

$$n(p,q) = |\,\mathrm{Tight}(S_\infty;(q/p)^a)| \cdot |\,\mathrm{Tight}(S^0;(q/p)^c)|$$

is an upper bound on the number of contact structures on $\mathrm{Tight}_0(C;\infty)$.

We now show that $n(p,q)$ is also a lower bound on the number of contact structures. To this end we first consider a topological Dehn filling. That is if we glue a solid torus S to C so that the meridian goes to a pq curve on ∂C then the result is $L(p,-q)\#L(q,-p)$. The reason for this is that one can use two meridian disks in S to cap off the boundary components of A' to get a 2-sphere that will divide the resulting manifold into two pieces. Once piece V_1' is V_1 with a 2–handle h_1 attached along the q/p curve and the other V_2' is V_2 with a 2–handle attached h_2 to V_2 along the q/p curve (notice S minus the two meridian disks can be thought of as two 2–handles, $h_1 \cup h_2$). Now if one glues a 3-ball to each of these pieces one gets the claimed lens spaces.

Now we return to contact geometry. Given a contact structure $\eta \in \mathrm{Tight}(V_1,(q/p)^a)$ and $\eta' \in \mathrm{Tight}(V_2,(q/p)^c)$ we can connect them with an I invariant contact structure on $N(A) = A \times I$ to get a contact structure on C. We first show this is indeed tight. To this end we Dehn fill C with the solid torus S as above. Notice that the solid torus glued in has meridional slope pq and we are gluing it to a convex torus with dividing slope ∞. Thus there is a unique tight contact structure on S with these boundary conditions. We claim this contact structure on $L(p,-q)\#L(q,-p)$ is tight, and hence the one on C must have been too. To see this notice that each of the 2-handles h_1 and h_2 can be thought of an an I-invariant neighborhood of a meridian disk. So gluing a tight 3-ball to $V_1' = V_1 \cup h_1$ is the same as gluing a tight solid torus to V_1 so that its meridian goes to the q/p curve, in other words one gets the tight contact structure on $L(p,-q)$ determined by the path in the Farey graph corresponding the the path determined by the contact structure η on V_1. Similarly we get a tight structure on $L(q,-p)$ determined by η'. Thus the contact structure on the Dehn filling of C is indeed a tight contact structure on $L(p,-q)\#L(q,-p)$. Colin [4] showed there is a one to one correspondence between tight contact structures on $M_1\#M_2$ and pairs of contact structures, one on M_1 and one on M_2. Thus the lower bound is $n(p,q)$. □

Lemma 6.7. *Let $n(p,q)$ be the number of tight contact structures on $L(p,-q)\#L(q,-p)$ then for the complement C of the (p,q)–torus knot and any integer $n > pq$, we have*

$$|\,\mathrm{Tight}_0(C;n)| = 2n(p,q),$$

unless $pq<0$ and $n = |pq|-|p|-|q|$, in which case we have

$$|\,\mathrm{Tight}_0(C;n)| = 2n(p,q)+1.$$

Proof. We begin with positive (p,q)–torus knots. By Lemma 6.1 and the proof of Lemma 6.6 we know that for any $n > pq$ and $\xi \in \mathrm{Tight}_0(C;n)$ there is a subset C' of C diffeomorphic to C such that $\xi|_{C'} \in \mathrm{Tight}_0(C;\infty)$ and $C \setminus C'$ is $T^2\times[0,1]$ and $\xi|_{T^2\times[0,1]} \in \mathrm{Tight}^{min}(T^2\times[0,1];n,\infty)$. Since $\mathrm{Tight}^{min}(T^2\times[0,1];n,\infty)$ contains exactly two elements we see that an upper bound on $|\,\mathrm{Tight}_0(C;n)|$ is $2n(p,q)$.

We now show that the obvious map

$$\mathrm{Tight}_0(C;\infty)\times\mathrm{Tight}^{min}(T^2\times[1,2];n,\infty)\to\mathrm{Tight}_0(C;n)$$

is injective and thus $|\,\mathrm{Tight}_0(C;n)| = 2n(p,q)$. We first show that it is well defined, that is given $\eta \in \mathrm{Tight}_0(C;\infty)$ and $\zeta \in \mathrm{Tight}^{min}(T^2\times[1,2];n,\infty)$ the contact structure $\eta\cup\zeta$ on $C \cong C\cup(T^2\times[0,1])$ is in $\mathrm{Tight}_0(C;n)$. Suppose that ζ is a positive basic slice. Recall

in the proof of Lemma 6.6 we showed that the result of gluing a solid torus S to (C,η) with meridional slope pq and extended η by the unique tight contact structure on S, was a tight contact structure on $L(p,-q)\#L(q,-p)$. Notice that S is a standard neighborhood of a Legendrian knot L in $L(p,-q)\#L(q,-p)$. If we stabilize L positively and let S' be a standard neighborhood of that knot, then $S\setminus S'$ is a positive basic slice $\zeta'\in \mathrm{Tight}^{min}(T^2\times[0,2];pq+1,\infty)$. We may find a convex torus $T=T^2\times\{1\}$ in $S\setminus S'$ with two dividing curves of slope n and this torus splits ζ' into a ζ on $T^2\times[1,2]$ and some other contact structure on $T^2\times[0,1]$. Thus we see that $\eta\cup\zeta$ is sitting in the contact Dehn filling of (C,η) which is tight. Thus $\eta\cup\zeta$ is tight. To see that it is actually in $\mathrm{Tight}_0(C;n)$ we note that it cannot contain a convex torus parallel to the boundary with dividing slope pq or else the contact structure on $L(p,-q)\#L(q,-p)$ would not be tight. If ζ were a negative basic slice then we could similarly show $\eta\cup\zeta$ is in $\mathrm{Tight}_0(C;n)$ by negatively stabilizing L.

To see that the above map is injective, we take η and η' in $\mathrm{Tight}_0(C;\infty)$ and ζ and ζ' are the two distinct elements in $\mathrm{Tight}^{min}(T^2\times[1,2];n,\infty)$, say the first is the positive basic slice and the second the negative one. We first note that $\eta\cup\zeta$ and $\eta'\cup\zeta'$ must be distinct for any two η and η' (even if they are the same). To do this we consider Dehn filling $C\cup(T^2\times[1,2])$ by a solid torus S'' with meridional slope pq. When $n>pq+1$, there are two ways we can extend the contact structures over the added torus as a universally tight contact structure (there is a unique contact structure on S'' when $n=pq+1$, we will discuss this case below). One will have a positive basic slices ξ and the other will have all negative ones ξ'. Suppose we choose the one with all positive basic slices, then on $(T^2\times[0,1])\cup S''$ the contact structure $\zeta\cup\xi$ is tight and $\zeta'\cup\xi$ is overtwisted. But $\zeta\cup\xi$ is simply the unique tight contact structure on the solid torus S from the previous paragraph. That is $\eta\cup\zeta\cup\xi$ is a tight contact structure on $C\cup(T^2\times[0,1])\cup S''=L(p,-q)\#L(q,-p)$ while $\eta'\cup\zeta'\cup\xi$ is overtwisted. Thus $\eta\cup\zeta$ and $\eta'\cup\zeta'$ are distinct.

We are left to see that if $\eta\cup\zeta$ is isotopic to $\eta'\cup\zeta$ then η is isotopic to η' (and similarly for ζ'). This is clear since gluing S'' with the contact structure ξ will result in the same contact structures on $L(p,-q)\#L(q,-p)$ and these will also be the result of Dehn filling (C,η) and (C,η'). From the proof of Lemma 6.6 we know that this implies η is isotopic to η'. (Notice this argument also works when $n=pq+1$.)

We must now see that $\eta\cup\zeta$ and $\eta\cup\zeta'$ are not isotopic when $n=pq+1$. This follows as the relative Euler classes of these two contact structures evaluate differently on a Σ where Σ is a minimal genus Seifert surface for the (p,q)–torus knot in C.

We now turn to the case of negative torus knots $-q>p>0$. If $n\neq|pq|-|p|-|q|$ then the argument is identical to the above argument using Lemma 6.2, the proof of Lemma 6.6, and Remark 6.3. When $n=|pq|-|p|-|q|$ then we get the upper bound of $2n(p,q)+1$ since Lemma 6.2 gave an extra contact structure on this case. From Lemma 6.2 we know that this extra contact structure ξ is tight and any convex torus parallel to the boundary of C has dividing slope n. Thus $\xi\in\mathrm{Tight}_0(C;n)$ and it is distinct from the other contact structures since they all contain convex tori parallel to the boundary with dividing slope ∞. □

Before our next result we establish some notation:

$$\mathcal{L}(p,q) = \{\text{Legendrian realizations of } (p,q)\text{–torus knot with tb} = pq \text{ in some contact structure on } S^3 \text{ whose complement is tight without convex Giroux torsion}\}.$$

Lemma 6.8. *Let* $m(p,q) = |Tight(S^1 \times D^2; p/q)| \cdot |\,\text{Tight}(S^1 \times D^2; q/p)|$. *Then*

$$|\mathcal{L}(p,q)| = m(p,q).$$

Proof. We will try to understand contact structures on $\text{Tight}_0(C; pq)$. While we will not quite get a classification of these, we will come close enough to identify all Legendrian realizations of (p,q)–torus knots.

Recall from Section 6.1 that we can take $V_1 \cup (S^1 \times P) \cup V_2$ as a model for C and we will use the notation established there for $\partial(S^1 \times P) = T_1 \cup T_2 \cup T_3$ and the coordinates on the T_i discussed there as well.

Since any $\xi \in \text{Tight}_0(C; pq)$ has dividing curves of slope pq on ∂C, we know they are isotopic to $S^1 \times \{pt\} \subset S^1 \times P$. We can then use convex annuli between ∂C and ∂V_i to thicken the solid tori V_i until they have dividing slope q/p.

The contact structure ξ on $S^1 \times P$ has dividing curves on all boundary components isotopic to the S^1–fibers. We can make the ruling curves have ∞ slope and arrange them for $\partial P = \{\theta\} \times \partial P$ to be ruling curves and then make P convex. According to Lemma 2.21, there is a unique contact structure on $S^1 \times P$ up to isotopy (not fixing the boundary point-wise). But notice that when V_1 and V_2 are glued back into $S^1 \times P$, the fact that the isotopy did not fix T_1 or T_2 is irrelevant because the rotation of these T_i can be extended to the interior by rotating the V_i's. So the contact structure on C is uniquely determined, up to isotopy (not fixing the boundary of C point-wise) by the contact structures on V_1 and V_2. Now notice that when the neighborhood N of the (p,q)–torus knot is glued to ∂C, we again do not need to be concerned about the fact that the classification above allowed ∂C to move.

Thus when studying contact structures on C that come from the complement of non-loose Legendrian (p,q)–torus knots, there is a unique tight contact structure on $S^1 \times P$ that we need to consider and a model for it comes from taking a neighborhood $T^2 \times [0,1]$ of a convex torus with two dividing curves of slope q/p and then remove a neighborhood N of a dividing curve on $T^2 \times \{1/2\}$. Now gluing V_1 and V_2 into this model, we see that an upper bound on $|\mathcal{L}(p,q)|$ comes from the number of tight contact structures on V_1 and V_2. Since the dividing slope on $\partial V_1 = \partial V_2$ is q/p we see that $|\,\text{Tight}(V_1)| = |\,\text{Tight}(S_\infty; q/p)| = \text{Tight}(S^1 \times D^2; q/p)|$ and $|\,\text{Tight}(V_2)| = |\,\text{Tight}(S^0; q/p)| = |\,\text{Tight}(S^1 \times D^2; p/q)|$ (see Section 2.2 for notation about upper and lower meridians). This shows that $m(p,q)$ is the upper bound of $|\mathcal{L}(p,q)|$. Now we will describe all the possible elements in $\mathcal{L}(p,q)$ and find the lower bound.

Construction of contact structures on $\text{Tight}_0(C; pq)$**.** Consider a decorated Farey graph (P_1, P_2) representing q/p (see Section 2.3). Recall that the union of $P_1 \cup P_2$ gives a contact structure ξ_{P_1,P_2} on S^3 (it might or might not be the tight) and inside of it there is a convex torus T with dividing slope q/p. Let L_{P_1,P_2} be a Legendrian divide on T. Below we will show that L_{P_1,P_2} is in $\mathcal{L}(p,q)$ and all elements of $\mathcal{L}(p,q)$ can be constructed in this manner.

We now claim that all of these Legendrian knots are indeed in $\mathcal{L}(p,q)$, that is the complement of L_{P_1,P_2} is tight and has no convex Giroux torsion. This will follow by showing that Legendrian surgery on L_{P_1,P_2} results in a tight contact structure. To see this, recall that any L_{P_1,P_2} can be realized as a Legendrian knot shown in Figure 2, see Section 2.4. The Legendrian surgery on L_{P_1,P_2} cancel one of the (+1)–surgery components and we obtain a tight contact structure. From Lemma 2.20, we know that L_{P_1,P_2} and $L_{P_1',P_2'}$ have different rotation numbers and thus are not Legendrian isotopic if $(P_1,P_2)\neq(P_1',P_2')$. This gives the lower bound of $|\mathcal{L}(p,q)|$ and completes the proof. □

Remark 6.9. The non-looseness of the knots in Lemma 6.8 is seen by showing that Legendrian surgery on them is tight, but we note that the proof of Proposition 7.5 can also be applied here to show non-looseness using convex surfaces and state transition.

Referring to the construction of contact structure on $\mathrm{Tight}_0(C;pq)$ above, each one will be of the form ξ_{P_1,P_2} where P_1 is a minimal path in the Farey graph that goes from ∞ clockwise to q/p and decorate it so that it represents an element in $\mathrm{Tight}(S_\infty;q/p)$ and P_2 is a minimal path from q/p clockwise to 0 and decorate it so that it represents an element in $\mathrm{Tight}(S^0;q/p)$. Recall from Section 2.3 that $(A_1,A_3,\dots,A_{2n-1})$ and $(B_2,B_4,\dots,B_{2m})$ are the subdivisions of P_1 and P_2 into continued fraction blocks, respectively (there is a similar discussion when the indexing of the B_i is odd and the A_j is even). Suppose i is even (odd will be similar). We will call the paths P_1 and P_2 *i-consistent* if the signs of the decorations on the paths in $A_1,B_2,\dots,A_{i-1},B_i$ are all the same and we call the paths *i-inconsistent* if (P_1,P_2) is $(i-1)$-consistent but not i-consistent. If every decoration of $(A_1,A_3,\dots,A_{i-1})$ has the same sign and every decoration of $(B_2,\dots,B_i)$ has the opposite sign, then the paths are called *totally i-inconsistent*.

Lemma 6.10. *Let $\xi'_{P_1,P_2}\in\mathrm{Tight}_0(C;pq)$ be the complement of L_{P_1,P_2}. In ξ'_{P_1,P_2}, all convex tori parallel to ∂C have slope pq if and only if P_1 and P_2 are 2-consistent. Moreover, if P_1 and P_2 are 2-inconsistent, then there is a subset C' of C that is isotopic to C and $(\xi'_{P_1,P_2})|_{C'}\in\mathrm{Tight}_0(C;\infty)$.*

Remark 6.11. Notice that by the proof of Lemma 6.6 any element in $\mathrm{Tight}_0(C;\infty)$ is described by a pair of paths P_1',P_2' where P_1' is a path from $(q/p)^a$ anti-clockwise to ∞ and P_2' is a path from $(q/p)^c$ clockwise to 0. One can extend P_i' to start at q/p and then add a $\pm$ sign to one and a $\mp$ to the other edges added. This will result in two different 2-inconsistent paths corresponding to the element in $\mathrm{Tight}_0(C;\infty)$ that give two elements in $\mathrm{Tight}_0(C;pq)$ described by 2-inconsistent paths. This observation, coupled with the above lemma implies that the number of 2-inconsistent elements in $\mathrm{Tight}_0(C;pq)$ is $2|\mathrm{Tight}_0(C,\infty)|$.

Proof. We first show that if P_1 and P_2 are 2-inconsistent, then we can find C' such that $(\xi'_{P_1,P_2})|_{C'}\in\mathrm{Tight}_0(C;\infty)$. As discussed in Section 6.1 we write C as $V_1\cup(S^1\times P)\cup V_2$ and use the notation there for $\partial(S^1\times P)=T_1\cup T_2\cup T_3$ and the coordinates on the T_i given there as well.

We can arrange that the ∂V_i are convex and the slope of the dividing curves on ∂V_1 is $(q/p)^a$ and the slope on ∂V_2 is $(q/p)^c$. Using the coordinates on $T_i=\partial V_i$ coming from $S^1\times P$, we see that the slope of the dividing curves on T_1,T_2, and T_3 is $-1,\infty$, and 0, respectively. Moreover, there are convex tori T_i' in $S^1\times P$ parallel to T_i with dividing slope 0, for $i=1,2$.

The thickened tori N_i cobounded by T_i and T_i' are basic slices. Because the paths P_1 and P_2 are 2-inconsistent, we know we can arrange these basic slices to have the same sign. To see this, notice that P_i describes a contact structure on V_i and we took the outermost basic slice and added it to $S^1 \times P$. By assumption we can arrange that the outermost basic slices of V_1 and V_2 have opposite signs, but recall the contact structure on V_2 is described as an element of $\text{Tight}(S^0; q/p)$. Thus this outermost basic slice, when oriented as a basic slice in $S^1 \times P$, has the same sign as the one coming from V_1. Now Lemma 2.22 says there is a convex annulus A going from a 0 slope ruling curve on T_1 to a ruling curve on T_2 that has dividing curves running from one boundary component to the other. As in the proof of Lemma 6.1, if we round the corners of $T_1 \cup T_2 \cup N(A)$, the convex torus $T = \partial(T_1 \cup T_2 \cup N(A))$ will have dividing curves with ∞ slope. The torus T is parallel to $T_3 = \partial C$ and again as in the proof of Lemma 6.1, the dividing slope of T in Seifert coordinates is still ∞. Thus T and T_3 cobound a thickened torus N that is a basic slice. So ξ_{P_1,P_2} can be written as the union of a contact structure on $\text{Tight}_0(C; \infty)$ and a basic slice in $\text{Tight}_0(T^2 \times [0,1]; pq, \infty)$.

By the proof of Lemma 6.6 we know that if there is a subset C' of C such that $(\xi'_{P_1,P_2})|_{C'} \in \text{Tight}_0(C; \infty)$, then $(\xi'_{P_1,P_2})|_{C'}$ will be as described in the previous paragraph and hence P_1 and P_2 will be 2-inconsistent. Now the proof of Lemma 6.1 shows that for $pq > 0$, if ξ_{P_1,P_2} is a contact structure on $\text{Tight}_0(C; pq)$ and there is a torus T parallel to ∂C with slope different from pq then there will be a subset C' of C such that $(\xi'_{P_1,P_2})|_{C'} \in \text{Tight}_0(C; \infty)$ (since if T has slope different from pq, then we can assume it has slope slightly larger than pq). Thus P_1 and P_2 are 2-inconsistent. If $pq < 0$, then Lemma 6.2 says if ξ'_{P_1,P_2} is a contact structure on $\text{Tight}_0(C; pq)$ and there is a torus T parallel to ∂C with slope different from pq then either there will be a subset C' of C such that $(\xi'_{P_1,P_2})|_{C'} \in \text{Tight}_0(C; \infty)$, or there will be a subset C'' that is isotopic to C and $\partial C''$ is convex with dividing slope $|pq| - |p| - |q|$. In the latter case, in $C \setminus C''$ we can find a convex torus T with dividing slope $|pq| - |p| - |q| - 1$ and Proposition 7.22 below says that inside the component of $C \setminus T$ that is not a thickened torus, we can find a subset C' such that $(\xi'_{P_1,P_2})|_{C'} \in \text{Tight}_0(C; \infty)$. So in either case, we see again that P_1 and P_2 are 2-inconsistent. Thus we have that in ξ_{P_1,P_2} there is a convex torus parallel to ∂C have slope different from pq if and only if P_1 and P_2 are 2-inconsistent; moreover, in this case there is a subset C' of C such that $(\xi'_{P_1,P_2})|_{C'} \in \text{Tight}_0(C; \infty)$. □

We can also see that for almost all contact structures in $\text{Tight}_0(C; \infty)$ any convex tori parallel to ∂C will have dividing slope ∞.

Lemma 6.12. *If $pq < 0$, then for any contact structure on $\text{Tight}_0(C; \infty)$, any convex torus parallel to ∂C will have dividing slope ∞. If $pq > 0$, the same is true for all contact structures but two. These contact structures are obtained from the complement of a standard neighborhood of Legendrian (p, q)–torus knots with maximal Thurston-Bennequin invariant in (S^3, ξ_{std}) by adding a $\pm$ basic slice in $\text{Tight}_0(T^2 \times [0,1]; \infty, pq - p - q)$.*

For context we recall that there is a unique maximal Thurston-Bennequin invariant Legendrian (p, q)–torus knots when $pq > 0$, see [16].

Proof. Suppose $pq < 0$ and $\xi \in \text{Tight}_0(C, \infty)$. If there is a convex torus in (C, ξ) parallel to the boundary that has dividing slope s different from ∞ then it separates off a $T^2 \times [0,1]$ where the contact structure rotates from ∞ to s, so there will be a convex torus parallel

to ∂C with dividing slope n for some negative integer n. Now according to Lemmas 6.2 and 6.5 if $n \neq |pq|-|p|-|q|$, then there is another torus T that is parallel to ∂C, has dividing slope ∞ or pq. If the slope of T is ∞, then T separates off $T^2 \times [0,1]$ that is a convex half Giroux torsion layer, contradicting the fact that $\xi \in \mathrm{Tight}_0(C, \infty)$.

If the slope of T is pq, then by Lemma 6.10 it may happen that all convex tori further from ∂C than T will have dividing slope pq. This happens when T separates C into $T^2 \times [0,1]$ and C' where $\xi|_{C'}$ is in $\mathrm{Tight}_0(C; pq)$ and corresponds to a pair of 2-consistent decorated paths P_1, P_2. In particular, $\xi|'_C$ is ξ'_{P_1,P_2}, which is the complement of $L_{P_1,P_2} \subset (S^3, \xi_{P_1,P_2})$. Thus (C, ξ) is the union of a basic slice in $\mathrm{Tight}(T^2 \times [0,1]; \infty, pq)$ and (C', ξ'_{P_1,P_2}) and by Lemma 6.13, ξ is overtwisted, contradicting that $\xi \in \mathrm{Tight}_0(C, \infty)$.

Now if $pq > 0$ and $\xi \in \mathrm{Tight}_0(C, \infty)$, then we can argue as above, using Lemmas 6.1 and 6.5, and see that if there are convex tori in C parallel to ∂C with slope different from ∞ then there is one T with slope $pq - p - q$. In this case T separates C into $T^2 \times [0,1]$ and C'. The contact structure restricted to the former space is simply a bypass with dividing slopes ∞ and $pq - p - q$. According to Case 1 of the proof of Lemmas 6.1 and [18, Section 3.1] we see that $\xi|_{C'}$ is simply the complement of the unique maximal Thurston-Bennequin Legendrian representative L of the (p, q)–torus knot in (S^3, ξ_{std}).

We now know the only possibilities for (C, ξ) to have a convex torus of slope different from ∞, but need to prove that the contact structure described above is indeed tight and so in $\mathrm{Tight}_0(C; \infty)$. But this was already proven in [22, Lemma 3.1]. □

The next two lemmas will show that 2-inconsistency also controls when one may attach certain basic slices to a contact structure in $\mathrm{Tight}_0(C; pq)$ and get a tight contact structure.

Lemma 6.13. *Let ξ'_{P_1,P_2} be a contact structure on $\mathrm{Tight}_0(C; pq)$ such that P_1 and P_2 are not totally 2-inconsistent. Gluing any basic slice in $\mathrm{Tight}_0(T^2 \times [0,1]; \infty, pq)$ to (C, ξ'_{P_1,P_2}) will result in an overtwisted contact structure.*

Remark 6.14. Note that Lemmas 6.10 and 6.13 show that if a contact structure in $\mathrm{Tight}_0(C; pq)$ has all convex tori parallel to ∂C having dividing slope pq, then adding a basic slice in $\mathrm{Tight}_0(T^2 \times [0,1]; \infty, pq)$ to C will yield an overtwisted contact structure.

Proof. Let ξ be the contact structure on C resulting from gluing any basic slice in $\mathrm{Tight}_0(T^2 \times [0,1]; \infty, pq)$ to ξ_{P_1,P_2}. We can decompose C as two solid tori V_1 and V_2 and $S^1 \times P$ as in Section 6.1 and arrange that the dividing slope of $\partial V_1 = T_1, \partial V_2 = T_2$, and $\partial C = T_3$ is $(q/p)^a, (q/p)^c$, and ∞, respectively. Using the coordinates on T_i coming from $S^1 \times P$, we see the dividing slope on T_1, T_2, and T_3 is $-1, \infty$, and ∞, respectively. Now there is a convex torus T'_i in $S^1 \times P$ parallel to T_i that has dividing slope 0. Let N_i be the thickened tori that T_i and T'_i cobound and set $S^1 \times P' = (S^1 \times P) \setminus \cup_{i=1}^3 N_i$. Notice that $\xi|_{N_3}$ is the basic slice that was added to ξ_{P_1,P_2}. By the hypothesis that P_1 and P_2 are not totally 2-inconsistent paths, we know that N_1 and N_2 can be taken to be basic slices with different signs, so one of them has the same sign as N_3 (recall, as in the proof of Lemma 6.10, a basic slice as seen in V_2 has the opposite sign when seen as a basis slice in $S^1 \times P$).

Suppose that N_1 and N_3 have the same sign. By Lemma 2.22 we know that there is a convex annulus A with boundary 0 sloped ruling curves on T_1 and T_3 and the dividing curves on A run from one boundary component to the other. If we now cut $(S^1 \times P') \cup N_1 \cup$

$N_2 \cup N_3$ along this annulus we will obtain $T^2 \times [0,1]$ with one boundary component T_2 and the other boundary component having dividing slope

$$\frac{1}{1+0-1} = \infty.$$

Since N_2 contains a 0-twisting vertical Legendrian curve, $T^2 \times [0,1]$ is a convex half Giroux torsion layer and the union of this and V_2 (which is contained in (C, ξ)) is overtwisted.

Similarly if N_2 and N_3 have the same sign then we write N_2 as the union of two basic slices N_2' and N_2'' where N_2' had dividing slopes -1 and 0. Now Lemma 2.22 again implies the existence of a 0 sloped convex annulus A between T_3 and one boundary component of N_2' with dividing slope -1. The dividing curves on A run from one boundary component to the other. As N_2'' has a similar annulus we can extend A to an annulus in $(S^1 \times P) \cup N_1 \cup N_2 \cup N_3$ between T_2 to T_3. If we now cut $(S^1 \times P') \cup N_1 \cup N_2 \cup N_3$ along this annulus we will obtain $T^2 \times [0,1]$ with one boundary component T_1 and the other boundary component having dividing slope

$$\frac{1}{0+0-1} = -1$$

Again, this $T^2 \times [0,1]$ is a convex half Giroux torsion layer and the union of this and V_1 (which is contained in (C, ξ)) is overtwisted. □

Lemma 6.15. *Let (P_1, P_2) be a totally 2-inconsistent pair of paths and $\xi'_{P_1,P_2} \in \mathrm{Tight}_0(C; pq)$. Gluing one basic slice $(T^2 \times [0,1]; \infty, pq)$ to (C, ξ'_{P_1,P_2}) will result in a tight contact structure ξ on C with ∞ dividing slope on ∂C, while gluing the other basic slice will result in an overtwisted contact structure. Moreover, adding any amount of convex Giroux torsion to (C, ξ) will result in a tight contact structure.*

Proof. Given a contact structure ξ'_{P_1,P_2} as in the statement of the lemma, we know from the proof of Lemma 6.10 that it is the union of a contact structure $\xi' \in \mathrm{Tight}_0(C; \infty)$ and a $\pm$-basic slice $\eta_\pm \in \mathrm{Tight}_0(T^2 \times [0,1]; pq, \infty)$. Now let $\zeta_\pm$ be the $\pm$-basic slice in $\mathrm{Tight}_0(T^2 \times [0,1]; \infty, pq)$. Gluing $\zeta_\mp$ to $\eta_\pm$ is overtwisted, we see that attaching one of the basic slices to ξ'_{P_1,P_2} will result in an overtwisted contact structure. We will now see that gluing the other results in a tight contact structure.

To be specific, suppose ξ'_{P_1,P_2} is the union of ξ' and η_-. We will show that gluing ζ_- and a convex Giroux torsion layer to it will result in a tight contact structure. Let ξ be the contact structure resulting from this gluing. As usual, we consider (C, ξ) as the union of two solid tori V_1 and V_2 and $S^1 \times P$. We will use the notation from Section 6.1 except that we will use the coordinates on T_1 and T_2 coming from the longitude-meridian coordinates on ∂V_1 and the coordinates on T_3 coming from the longitude-meridian coordinates on ∂C. In particular, we can take the dividing curves on T_1 to have slope $(q/p)^a$, on T_2 to have slope $(q/p)^c$ and on T_3 to have slope ∞. Moreover, we can thicken V_1 and V_2 so that the slope of T_1 and T_2 become q/p, notice that in the coordinates on ∂V_i, $i = 1, 2$, coming from $S^1 \times P$ the slopes are 0. Honda [35, Lemma 5.1] showed that this $P \times I$ is universally tight even after adding a universally tight rotative $T^2 \times I$ layer to T_i (with the correct sign). Thus it is tight after we add convex Giroux torsion layer to T_3. After we make P convex we

obtain the dividing curves on P as shown in Figure 19 (see the proof of Lemma 7.25 how to rule out other possibilities).

Let A' be an annulus in $S^1 \times P$ separating T_1 from T_2, such that the boundary is two pq slope ruling curves on T_3. See the first drawing of Figure 18. We can perturb A' rel boundary so that it becomes convex and the intersection between P and A' is the Legendrian arc as shown in Figure 19. It is not hard to see that A' contains 0-twisting Legendrian curve, so we obtain two non-rotative layers N_1 and N_2 once we cut $S^1 \times P$ along A'. By Theorem 2.28, $\widehat{V}_1 := V_1 \cup N_1$ and $\widehat{V}_2 := V_2 \cup N_2$ are tight. By adding a sufficiently large amount of convex Giroux torsion to T_3, we can assume that $\widehat{V}_1$ and $\widehat{V}_2$ have a large number of dividing curves.

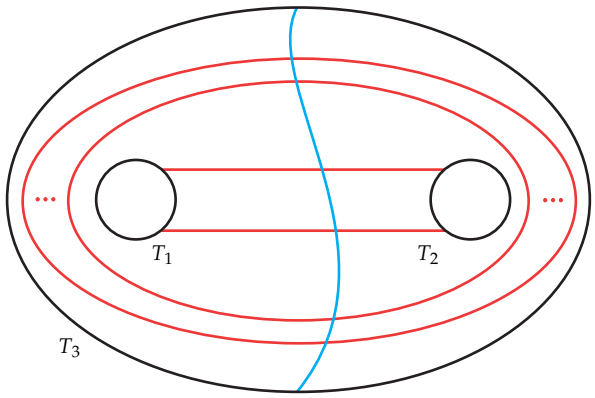

FIGURE 19. A dividing set on the pair of pants P. The blue arc is a Legendrian arc, which is the intersection of A' and P.

Suppose (C, ξ) was not tight. Then we can smoothly isotope A' so that it would be disjoint from an overtwisted disk. We can then use isotopy discretization (Theorem 2.30) to find a sequence of convex annuli $A_1 = A', A_2, \dots, A_n$ such that there is an overtwisted disk in the complement of A_n and each A_i is obtained from A_{i-1} by a bypass attachment. We will inductively show that A_i is contained in an I-invariant neighborhood $A \times [1,2]$, where A is contact isotopic to A' rel boundary. Then clearly $C \setminus A_i$ is tight for all i and this contradiction will establish the tightness of ξ.

Clearly A_1 satisfies the inductive hypothesis. Now assume that A_{i-1} satisfies the inductive hypothesis. We know A_i is obtained by attaching a bypass to A_{i-1}. We assume the bypass was contained in $\widehat{V}_1^{i-1}$. The argument when the bypass is contained in $\widehat{V}_2^{i-1}$ is almost identical, except for one issue that is discussed in Remark 6.18. By the inductive hypothesis, A_{i-1} is contained in an I-invariant neighborhood $A \times [1,2]$. Since $A \times \{2\}$ is contact isotopic to A' we know that $C \setminus (A \times \{2\})$ consists of two solid tori contact isotopic to $\widehat{V}_1$ and $\widehat{V}_2$, so we will think of $C \setminus (A \times \{2\})$ as $\widehat{V}_1 \cup \widehat{V}_2$. We know that A_i is contained in $\widehat{V}_1$ and A_i cuts C into two solid tori, one of them is contained in $\widehat{V}_1$. Denote the boundary of this solid torus by T_i. We need to find an annulus A_i' inside of the solid torus bounded by T_i and contact isotopic to $A \times \{2\}$. When we do this, A_i' and $A \times \{2\}$ will co-bound a thickened annulus $A \times [1,2]$ containing A_i on which the contact structure is I-invariant, thus completing the inductive step.

Since A_{i-1} is contained in an I-invariant neighborhood $A \times [1,2]$, the number of dividing curves on A_{i-1} is greater than or equal to the number of dividing curves on $A \times \{2\}$. If the number of dividing curves are the same, then A_{i-1} and $A \times \{2\}$ are contact isotopic. We claim that the number of dividing curves on A_i is also greater than or equal to the number of dividing curves on $A \times \{2\}$. To prove the claim, we only need to consider the case when the number of dividing curves on A_{i-1} is the same as the number of dividing curves on $A \times \{2\}$ (since the number of dividing curves on A_i can only differ from those on A_{i-1} by 2). In this case, A_{i-1} is contact isotopic to $A \times \{2\}$ and the torus T_{i-1} is contact isotopic to $\partial \widehat{V}_1$. Label the dividing curves on ∂T_{i-1} (and $\partial \widehat{V}_1$) as shown in first drawing of Figure 15 (notice that the annulus in the figure is equivalent to the horizontal annulus for $\widehat{V}_1 \setminus V_1$, which is the subsurface of $\{\theta\} \times P$ as shown in Figure 19). To proceed we note the following result which will be established later.

Lemma 6.16. *Suppose (P_1, P_2) is totally 2-inconsistent. Then there exist no effective bypasses in $\widehat{V}_1$, except for the ones for p_1.*

Notice that A_{i-1} contains all dividing curves of T_{i-1} except for the one containing p_1. By Lemma 6.16, there is no effective bypass on A_{i-1}, so any bypass cannot reduce the number of dividing curves on A_{i-1} and this completes the claim. Thus the solid torus bounded by T_i contains a solid torus $\overline{V}_1$ with two dividing curves of the same slope as the dividing curves on T_i (which is the same slope as the dividing curves on $\partial \widehat{V}_1$). Now $\widehat{V}_1 \setminus \overline{V}_1$ and $\widehat{V}_1 \setminus V_1$ are both non-rotative outermost layers and so by Theorem 2.27 we know that $\overline{V}_1$ and V_1 are contactomorphic.

Now consider a horizontal annulus $\widehat{A}$ for the thickened torus bounded by T_i and $\partial \widehat{V}_1$ that is isotopic to a subsurface of $\{\theta\} \times P$ and then extend it to $\overline{A}$, a horizontal annulus for the thickened torus bounded by $\partial \overline{V}_1$ and $\partial \widehat{V}_1$. We can make these annuli convex with Legendrian boundary. By Theorem 2.26 and Lemma 6.16, the horizontal annulus $\overline{A}$ must be disk equivalent to the horizontal annulus for $\widehat{V}_1 \setminus V_1$. Label the points where $\overline{A}$ intersects the dividing curves on $\partial \widehat{V}_1$ as shown in first drawing of Figure 15.

Notice that $\partial \widehat{V}_1$ and T_i agree in a neighborhood of the dividing curve corresponding to p_1. From this we can see that the dividing set on $\widehat{A}$ does not have any bypasses for $\partial \widehat{V}_1$. This is because the only effective bypasses for $\partial \widehat{V}_1$ in $\widehat{V}_1$ are bypasses for p_1, but since the dividing curves corresponding to p_1 is not moved when going from ∂V_1 to T_i there is no bypass here either. Notice this implies every dividing curve on $\widehat{A}$ that starts on $\widehat{A} \cap \partial \widehat{V}_1$ must end on $\widehat{A} \cap T_i$. Now inside of $\overline{A} \setminus \widehat{A}$, we can find a closed curve parallel to $\partial \overline{A}$ that intersects the dividing set the same number of times that $\overline{A} \cap \partial \widehat{V}_1$ does. Legendrian realize this curve and take a convex torus T parallel to T_i intersecting $\overline{A}$ in that curve. The thickened torus between T and $\partial \widehat{V}_1$ is an I-invariant neighborhood of $\partial \widehat{V}_1$ containing T_i (and hence A_i) (note this follows since both boundary components have the same number of dividing curves and the horizontal annulus connecting them has all the dividing curves running from one boundary component to the other). Again, since the dividing curves corresponding to p_1 is not moved when going from ∂V_1 to T, we can fix the surface $S =$

$\partial V_1 \setminus A \times \{2\}$ in the I-invariant neighborhood. This implies that $A \times \{2\}$ and $T \setminus S$ are contact isotopic. This completes the inductive step. □

To prove Lemma 6.16, we need a preliminary observation. Lemma 6.16 and the following lemma both apply to $\widehat{V}_2$ once we use the mirror image of the first drawing in Figure 15.

Lemma 6.17. *In $\widehat{V}_1$, the only points which can have an effective bypass are p_1 and p_{k+1}. If there exists an effective bypass for p_{k+1}, then there exist length $k-1$ nested bypasses for p_1 which are disjoint from a, possibly different, effective bypass for p_{k+1}.*

Proof. According to Theorem 2.26, any two horizontal annuli for $\widehat{V}_1$ are disk-equivalent. The first horizontal annulus for $\widehat{V}_1$ is shown in Figure 19 and is obtained by cutting the pair-of-pants along the blue Legendrian arc in the figure. So any other horizontal annulus for a non-rotative outer layer in $\widehat{V}_1$ will be disk equivalent to this one and all such possibilities are shown in Figure 15. If there is an effective bypass for p_i when $i \neq 1, k+1$, then we can attach it to reduce the number of dividing curves on $\partial \widehat{V}_1$. We can then find further bypasses to get a torus T with just two dividing curves of slope 0 (the same slope as the dividing cures on $\partial \widehat{V}_1$). Now we can find a horizontal annulus for the region between $\partial \widehat{V}_1$ and T on which the original bypass sits. This annulus cannot be disk-equivalent to the one for $\widehat{V}_1$. Thus there is no effective bypass for p_i when $i \neq 1, k+1$.

Now suppose there is an effective bypass for p_{k+1}. To find the claimed bypasses for p_1 we will construct a meridian disk for $\widehat{V}_1$ form the horizontal annulus shown in Figure 19. To this end recall that the horizontal annulus is for the non-rotative layer $\widehat{V}_1 \setminus V_1$ and the boundary of the meridian for V_1 is a $-p/q'$ slopes curve in the coordinates on ∂P coming from $S^1 \times P$ (we are using the change of coordinates ϕ from Section 6.1). We want to extend this meridian to a meridian for $\widehat{V}_1$ by using copies of the horizontal annulus H (which has slope ∞). Smoothly we can do this by taking p copies of H, labeled $H_0, \dots, H_{p-1}$, cutting each of them p' times by an arc running from one boundary component to the other and then gluing one side of the cut on H_i to the other side of the cut on H_{i+1} (with indices taken modulo p). See the blue curves in Figure 20 (there $p = 5$ and $p' = 2$). This will give an annulus in $\widehat{V}_1 \setminus V_1$ that can be extended to a meridian disk for $\widehat{V}_1$.

We will now perform the construction paying attention to the contact geometry. Consider the torus T formed by taking the product of S^1 with the blue arc on the left of Figure 15 and the black arc containing p_{k+1} and connecting the end points of the blue arc. Notice that ∂V_1 intersected with H is the inner circle in Figure 15 and we see that the region R bounded by T and ∂V_1 is a thickened torus with an I-invariant contact structure we denote the outer boundary component by $\partial_o R$ and the inner boundary component by $\partial_i R$. We now take p copies of the convex horizontal annulus H shown on the left of Figure 15 and will perform the construction above, but the cutting and re-glueing of the annuli will take place in a small neighborhood of a horizontal arc connecting p_{k+1} on $H \cap \partial \widehat{V}_1$ to $H \cap \partial V_1$. In particular, we will modify our annuli in the region R where the contact structure is I-invariant. Let $H' = H \cap R$ and we can assume this is a horizontal annulus for R. In a neighborhood of the dividing curve corresponding to p_{k+1} the characteristic foliation can be assumed to be as shown on the left of Figure 20

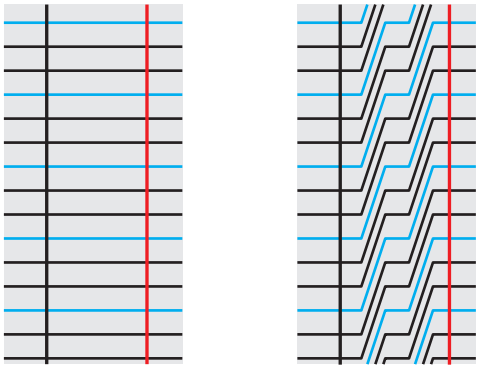

FIGURE 20. The gray is an annular neighborhood of the dividing curve corresponding to p_{k+1}, shown in red (the top and bottom of the rectangle are identified). On the right we see the original annulus with a Legendrian divide shown vertically and the horizontal curves are ruling curves. The blue curves are the intersection of the copies of H' with the region (they are also ruling curves). The annulus can be isotoped relative to its boundary so the foliation is as shown on the right hand side. Notice that the blue will now be a single curve on $\partial_o R$.

and the copies of H' intersecting this region are also shown. By a small perturbation of $\partial_i R$ we can arrange the characteristic foliation to be as shown on the right of Figure 20. Notice that the green curve (when extended to the rest of $\partial_o R$ by arcs in copies of $H' \cap \partial_o R$) is a p/p' curve γ and can be assumed to agree with copies of $H' \cap \partial_o R$ outside of the region shown in the figure. We can make this same perturbation to the torus making up the inner boundary component of R. When we have done this to both boundary components of R we can again assume that the contact structures is I-invariant on R and $\gamma \times I$ will be an annulus. This annulus must have $2p$ dividing curves running from one boundary component to the other and agrees with copies of H' outside a small neighborhood of the dividing curve corresponding to p_{k+1} times I. The copies of H' already had $2p$ dividing curves in the region where they agree with $\gamma \times I$ and so we can take these to be the dividing curves on $\gamma \times I$. Notice that on $\partial_o R$ we can glue copies of $H \setminus H'$ to $\gamma \times I$ to get an annulus A_m for $\widehat{V}_1 \setminus V_1$ that can be extended by a meridian disk D' for V_1 to a meridian disk of $\widehat{V}_1$. By construction the dividing set on A_m will be obtained from H taking a p-fold cover, the dividing set on D' will consist of p arc (of which we have no control).

A potential dividing set for the meridian disk $D = A_m \cup D'$ is shown in Figure 21. For some configurations of dividing curves on D' we will immediately see a bypass for p_{k+1}. If this happens then we can take the bypass for p_{k+1} to be on this meridian disk and then the length $(k-1)$ nested bypasses for p_1 can be found on a parallel copy of the meridian disk.

We now suppose that there is not a bypass for p_{k+1} on D. By hypothesis there is an effective bypass for p_{k+1} and as we did in the first paragraph of this proof, we can assume that it is on some meridian disk for $\widehat{V}_1$ and by sliding the boundary of this disk along $\partial \widehat{V}_1$ we can assume that it has the same boundary os D. By the isotopy discretization (Theorem 2.30), we obtain a sequence of disks $D_0 = D, D_1, \ldots, D_{n-1}, D_n = D'$ such that

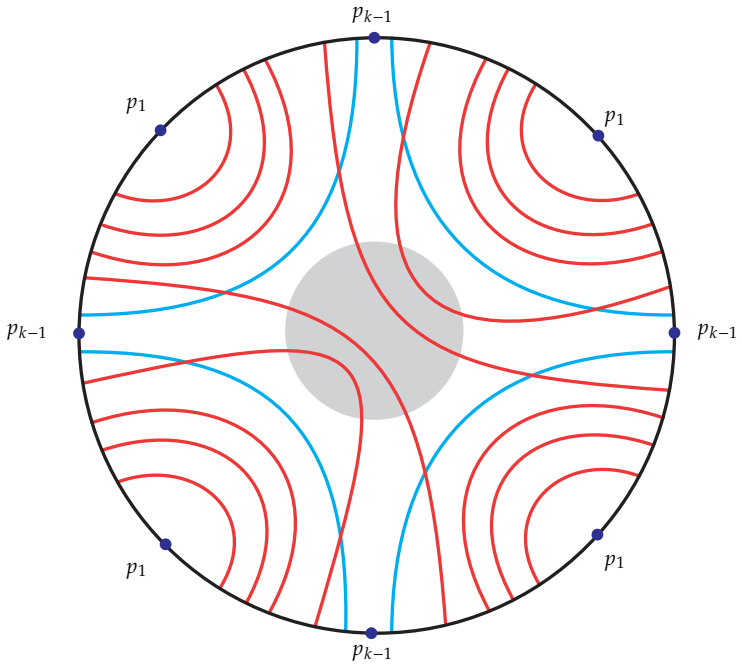

FIGURE 21. Some possible meridian disk for $\widehat{V}_1$ constructed from horizontal annuli. The shaded center region is D'. Here, $p = k = 4$.

D_{i+1} can be obtained by a single bypass attachment from D_i. Then by the construction of D, there is an integer j such that D_j does not contain a non-nested bypass for p_{k+1} and D_{j+1} contains a non-nested bypass for p_{k+1}.

Consider the maximal nested bypasses for p_1. If one of these has length $k-1$, then the proof is done. This is because D_{j+1} is obtained from a single bypass attachment from D_j, so we can make D_j and D_{j+1} disjoint after perturbation. Then the bypass for p_{k+1} on D_{j+1} is disjoint from the bypasses on D_j.

Recall that from the first part of the proof and our assumption that there is no bypass for p_{k+1} on D_j, we know that the only boundary parallel dividing curves (by which we mean that it co-bounds with an arc in ∂D_j a disk containing no other dividing curves) are bypasses for p_1. We also know from the construction of our meridian disk that there are pk arcs in the dividing set and their end points are interlaced with the p copies of each of the points p_i. We claim that the combinatorics of arcs on a disk as described above implies that one of the p_1 must have nested bypass of length $k-1$ and so the proof is complete. To see this suppose that all of the nested bypasses for p_1 on D_j have length less than $k-1$. Consider a sub-disk D_j' of D_j such that the annulus $D_j \setminus D_j'$ contains all of the nested bypasses for the copies of p_1 and the rest of the dividing curves just run from one boundary component to the other. Since we are assuming all the nested bypasses for p_1 have length less than $k-1$, there will still be at least $2p$ arc in D_j'. Thus there will be a boundary parallel arc γ on D_j'. We can extend γ across the annulus $D_j \setminus D_j'$ and it will either be boundary parallel on D_j or not. If it is boundary parallel then it gives a bypass for $\partial\widehat{V}_1$ along some p_i with $i \neq 1$, which is a contradiction. But if the arc is not boundary parallel,

then it will surround one of the nested bypasses for p_1, but this is also a contradiction since we said all the nested bypasses for p_1 were outside of D'_j. Thus p_1 must have a nested bypass of length at last $k-1$, as claimed. □

We are now ready to proof Lemma 6.16.

Proof of Lemma 6.16. Suppose there is an effective bypass for p_{k+1}. We claim that the sign of this bypass is different from the sign of the first continued fraction block of V_1 (it has the single sign since (P_1, P_2) is totally 2-inconsistent). To see this we first notice that the sign of the bypass will agree with the sign of the region on the convex surface P between the two horizontal dividing curves in Figure 19. (To see this we will always orient the attaching arc of a such a bypass so that is passes the dividing curves corresponding to p_{k+1} in the same direction that ∂H does. Now the co-orientation on a contact structure orients the dividing curve corresponding to p_{k+1}. The sign of a bypass is determined by whether or not the orientation no the dividing curve agrees with the co-orientation on the bypass disk when oriented as above and so is fixed by the contact structure and orientation on its attaching arc.) We claim this sign must be opposite to the sign in the first continued fraction block of V_1. We assume this is not the case and derive a contradiction. We can do this by replacing V_1 and V_2 in C with the universally tight solid tori whose sign of the first continued fraction block is the same as V_1 and V_2, respectively. By Lemma 7.1, this is contactomorphic (possibly co-orientation reversing) to the complement of the binding of an open book supported by (p, q)–torus knot with a convex Giroux torsion layer added. By Colin's gluing theorem, the contact structure is universally tight even after adding any amount of convex Giroux torsion. Inside V_1 we have another solid torus V'_1 with dividing slope $(q/p)^a$ and if we extend the convex pair of pants P across an annulus running between ∂V_1 and $\partial V'_1$ we will see a bypass on this annulus with sign given by the sign of the bypasses in the first continued fraction block of V_1. Since we are assuming that it is the same sign as the region between the horizontal lines in Figure 19, we see that it will give a bypass for V_2. Attaching this bypass will result in a torus about V_2 with dividing slope $(q/p)^a$. Since there are vertical ruling curves on A' disjoint from the attached bypass, we can thicken this torus further to have slope q/p. This gives a Giroux torsion layer in a solid torus so the contact structure would be overtwisted, but we know that is not the case. So the sign of the region bounded by the horizontal dividing curves in Figure 19 is opposite from the signs of the first continued fraction block of V_1.

We now return to the setting where V_1 and V_2 are given by any decorated pair of paths that is totally 2-inconsistent. We still know that the sign of the region bounded by the horizontal dividing curves in Figure 19 is opposite that of the signs in the first continued fraction block of V_1. Thus any effective bypass for p_{k-1} will have sign opposite as well.

From Lemma 6.17, we can find an effective bypass for p_{k+1} disjoint from the length $k-1$ nested bypasses for p_1. Attach these nested bypasses to obtain a solid torus with two dividing curves inside of $\widehat{V}_1$, which is contactomorphic to V_1 by Theorem 2.27. Thus we just call this solid torus V_1. While attaching the nested bypasses, we never modify the dividing curve on $\partial\widehat{V}_1$ passing through p_{k+1}, so the bypass for p_{k+1} is also effective for V_1. However, the sign of the effective bypass for p_{k+1} is different from the sign of the first continued

fraction block of V_1. This is impossible since the sign of the first continued fraction block is determined by the sign of effective bypasses in a solid torus. This contradiction implies that there is no effective bypass for p_{k+1} in $\widehat{V}_1$. Combining with Lemma 6.17, the only effective bypasses in $\widehat{V}_1$ are a bypass for p_1. □

Remark 6.18. Lemma 6.16 and 6.17 also hold for $\widehat{V}_2$ and the proofs are the same except for a part of the proof of Lemma 6.17. Specifically, in that proof we used the fact that we could find the bypass for $V_1 \setminus V_1'$ on P. This is because in the coordinates on ∂V_1 coming from $S^1 \times P$ we see that the dividing slope on ∂V_1 is 0 and on V_1' is ∞. Thus the annulus in $V_1 \setminus V_1'$ that extends P, which has slope ∞, will contain a bypass for ∂V_1. When we consider $\widehat{V}_2$ the relevant slopes on ∂V_2 and $\partial V_2'$ are 0 and -1, respectively. Thus we cannot find a bypass for ∂V_2 on an annulus of slope ∞. To proceed in this case we need to change the section of $S^1 \times P$ that we are using. Specifically, if we take $\{\theta\} \times P$ and cut it along an arc connecting $\partial V_1 \cap P$ to $\partial V_2 \cap P$, we can then push one side of the cut along the S^1 fibers until it returns and is glued to the other side of the cut. Notice that if one pushed in the correct direction, then the slope of this new section, call it P', on ∂V_2 is -1. Now running the whole argument with $S^1 \times P'$ instead of $S^1 \times P$ will prove the lemma for $\widehat{V}_2$.

We now turn to contact structures on C with convex Giroux torsion.

Lemma 6.19. *For any (p, q)–torus knot and integer k we have that*

$$|\operatorname{Tight}_l(C; k)| = 2|(a_1 + 1) \cdots (a_{m-1} + 1)||(b_1 + 1) \cdots (b_{n-1} + 1)|$$

for any $l \in \frac{1}{2}\mathbb{N}$, where the a_i and b_i are defined in Section 1.2. This is the same as the number of totally 2-inconsistent pairs of paths representing q/p.

Proof. We begin by considering $\operatorname{Tight}_l(C; pq)$. Given a contact structure $\xi \in \operatorname{Tight}_l(C; pq)$, there is an embedding of a convex l Giroux torsion layer, i.e. there is an embedding of $T^2 \times [0, 1]$ such that $T^2 \times \{0\} = \partial C$ and ξ restricted to $T^2 \times [0, 1]$ has convex l Giroux torsion. Let $C' = C \setminus T^2 \times [0, 1]$ and ξ' be ξ restricted to C'. Notice that (C', ξ') has no convex Giroux torsion, otherwise (C, ξ) would have torsion larger than l. Thus $\xi' \in \operatorname{Tight}_0(C; pq)$ and the contact structure on $C \setminus C'$ is $T^2 \times [0, 1]$ with convex l Giroux torsion. By Lemma 6.13, the pair of paths describing ξ' must be totally 2-inconsistent. Theorem 2.4 says there are two possibilities for the contact structure on $T^2 \times [0, 1]$, but by Lemma 6.15 we see that only one can possibly result in ξ being tight. Thus for every element in $\xi \in \operatorname{Tight}_l(C; pq)$ there is a unique element $\xi' \in \operatorname{Tight}_0(C; pq)$ corresponding to a totally 2-inconsistent pair of paths and a unique convex l Giroux torsion layer on $T^2 \times [0, 1]$. Moreover, given an element in $\operatorname{Tight}_0(C; pq)$ described by a totally 2-inconsistent pair of paths there is a unique convex l Giroux torsion layer on $T^2 \times [0, 1]$ that can be glued to it to give a tight contact structure.
Claim A: *The convex Giroux torsion of this contact structure is exactly l.*

Thus from above we see that $|\operatorname{Tight}_l(C; pq)|$ is bounded above by the number of totally 2-inconsistent paths describing q/p.
Claim B: *Adding convex l Giroux torsion to two distinct elements of* $\operatorname{Tight}_0(C; pq)$ *results in distinct contact structures.*

We now know that $|\operatorname{Tight}_l(C; pq)|$ is the number of totally 2-inconsistent paths describing q/p. We will prove these claims below, but finish the proof assuming they are true.

To see that the number of such paths is given by the formula in the lemma we note that the first continued fraction block in P_1 must be all one sign and the first in P_2 must be of the opposite sign. Thus there are 2 possibilities for these two continued fraction blocks. The number of possible decorations on the remainder of P_1 is $|(a_1+1)\cdots(a_{m-1}+1)|$ and on P_2 is $|(b_1+1)\cdots(b_{n-1}+1)|$.

Now given $k > pq$ we know by Lemma 6.7 and Remark 6.11 that for each $\xi \in \mathrm{Tight}_0(C;k)$ there is a unique 2-inconsistent path describing a contact structure $\xi' \in \mathrm{Tight}_0(C;pq)$ such that ξ embeds in (C,ξ'). Thus we can clearly add convex Giroux torsion to ξ to get an element in $\mathrm{Tight}_l(C;k)$. Moreover, given any element in $\mathrm{Tight}_0(C;pq)$ there will be a unique element in $\mathrm{Tight}_0(C;k)$ embedded in it. Thus $|\mathrm{Tight}_l(C;k)|$ is the number of totally 2-inconsistent paths describing q/p.

Suppose that $k < pq$ and if $pq > 0$ then assume $k > pq - p - q$. If $\xi \in \mathrm{Tight}_0(C;k)$ then we can glue in a solid torus to get a non-loose Legendrian knot in S^3 and by Lemma 6.5 that knot must destabilize to a knot with $\mathrm{tb} = pq$. In other words, there is a subset C' of C such that $\xi|_{C'} = \xi'$ is in $\mathrm{Tight}_0(C;pq)$. Now if ξ' is described by a 2-inconsistent pair of paths, then as above we see that we can add convex Giroux torsion to ξ to get an element in $\mathrm{Tight}_l(C;k)$. If the Legendrian corresponding to ξ cannot be destabilized to a contact structure on $\mathrm{Tight}_0(C;pq)$ corresponding to a totally 2-inconsistent pair of paths, then after adding twisting to ξ so that the boundary slope is ∞ the contact structure will be overtwisted by Lemma 6.13. Thus once again we see that $|\mathrm{Tight}_l(C;k)|$ is the number of totally 2-inconsistent paths representing q/p.

Finally, if $pq > 0$ and $k \leq pq - p - q$, then we can make the same argument as above, except notice that according to Lemma 6.12 two of the elements in $\mathrm{Tight}_0(C;pq)$ corresponding to totally 2-inconsistent paths contain a convex torus T with two dividing curves of slope $pq - p - q$ and the rest contain a convex torus T with two dividing curves of slope ∞ (and in both cases any torus further from the boundary have the same dividing slope). Thus adding a contact structure on $T^2 \times [0,1]$ with dividing slopes k and pq on the boundary to C with the first two contact structures will have convex $1/2$ Giroux torsion, while adding the same contact structure to the other contact structures will still have no convex Giroux torsion. However, we can add a convex $1/2$ Giroux torsion layer to these to get contact structures on $\mathrm{Tight}_{1/2}(C;k)$ and thus the count of such structures is still the same. One can similarly argue for $\mathrm{Tight}_l(C;k)$. □

Proof of Claim A. We begin with a specific example. Consider the pair of paths (P_1,P_2) representing q/p with all the signs of P_1 positive and all the signs of P_2 negative. From Lemma 7.1 below, we know that when $pq < 0$, the contact structure ξ_{P_1,P_2} is the one supported by the open book with binding the (p,q)–torus knot and when $pq > 0$, the contact structure is obtained from the tight contact structure on S^3 by a half Lutz twist.

Let ξ_l be the contact structure obtained from ξ_{P_1,P_2} by performing an l-fold Lutz twist on a transverse push-off of L_{P_1,P_2} for $l \in \frac{1}{2}\mathbb{N} \cup \{0\}$. Similarly ξ_l can also be obtained from the complement of L_{P_1,P_2} by attaching a $T^2 \times [0,1]$ with convex l Giroux torsion and then a tight solid torus that is a neighborhood of a Legendrian knot L_l in ξ_l with $\mathrm{tb} = pq$. In [15, Section 5], it was shown that $\mathrm{tor}(L_l) = l$. Let (C,ξ_l') be the contact structure on the

complement of L_l. Clearly (C, ξ_l') has convex Giroux torsion l, but not $l+1$. Thus we have established the claim for the contact structure ξ_{P_1,P_2}.

The key to proving ξ_l has Giroux torsion l from [15] is to consider a specific arc γ on a Seifert surface for the torus knot and showing that in ξ_l the maximal twisting $\overline{tw}(\gamma) = -2l$ where $\overline{tw}(\gamma)$ is defined to be the maximum of the twisting of the contact planes along any Legendrian approximation of γ (with endpoints fixed) with respect to the framing on γ coming from the Seifert surface. It is easy to see that $\overline{tw}(\gamma) \leq -2l$, but to show it is exactly $-2l$ one needs to use that the contact structure on the complement of the torus knot is universally tight. Thus we can only apply this argument to the contact structure considered above (for the universally tightness, see the proof of Lemma 7.1).

To prove Claim A for the other contact structures we proceed as follows. Recall that C can be thought of as the union of two solid tori V_1 and V_2 and $S^1 \times P$ (see Section 6.1). A Seifert surface for the (p,q)–torus knot can be constructed by taking q meridian disks in V_1, p meridian disks in V_2 and pq, 1-handles in $S^1 \times P$ that connect the disks. The arc γ above can be taken to be a co-core to one of these 1-handles and hence lives in $S^1 \times P$. Also recall there is an annulus A' that has both boundary components on ∂C and when C is cut along A' one obtains two solid tori, one containing V_1 and the other V_2. The curve γ can also be taken to be a curve on A' and the framing given to γ by the Seifert surface is the same as the one given by A'. Thus we can measure $\overline{tw}(\gamma)$ using the A' framing.

Now since we are considering pairs of decorated paths P_1 and P_2 that are totally 2-inconsistent, we know the contact structure on $S^1 \times P$ is contactomorphic to $\xi_{\pm\pm}$ and hence (up to switching co-orientations on the contact planes) independent of the choice of totally 2-inconsistent pairs of paths. Now let $\widetilde{\xi}_l$ be the result of attaching l convex Giroux torsion to $S^1 \times P$ along ∂C. We have that $\overline{tw}(\gamma)$ in $\widetilde{\xi}_l$ is $-2l$. This is because it must be greater than or equal to $-2l$ by construction, but it cannot be larger than $-2l$ since if it were, that would contradict the fact that in ξ_l' considered above we have that $\overline{tw}(\gamma) = -2l$ (recall that $\widetilde{\xi}_l$ is a subset of ξ_l').

Finally consider any totally 2-inconsistent pair of paths (P_1, P_2). We can construct contact structures ξ_l' as above associated to ξ_{P_1,P_2} and inside ξ_l' we have the contact structures $\widetilde{\xi}_l$ on $S^1 \times P$. We can again consider $\overline{tw}(\gamma)$ in ξ_l' and we again clearly have $\overline{tw}(\gamma) \geq -2l$. Suppose $\overline{tw}(\gamma) > -2l$. Then we can smoothly isotope the annulus A' (relative to its boundary), so that it contains a Legendrian realization of γ with twisting larger than $-2l$. As in the proof of Lemma 6.15 we can use the isotopy discretization (Theorem 2.30) to get annuli $A_1 = A', \dots A_k$ such that A' is our original annulus (that by construction contains a Legendrian realization of γ with twisting $-2l$) and A_k contains a Legendrian realization of γ with twisting larger than $-2l$, and A_i is obtained from A_{i-1} by a bypass attachment. But recall, in the proof of Lemma 6.15 we showed by induction that A_i is contained on $S^1 \times P$ with a contact structure contactomorphic to $\widetilde{\xi}_l$. This contradicts that $\overline{tw} = -2l$ in $\widetilde{\xi}_l$ and completes the proof of the claim. □

Proof of Claim B. Suppose that ξ and ξ' are two contact structures on $\mathrm{Tight}_0(C; pq)$ associated to totally 2 inconsistent pairs of decorated paths (P_1, P_2) and (P_1', P_2') representing q/p, respectively, such that $(P_1, P_2) \neq (P_1', P_2')$. Now let ξ_l and ξ_l' be the result of adding convex

l Giroux torsion to ξ and ξ', respectively. We first note that by Claim A we know that ξ_l is not contactomorphic to ξ'_k if $l \neq k$, so we are left to see that ξ_l and ξ'_l are distinct.

From Lemma 2.20, we know that $\mathrm{rot}(L_{P_1,P_2}) \neq \mathrm{rot}(L_{P'_1,P'_2})$. Recall that the rotation number is the relative Euler class of the contact structure evaluated on a Seifert surface of the knot. Since adding full torsion does not change the relative Euler class and adding half torsion changes the sign of the relative Euler class, we see that the relative Euler class of ξ_l and ξ'_l are distinct for all $l \in \frac{1}{2}\mathbb{N}$, thus proving Claim B. □

7. Classification of non-loose torus knots

In this section, we begin by identifying some special contact structures and their associated pairs of decorated paths, and end by proving that our algorithm from Section 3 really does give a compete classification of non-loose Legendrian (p,q)–torus knots. To this end, we first understand non-loose Legendrian torus knots without convex Giroux torsion. The classification of these non-loose Legendrian torus knots hinges on the classification of such knots with $\mathrm{tb} = pq$. All others, except for the one when $pq < 0$ and $\mathrm{tb} = |pq| - |p| - |q|$, will either be stabilizations or destabilizations of these. The homotopy classes of overtwisted contact structures where the non-loose Legendrian (p,q)–torus knots with $\mathrm{tb} = pq$ live were determined in Section 2.5. In Section 7.2, we will see when the stabilizations of non-loose knots with $\mathrm{tb} = pq$ stay non-loose and when stabilizations of two different non-loose knots with $\mathrm{tb} = pq$ become equivalent. We then consider in Section 7.3 which non-loose knots with $\mathrm{tb} = pq$ destabilize. In Section 7.4, we consider the extra non-loose Legendrian when $pq < 0$ and $\mathrm{tb} = |pq| - |p| - |q|$, and how they relate to the other non-loose Legendrian knots. In the following section, we will determine the convex Giroux torsion of these examples is zero (except in one case where it is a half). In Section 7.6 we consider non-loose Legendrian knots with convex Giroux torsion in the complement and finally in the last section we prove that our algorithm from Section 3 really does give a compete classification of non-loose Legendrian (p,q)–torus knots.

7.1. Contact structures described by special pairs of decorated paths.

It will be useful to understand explicitly some of the contact structures associated with pairs (P_1,P_2) of decorated paths in the Farey graph for the (p,q)–torus knot. The first statement of the following lemma was observed in [43] and previously for some negative torus knots in [25], in terms of contact surgery diagrams.

Lemma 7.1. *Let (P_1,P_2) be a pair of paths representing q/p and decorated such that P_1 has only positive signs and P_2 has only negative signs. We have the following:*

1. *If $pq < 0$ then $\xi_{\pm P_1,\pm P_2}$ is the contact structure $\xi_{|pq|-|p|-|q|+1}$ and is supported by the open book with binding the (p,q)–torus knot $T_{p,q}$.*
2. *If $pq > 0$ then $\xi_{\pm P_1,\pm P_2}$ is the contact structure $\xi_{-pq+p+q}$ which is obtained from ξ_{std} by a half Lutz twist on the unique maximal self-linking number transverse representative of $T_{p,q}$ in (S^3,ξ_{std}).*

Proof. Consider a contact structure $\xi'_{P_1,P_2} \in \mathrm{Tight}_0(C;pq)$, which is constructed by gluing two solid tori together with contact structures determined by the decorated paths (P_1,P_2) and then removing a neighborhood of a Legendrian divide from the torus. Notice that

when pulled back to the universal cover of C the solid tori will complete unwrap (that is their pre-image under the covering map will be copies of the universal cover of the solid tori). Thus for ξ'_{P_1,P_2} to be universally tight, each path can have only one sign. So there are at most four universally tight contact structures. Moreover, if (P_1, P_2) are not totally 2-inconsistent then Lemma 6.13 says adding Giroux torsion to (C, ξ'_{P_1,P_2}) will result in an overtwisted contact structure; while by Lemma 6.15 if (P_1, P_2) are totally 2-inconsistent, then (C, ξ'_{P_1,P_2}) remains tight even after one adds Giroux torsion to it. Thus $\xi_{\pm P_1,\pm P_2}$ are the only two possible contact structures that are universally tight and remain tight when Giroux torsion is added; in addition, Section 2.5 says ξ_{P_1,P_2} and $\xi_{-P_1,-P_2}$ are isotopic (since they are homotopic as plain fields). In [22], the first author and Vela-Vick showed that for a closed contact 3–manifold (M, ξ), the complement of a neighborhood of transverse knot supporting (M, ξ) is universally tight, and after adding convex Giroux torsion to its boundary, it remains tight. In Proposition 7.5, we will see that all the negative stabilizations of L_{P_1,P_2} are non-loose and hence the transverse push-off of L_{P_1,P_2} has both these properties, and it is the only Legendrian with these properties (the contact structure $\xi_{-P_1,-P_2}$ also has these properties, but the transverse push-off of $L_{-P_1,-P_2}$ will be loose since a single negative stabilization of it is loose, see Proposition 7.5 below). Thus ξ_{P_1,P_2} is the contact structure supported by $T_{p,q}$ when $pq < 0$. The d_3-invariant can be computed from [33, Theorem 1.2] or [1, Corollary 1.2] (note those papers consider the Hopf invariant, which in our context is $-d_3$).

When $pq > 0$, $T_{p,q}$ supports ξ_{std}, but adding a half Lutz twist to ξ_{std} along the maximal self-linking number representative of $T_{p,q}$ will also have these properties and contain a non-loose Legendrian realization of $T_{p,q}$ with $\mathrm{tb} = pq$ and $\mathrm{tor} = 0$. Thus the contact structure must be ξ_{P_1,P_2}. The d_3-invariant changes by subtracting the self-linking number of the transverse knot [23, Proof of Theorem 4.3.1] thus we see the contact structure is $\xi_{-pq+p+q}$. □

We explicitly identify another contact structure on terms of decorated paths. This was also observed in [43] in terms of contact surgery diagrams.

Lemma 7.2. *Let (P_1, P_2) be a pair of decorated paths in the Farey graph for the (p, q)–torus knot. Suppose that the signs of all basic slices in P_1 and P_2 are the same, then $\xi_{P_1,P_2} = \xi_{std}$ for $pq < 0$, and $\xi_{P_1,P_2} = \xi_1$ for $pq > 0$.*

Remark 7.3. If $q/p < -2$, then Lemma 7.2 remains true even if the basic slices in the last continued fraction block in P_2 have any signs.

Proof. When $pq < 0$, the last continued fraction block in P_2 is $n+1, n+2, \dots, -1$ for $n = \lfloor q/p \rfloor$. Given the hypothesis on (P_1, P_2), the concatenated path $\overline{P_1} \cup P_2$ can be shortened to $n, n+1, \dots, -1$ where each edge in the path has some sign (notice the edge from n to $n+1$ represents a basic slice since all of the edges that were shortened had the same sign). Now extending this path by adding the edge from ∞ to n, we may think of this path as describing a contact structure on the solid torus with lower meridian ∞ and dividing slope -1. According to Lemma 2.6, we know this contact structure is tight and by Theorem 2.5 it is unique. Now the path from 0 to -1 also represents the unique tight structure on this

solid torus. The union of these two tight contact structures on the solid tori now gives the tight contact structure on S^3.

When $pq > 0$, the same argument shows that ξ_{P_1,P_2} is obtained by gluing a solid torus with lower meridian ∞ and dividing slope 1 to a solid torus with upper meridian 0 and dividing slope 1. This is clearly the result of performing a half Lutz twist on the maximal self-linking number unknot in the standard tight contact structure on S^3 and hence ξ_1. □

It will be useful to have an explicit description of ξ_1 in terms of torus knots. This is given in the following lemma, but we first need another description of ξ_1 in terms of pairs of paths. At the end of Section 2.3 we saw that ξ_1 is also described by paths P_1' and P_2' such that all the signs of the basic slices in P_1' are $\mp$, except the first one which is $\pm$ and all the basic slices of P_2' are $\pm$, except the first one which is $\mp$.

Lemma 7.4. *For any positive (p,q)–torus knot $T_{p,q}$, the contact structure ξ_1 can be described as follows. Let (C,ξ) be the complement of a standard neighborhood of the Legendrian representative of $T_{p,q}$ with $\mathrm{tb} = pq - p - q$ in (S^3,ξ_{std}). Attach a basic slice in $\mathrm{Tight}^{min}(T^2\times[0,1];\infty,pq-p-q)$ to (C,ξ) and then a basic slice in $\mathrm{Tight}^{min}(T^2\times[0,1];pq,\infty)$ with the opposite sign to the result. Finally glue the unique tight contact structure on a solid torus with meridional slope ∞ and dividing slope pq.*

The final torus is a standard neighborhood of a non-loose (p,q)–torus knot with $\mathrm{tb} = pq$ that is described by the pair of decorated paths (P_1',P_2') where the first edge in P_1' is $\pm$ and all the others are $\mp$ while the first edge of P_2' is $\mp$ and all the others are $\pm$.

Proof. Let $\xi_\pm$ be the contact structure which is the result of attaching a $\pm$–basic slice to C with dividing slopes ∞ and $pq-p-q$. Since we discussed that $\xi_1 = \xi_{P_1',P_2'}$ above, it is sufficient to show that $\xi_{P_1',P_2'}$ is the result of attaching a $\mp$–basic slice to $\xi_\pm$ with dividing slopes pq and ∞.

Since the basic slices in (P_1',P_2') adjacent to q/p are of opposite signs, we may argue as in the proof of Lemma 6.10 that $\xi_{P_1',P_2'}$ may be factored into two solid tori V_1' and V_2' and $S^1\times P$, where P is a pair of pants. Also the contact structure on $S^1\times P$ admits a convex annulus A running from $\partial V_1'$ to $\partial V_2'$ with two dividing curves that run from one boundary component to the other. Moreover, the contact structure on V_1' is described by a path in the Farey graph whose signs are all $\mp$ and the path for V_2' has all signs $\pm$. Notice that adding an I-invariant neighborhood of A to $V_1'\cup V_2'$ yields a manifold C' that is isotopic to C and $\partial C'$ is convex with dividing slope ∞. Thus $C\setminus C'$ is $T^2\times[0,1]$ and the contact structure $\xi_{P_1',P_2'}$ restricted to $T^2\times[0,1]$ will be a basic slice with dividing slopes pq and ∞. Below we will see that the contact structure on C' is $\xi_\pm$ discussed above and the basic slice has sign $\mp$.

Now consider the pair of paths (P_1,P_2) representing q/p with P_1 having all signs $\pm$ and P_2 having all signs $\mp$. From Lemma 7.1 we know that ξ_{P_1,P_2} is obtained from performing a half-Lutz twists on the maximal self-linking transverse representative of $T_{p,q}$ in ξ_{std} and then removing a solid torus with convex boundary having dividing slope pq. Notice that this contact structure can be described by taking $\xi_\pm$ on C' and then adding another basic slice with dividing slopes pq and ∞ with sign $\pm$.

We note that ξ_{P_1,P_2} can be decomposed into piece as we did for $\xi_{P_1',P_2'}$. In particular inside (C, ξ_{P_1,P_2}) we see a submanifold C' isotopic to C such that $C \setminus C'$ is a basic slice with dividing slopes pq and ∞, and sign $\pm$. Moreover, we see that ξ_{P_1,P_2} and $\xi_{P_1',P_2'}$ restricted to C' are the same since they are given by attaching a thickened annulus to V_1' and V_2' with the same contact structures on them. Thus the only difference between ξ_{P_1,P_2} and $\xi_{P_1',P_2'}$ is the sign of the bypass added, thus giving the desired result. (Notice that ξ_{P_1,P_2} and $\xi_{P_1',P_2'}$ cannot be the same contact structure since they are contact structures on the complement of Legendrian knots with different rotation number, see Lemma 2.20.) □

7.2. **Non-loose torus knots with** tb $\leq pq$**.** In this section we will classify non-loose (p,q)–torus knots with tb $\leq pq$ that are stabilizations of the Legendrian knots L_{P_1,P_2} constructed in the proof of Lemma 6.8 and determined by pairs of decorated paths. In Section 2.5 we determined the homotopy class of plane fields that support such torus knots with tb $= pq$ and determining the rotation numbers of them. Here we will see how each of these non-loose tb $= pq$ torus knots generates a "wing" or a "diamond" and see how the wings and diamonds for different tb $= pq$ torus knots interact. This will lead to the desired classification.

7.2.1. *Wings for i-inconsistent paths.* We now consider a pair of decorated paths (P_1, P_2) that is i-inconsistent for some $i \geq 2$ that describe a (p,q)–torus knot. We assume here that (P_1, P_2) does not describe a positive torus knot in (S^3, ξ_1) or a negative torus knot in the tight contact structure ξ_{std}. As above, see the beginning of this section or Section 2.3, we break the truncated paths (P_1, P_2) into the continued fraction blocks

$$(A_2, \dots, A_{2n}) \text{ and } (B_1, B_3, \dots, B_{2m-1}).$$

(we will only discuss this case here, with the case of $(A_1, \dots, A_{2n-1})$ and $(B_2, \dots, B_{2m})$ being analogous). Let s_k be the slope in A_k or B_k which is farthest from q/p, T_k the convex torus in V_1 or V_2 with two dividing curves of slope s_k, and L_k a Legendrian ruling curve on T_k of slope q/p. Finally set $n_k = |s_k \bullet \frac{q}{p}|$.

Proposition 7.5. *If $pq > 0$ then we assume that the ambient contact structure is not ξ_1 and if $pq < 0$ we assume that the ambient contact structure is not ξ_{std}. Given an i-inconsistent pair of paths (P_1, P_2) for q/p as above assume that i is even and all the the basic slices in the continued fractions blocks $A_2, \dots, A_{i-2}, B_1, \dots, B_{i-1}$ are negative while some in A_i are positive. Then we have $S_+^{n_{i-1}}(L_{P_1,P_2})$ is loose and any Legendrian $S_+^k S_-^l(L_{P_1,P_2})$ for $k < n_{i-1}$ and $l \geq 0$ is non-loose.*

Similarly, for $S_-^{n_{i-1}}(L_{-P_1,-P_2})$ is loose and any Legendrian $S_+^k S_-^l(L_{-P_1,-P_2})$ for $k \geq 0$ and $l < n_{i-1}$ is non-loose. See Figure 22.

When i is odd, the same result holds if all basic slices in the continued fraction blocks $A_2, \dots, A_{i-1}$, $B_1, \dots, B_{i-2}$ are positive and some in B_i are negative.

We will call the set

$$W(L_{P_1,P_2}) = \{S_+^k S_-^l(L_{P_1,P_2}) \text{ for } k < n_{i-1} \text{ and } l \geq 0\},$$

the *wing of* L_{P_1,P_2}, and similarly for $L_{-P_1,-P_2}$. We think of these as the non-loose Legendrian knots generated by $L_{\pm P_1,\pm P_2}$. See Figure 22.

When $pq < 0$ and $\mathrm{tb} < pq$ this proposition also follows from [43, Corollary 4.3], though the structure of the wings was not made explicit. The result for the negative trefoil and $\mathrm{tb} < -6$ or equal to 5 was also established in [25].

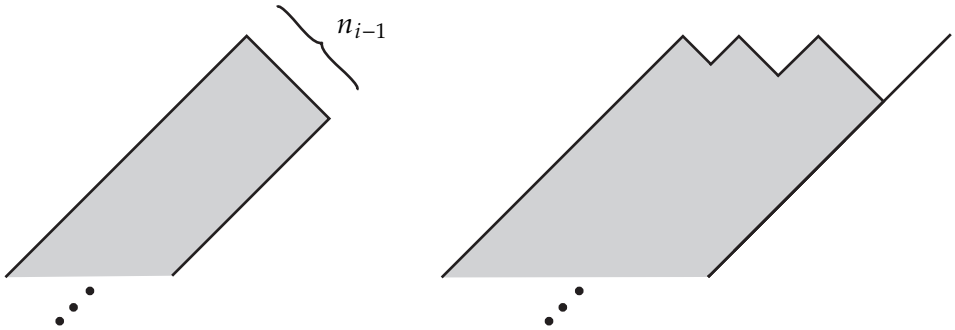

FIGURE 22. On the left is the wing $W(L_{P_1,P_2})$ from Proposition 7.5. On the right is the wing W from Proposition 7.10 generated from all the pairs of paths compatible with (P_1, P_2). Each integral point in the shaded region, whose coordinates sum to be odd, is realized by a unique non-loose Legendrian knot with tor = 0. The peaks are at $\mathrm{tb} = pq$ and there are $i-1$ peaks (for an i-inconsistent path) each corresponding to a k-inconsistent pair of paths (P_1^k, P_2^k) compatible with (P_1, P_2) for $2 \leq k \leq i$ and the distance between the peaks corresponding to (P_1^k, P_2^k) and (P_1^{k-1}, P_2^{k-1}) is $2n'_{k-1}$ (see the proof of Proposition 7.10). Once one computes a rotation number of one of the peaks using Lemma 2.19 the others are determined by the distance between the peaks. The wings for $(-P_1, -P_2)$ are obtained by reflecting these wings about a vertical line.

Remark 7.6. We will see in the proof below that stabilizations of the L_{P_1,P_2} become loose because they can be put on a convex torus that allows the path $\overline{P_1} \cup P_2$ to be shortened merging two basic slices with opposite sign. This does not happen if ξ_{P_1,P_2} is ξ_{std} since the ambient contact structure is tight. We will address the case when $pq > 0$ and ξ_{P_1,P_2} is $\xi_{-pq+p+q}$ at the end of this section and in Section 7.2.2 below we will see what is different when $pq > 0$ and ξ_{P_1,P_2} is ξ_1.

We first observe the following results.

Lemma 7.7. *With the notation above, the integers $n_i = |s_i \bullet \frac{q}{p}|$ start at 1 and are strictly increasing (unless $q/p = (2n+1)/2 < 0$ in which case $n_1 = n_2$).*

Proof. The claim for $q/p = (2n+1)/2 < 0$ can easily be checked, so we assume that we have some other q/p. By Lemmas 2.10 and 2.11 we know that there is an edge from q/p to s_1 and there is not an edge between q/p and s_2. Thus $n_1 = |\frac{q}{p} \bullet s_1| = 1 < |\frac{q}{p} \bullet s_2| = n_2$. We now inductively prove the n_i are strictly increasing. To this end we assume this has been proven for $i < j$ and establish that $n_i < n_j$. Recall, from Observation 2.13 we know that there is an edge from s_{j-1} to s_j and the minimal path from s_j to s_{j-2} is given by $v_0 =$

$s_j, v_1, \dots, v_k = s_{j-2}$, where $v_l = ls_{j-1} \oplus s_j$ for $0 \le l \le k$. Then we have

$$\begin{aligned} s_{j-2} \bullet \frac{q}{p} &= (ks_{j-1} \oplus s_j) \bullet \frac{q}{p} \\ &= (ks_{j-1} \bullet \frac{q}{p}) + (s_j \bullet \frac{q}{p}). \end{aligned}$$

Since $(s_{j-1} \bullet \frac{q}{p})$ and $(s_j \bullet \frac{q}{p})$ have opposite sign and $(s_{j-2} \bullet \frac{q}{p})$ and $(s_j \bullet \frac{q}{p})$ have the same sign, we have

$$\left|s_{j-2} \bullet \frac{q}{p}\right| + \left|(ks_{j-1}) \bullet \frac{q}{p}\right| = \left|s_j \bullet \frac{q}{p}\right|, \tag{5}$$

confirming that the n_i are increasing. □

Lemma 7.8. *Let $(T^2 \times [0,1], \xi)$ be a $\pm$ basic slice with dividing slopes s_i on $T^2 \times \{i\}$. Let L_0 be a Legendrian ruling curve of slope s_1 on $T^2 \times \{0\}$ and L_1 a Legendrian divide on $T^2 \times \{1\}$. Then L_0 is $S_\pm(L_1)$. Moreover, if L_0' is a Legendrian divide on $T^2 \times \{0\}$ and L_1' is a ruling curve of slope s_0 on $T^2 \times \{1\}$, then L_1' is $S_\mp(L_0')$.*

Let s be a vertex in the Farey graph outside the interval $[s_0, s_1]$ for which there are vertices in the Farey graph in $[s, s_0)$ with an edge to s_1. If L_i'' is a ruling curve of slope s on $T^2 \times \{i\}$ then L_0'' is $S_\pm^k(L_1'')$ where $k = |(s_1 \ominus s_0) \bullet s|$. Moreover, there is a similar statement when s is outside of $[s_0, s_1]$ for which there are vertices in the Farey graph in $(s_1, s]$ with an edge to s_0, and with the roles of L_0'' and L_1'' interchanged as in the previous paragraph.

Remark 7.9. Notice that this lemma implies that, with the notation above the q/p-sloped ruling curve L_k on T_k is Legendrian isotopic to $S_+^{n_k}(L_{P_1,P_2})$ if k is odd and $S_-^{n_k}(L_{P_1,P_2})$ if k is even (since the sign of bypass will change if we consider the basic slice is from $T^2 \times \{1\}$ to $T^2 \times \{0\}$).

Proof. We will show how to build a solid torus in $T^2 \times [0,1]$ that is a regular neighborhood of L_1 and isotope L_0 into this neighborhood so that it has a standard neighborhood with dividing slope $\mathrm{tb}(L_1) - 1$. This will establish that L_0 is a stabilization of L_1 and the sign of the stabilization is determined by the relative Euler class. That is, if A is an annulus in $T^2 \times [0,1]$ with boundary $L_0 \cup L_1$, then $\mathrm{rot}(L_0) - \mathrm{rot}(L_1)$ is the relative Euler class of the basic slice evaluated on A, which in turn is $\chi(A_+) - \chi(A_-)$, where $A_\pm$ are the positive and negative regions of A once it is made convex.

To construct the claimed solid torus, we take parallel copies T_i of $T^2 \times \{i\}$ inside of $T^2 \times [0,1]$ that are contact isotopic to the the respective boundary components. Clearly L_i still sits on T_i and we an take A be the annulus with boundary $L_0 \cup L_1$ sitting on $T_0 \cup T_1$. As the twisting of each component of ∂A is non-positive, we can make A convex. We claim that A can be chosen so that it has a single dividing curves, and it is an arc with both boundary components on L_0. Assuming this for the moment we complete our proof. Let $N = A \times [-1,1]$ be an $[-1,1]$-invariant neighborhood of $A = A \times \{0\}$. Notice that ∂N consists of four parts, $A_{-1} = A \times \{-1\}$, $A_1 = A \times \{1\}$, $L_0 \times [-1,1]$, and $L_1 \times [-1,1]$. The first 3 are convex surfaces, with the first two having dividing set the same as A while the third having dividing set being two arcs each running from one boundary component to the other. We can round the two corners between the first three surfaces to get a convex annulus A'

with one dividing curves isotopic to its center curve and intersecting L_0 twice. Notice that by choosing the correct dividing set on A to begin with, we can assume the characteristic foliation of A' has Legendrian boundary and each boundary component looks like a Legendrian divide, by which we mean the boundary components are circles of singularities in the foliation and near by the foliation is non-singular and transverse to the boundary, moreover one boundary will be an attracting circle of singularities and the other will be repelling.

We now have $A' \cup (L_1 \times [-1,1])$ is a torus bounding a solid torus. We now consider $L_1 \times [-1,1]$. This has characteristic foliation given by $L_1 \times \{t\}$ for $t \in [-1,1]$. That is, it is a pre-Lagrangian annulus and thus cannot be convex. But we build a standard model for a neighborhood of $L_1 \times [-1,1]$. Specifically, in $\mathbb{R}^3/\sim$, where $(x,y,z) \sim (x+1,y,z)$, with the contact structure $dz - y\,dx$ we find an open set around $S = \{(x,y,z) : y = 0, |z| \leq 1\}$ that is contactomorphic to a neighborhood of $L_1 \times [-1,1]$ by a contactomorphism taking S to $L_1 \times [-1,1]$ and a neighborhood of $\partial A'$ to constant z annuli with, say, positive y coordinate. In this local model we can deform $L_1 \times [-1,1]$ by slightly pushing its interior to have negative y coordinate. The characteristic foliation on this new annulus A'' now has Legendrian boundary and on the interior flow lines that spiral to one boundary component in positive time and the other in negative time. We can finally slightly modify A' in this local model so that the orbits near $\partial A' = \partial A''$ spiral towards the boundary components in the same way that those on A'' do. In particular, $A' \cup A''$ is not a convex torus with two dividing curves. One is in the center of A' and the other is in A''. In addition, we see that L_1 is isotopic to the Legendrian divides on $A' \cup A''$ and again, L_0 sits on this torus intersection one of the dividing curves twice. Let N be the solid torus bounded by $A' \cup A''$. This is a standard neighborhood of L_1 and we see that L_0 has contact twisting one less than L_1 and so when it is contact isotoped into the interior of N we see that it has a neighborhood as claimed above.

We are now left to establish our claim concerning the dividing set on A. Notice that the dividing curves of A intersect L_0 twice and L_0 zero times. Thus we know the dividing set is as claimed, except that there might also be some closed dividing curves isotopic to the core of A. We must show that A can be chosen so that this is not the case (one must be careful, as there are choices for A where there are such closed curves). To this end, notice that given the slopes s_0 and s_1 with an edge in the Farey graph connecting them, there will be exactly two slopes that both have an edge to s_0 and s_1. One will be in $[s_0, s_1]$ while the other s will be outside this interval. Let B be an annulus of slope s in $T^2 \times [0,1]$ with boundary a ruling curves on the $T^2 \times \{i\}$. We can make B convex and it must have exactly two dividing curves running from one boundary component to the other. This is because, if not, we could Legendrian realize the core curve in B with contact twisting 0 with respect to B. We could then find a torus T parallel to the boundary of $T^2 \times [0,1]$ containing this curve so that it also had twisting 0 with respect to T. This implies that T can be made convex with dividing slope s, contradicting the fact that, as a basic slice, $T^2 \times [0,1]$ is minimally twisting. Thus the dividing curves are as claimed. Now we can Legendrian realize a curve γ on B that runs from one boundary component to the other and has contact twisting 0, we can moreover assume that one boundary component of γ is one L_1 and the other is not on the Legendrian divides on $T^2 \times \{0\}$. Now we can isotope $T^2 \times \{0\}$, keeping if fixed near $\partial\gamma$

so that its ruling curves have slope s_1. This allows us to take an annulus A from L_0 to L_1 that contains γ. The twisting of γ with respect to this annulus is still 0, so we can make A convex relative to γ. Because the twisting of γ is 0 we see that it cannot intersect the dividing curves of A. This implied that there can be no closed curves in the dividing set of A and hence the dividing curves of A must be as claimed.

The proof for the analogous case with the Legendrian knots L_0' and L_1' is the same.

For the second statement, notice that the annulus A of slope s from $T^2 \times \{0\}$ to $T^2 \times \{1\}$ with boundary ruling curves cannot have a boundary parallel dividing curve on $T^2 \times \{1\}$, since if there were we could attach a bypass to $T^2 \times \{1\}$ and get a convex torus of dividing slope outside of $[s_0, s_1]$ contradicting the minimal twisting of a basic slice. Thus the dividing curves on A have some boundary parallel dividing curves on $A \cap (T^2 \times \{0\})$ and the rest run across from one boundary component to the other. We can use the bypasses to destabilize L_0'' and then isotope it to L_1''. The signs of the destabilization are determined by the sign of the bypass and then number has to be as indicated, otherwise there would be a bypass on $T^2 \times \{1\}$. □

Proof of Proposition 7.5. From Lemma 7.8 we know that L_{i-1} is the same as $S_+^{n_{i-1}}(L_{P_1,P_2})$. Notice, by Observation 2.13, there is an edge in the Farey graph from s_{i-1} to s_i. Thus the path $\overline{A}_i, \dots, \overline{A}_2, B_1, \dots B_{i-1}$ can be shortened. Since not all the signs of the basic slices in this path are the same, the resulting contact structure on $T^2 \times [0,1]$ is overtwisted. That is we have found an overtwisted disk in the complement of $S_+^{n_{i-1}}(L_{P_1,P_2})$.

Now we will show that $L := S_+^{n_{i-1}-1} S_-^l(L_{P_1,P_2})$ for $l \geq 0$ is non-loose. We can put L on a convex torus T, which is contained in V_2 with slope s_{i-3} (not as a standard ruling curve). To see this, notice that a ruling curve on T would be $S_+^{n_{i-3}}(L_{P_1,P_2})$ by Lemma 7.8 and $n_{i-3} < n_{i-1}$ by Lemma 7.7; thus any further stabilization can be put on T but not as a ruling curve. Let $\overline{S^3 \setminus T} = V_1' \cup V_2'$. Clearly, V_1' and V_2' are tight as the paths in the Farey graph describing them are either minimal or can be shortened to be minimal at vertices whose adjacent edges have the same sign.

Suppose L is loose. Then there is an overtwisted disk in the complement of a standard neighborhood N of L. Notice that $T \cap (\overline{S^3 \setminus N})$ is an annulus A and there is a smooth isotopy of A, rel boundary, to an annulus disjoint from the overtwisted disk. We can assume that the boundary of A is Legendrian curves and perturb A to be convex. By isotopy discretization (Theorem 2.30), there is a sequence of annuli $A_1 = A, \dots, A_k$ such that A_k is disjoint from the overtwisted disk and each A_j is obtained from A_{j-1} by attaching a bypass. Notice that the A_j can be extended to tori T_j containing L, which is just $A_j \cup (T \cap N)$ (after perturbation). Each T_j is obtained from T_{j-1} by a bypass attachment in the complement of L, and T_k is disjoint from the overtwisted disk.

Each T_j breaks S^3 into two solid tori V_1^j and V_2^j. By construction we know that V_1^1 and V_2^1 are both tight. We will inductively prove that each V_1^j and V_2^j is tight and this will contradict the fact that there is an overtwisted disk in the complement of T_k, thus showing that there could not have been an overtwisted disk in the complement of N and that L is non-loose.

We recall that in the part of the path $\overline{P_1} \cup P_2$ between s_{i-3} and s_{i-2} consists of all negative basic slices while the part between s_{i-2} and s_i contains some positive basic slices (and possibly some negative ones too).

We inductively assume that

- the slope t_{j-1} of the dividing curves on T_{j-1} is in (s_i, s_{i-1}),
- if $t_{j-1} \in (s_i, s_{i-2})$, then the contact structures on the tori are given by consistently dividing the path $\overline{P_1} \cup P_2$, by which we mean shortening the path at vertices whose adjacent edges have the same sign or dividing an edge into two edges of the same sign.

Notice that this condition guarantees that the contact structures on V_1^{j-1} and V_2^{j-1} are tight since the contact structures correspond to subdividing the path $\overline{P_1} \cup P_2$ at t_{j-1} and when doing this only the continued fraction blocks with the same sign can be shortened.

First, suppose $t_j \geq t_{j-1}$. By the inductive hypothesis, $t_j \in (s_i, s_{i-1}]$ and we will show that $t_j \neq s_{i-1}$. Assume $t_j = s_{i-1}$. Then the ruling curves on T_j is Legendrian isotopic to $S_+^{n_{i-1}}(L_{P_1,P_2})$ by Lemma 7.8 and any Legendrian curve on T_j is a stabilizations of the ruling curve. However, since $L = S_+^{n_{i-1}-1} S_-^l(L_{P_1,P_2})$, it cannot be a stabilization of the ruling curve and $t_j \neq s_{i-1}$.

Next, suppose $t_j < t_{j-1}$. By the inductive hypothesis, $t_j \in [s_i, s_{i-1})$. Assume $t_j < s_{i-2}$ and the sign of the basic slice between T_{j-1} and T_j is positive. Recall the proof of Lemma 7.7. We labeled the vertices in A_i as $v_0 = s_i, v_2, \dots, v_k = s_{i-2}$ and $v_l = l s_{i-1} \oplus s_i$ for $1 \leq l \leq k$. Also, from Equation (5), we have

$$\left| v_l \bullet \frac{q}{p} \right| = \left| s_i \bullet \frac{q}{p} \right| - l \left| s_{i-1} \bullet \frac{q}{p} \right|.$$

Clearly this implies

$$\left| v_l \bullet \frac{q}{p} \right| - \left| v_{l+1} \bullet \frac{q}{p} \right| = \left| s_{i-1} \bullet \frac{q}{p} \right|. \tag{6}$$

Returning to our problem, the sign of the basic slice implies that $t_{j-1} = v_{l+1}$ for some $0 \leq l < k$. This is because if v_{j-1} were between two v_i then v_j would also be between them and the basic slice would have to be negative (since the basic slice between the two v_i are negative by our hypothesis on t_{j-1}). Clearly $t_j \in [v_l, v_{l+1}]$ and by [3, Remark 2.13], we have

$$\left| v_l \bullet \frac{q}{p} \right| \leq \left| t_j \bullet \frac{q}{p} \right|.$$

Thus combining it with Equation (6), we can conclude

$$\begin{aligned} \left| s_{i-1} \bullet \frac{q}{p} \right| &= \left| v_l \bullet \frac{q}{p} \right| - \left| v_{l+1} \bullet \frac{q}{p} \right| \\ &\leq \left| t_j \bullet \frac{q}{p} \right| - \left| t_{j-1} \bullet \frac{q}{p} \right| \\ &\leq \left| (t_j \ominus t_{j-1}) \bullet \frac{q}{p} \right|. \end{aligned}$$

Therefore, the ruling curves on T_j is Legendrian isotopic to $S_+^k S_-^l(L_{P_1,P_2})$ for $k \geq n_i$ and $l \geq 0$ by Lemma 7.8 and any Legendrian curve on T_j is a stabilizations of the ruling curve. However, since $L = S_+^{n_{i-1}-1} S_-^l(L_{P_1,P_2})$, it cannot be a stabilization of the ruling curve and the basic slice cannot be positive. □

Let (P_1^i, P_2^i) be an i-inconsistent pair of paths that describes a (p,q)–torus knot and assume it is not compatible with and $(i+1)$-inconsistent pair of paths (see Section 2.5 for terminology); moreover, if $pq > 0$ assume that the contact structure given by the paths is not ξ_1. As discussed in Section 2.5, we know that these paths are compatible with a unique k-inconsistent pairs of paths (P_1^k, P_2^k) for all $k = 2, 3, \dots, i$. Let $L_{P_1^k,P_2^k}$ be the Legendrian (p,q)–torus knots corresponding to the paths (P_1^k, P_2^k). We know they are all in the same contact structure and each generates a wing by Proposition 7.5. We will see that all of these wings merge in the sense that when two Legendrian knots in different wings has the same classical invariants then they are isotopic.

As above, see the beginning of this section or Section 2.3, we break the decorated paths (P_1^k, P_2^k) into their continued fraction blocks

$$(A_2^k, A_4^k, \dots, A_{2n}^k) \text{ and } (B_1^k, B_3^k, \dots, B_{2m-1}^k).$$

Notice that the paths A_l^k and B_l^k in the Farey graph are independent of k, only the signs on the edges vary with k.

We will assume that i is even but the discussion for i odd is entirely analogous. Since the pair (P_1^i, P_2^i) is i-inconsistent, we can assume that all the basic slices in $A_2^i, \dots, A_{i-2}^i$, $B_1^i, \dots, B_{i-1}^i$ have the same sign, say negative (the positive case being entirely analogous), and A_i has some positive basic slices. In Section 2.3 we saw that one gets (P_1^{i-1}, P_2^{i-1}) from (P_1^i, P_2^i) as follows: the union of $A_2^i, \dots, A_{i-2}^i$, $B_1^i, \dots, B_{i-3}^i$ and all but the last basic slice of B_{i-1}^i can be shortened to a single edge in the Farey graph, which will have a negative sign, and that edge extends A_i^i to a longer continued fraction block. Thus we exchange the positive basic slice in A_i^i with this new edge and the break the new edge back into its previous edges, but now all having positive signs. Specifically, this means $A_l^{i-1} = A_l^i$ and $B_l^{i-1} = B_l^i$ for all $l > i$, A_i^{i-1} agrees with A_i^i except one of the positive basic slices has turned into a negative one, B_{i-1}^{i-1} consists of one negative basic slice and all the others are positive, and finally A_l^{i-1} and B_l^{i-1} all have only positive basic slices for $l < i-1$. Continuing this shuffling, one sees that the A_l^k and B_l^k for $l < k$ will all have the same sign and the signs are negative if k is even and positive is k is odd. See Figure 12.

As above let s_k be the slope in A_k^i or B_k^i which is farthest from q/p, T_k the convex torus in V_1 or V_2 with two dividing curves of slope s_k, and L_k a Legendrian ruling curve on T_k of slope q/p. We also set $n_k = |s_k \bullet \frac{q}{p}|$.

Proposition 7.10. *With the notation above, there is a fixed line of slope* ± 1 *that contains the lower edge of each wing* $W_{P_1^k,P_2^k}$ *and the union of the wings*

$$W = \bigcup_{k=2}^{i} W_{P_1^k,P_2^k}$$

is coarsely Legendrian simple, i.e. any two Legendrian knots in W with the same tb *and* rot *are equivalent. See Figure 22*

When $pq < 0$ and $\mathrm{tb} < pq$ this proposition also follows from [43, Corollary 4.3], though the coarse Legendrian simplicity was not made explicit.

Proof. We begin with the Legendrian simplicity of W. Consider the contact structure $\xi_{P_1^i,P_2^i}$. Let s'_{i-1} be the slope in B_{i-1} closest to q/p with an edge to s_{i-1} (that is, it is the slope of the second to the last vertex in B_{i-1}). Let T'_{i-1} be the convex torus in V_2 with two dividing curves of slope s'_{i-1} and let L'_{i-1} be a ruling curve on T'_{i-1} with slope q/p. By Lemma 7.8 we know that

$$L'_{i-1} = S_+^{n'_{i-1}}(L_{P_1^i,P_2^i})$$

for $n'_{i-1} = |s'_{i-1} \bullet \frac{q}{p}|$ (since the sign of all basic slices in $B_1, \dots, B_{i-1}$ are negative). Now consider two solid tori V'_1 and V'_2 that T'_{i-1} breaks S^3 into, and the contact structure on V'_1 is given by the path $\overline{P_1}$ followed by $B_1^i \cup \dots \cup B_{i-3}^i$ followed by all but the last edge in B_{i-1}. We can thus exchange the basic slices in the continued fraction block as discussed above. Now it is clear that T'_{i-1} is also a torus in the contact structure $\xi_{P_1^{i-1},P_2^{i-1}}$ and hence its ruling curve is

$$L'_{i-1} = S_-^{n'_{i-1}}(L_{P_1^{i-1},P_2^{i-1}}).$$

In other words, $S_+^{n'_{i-1}}(L_{P_1^i,P_2^i})$ is Legendrian isotopic to $S_-^{n'_{i-1}}(L_{P_1^{i-1},P_2^{i-1}})$. It is also the first time a stabilization of $L_{P_1^i,P_2^i}$ could be isotopic to a stabilization of $L_{P_1^{i-1},P_2^{i-1}}$. Moreover, it is clear that any Legendrian knot in

$$W(L_{P_1^i,P_2^i}) \cap W(L_{P_1^{i-1},P_2^{i-1}})$$

is a stabilization of L'_{i-1} and hence

$$W(L_{P_1^i,P_2^i}) \cup W(L_{P_1^{i-1},P_2^{i-1}})$$

is coarsely Legendrian simple. One may now similarly show that $W(L_{P_1^k,P_2^k}) \cup W(L_{P_1^{k-1},P_2^{k-1}})$ is coarsely Legendrian simple for all k, thus yielding the second part of the proposition.

We now consider the first statement that there is a fixed line which is the lower edge of all the wings. Notice that the lower boundary of all wings contained in a line of slope 1 (or -1 for $(-P_1, -P_1)$) and this line is determined by how many positive stabilizations make one of the $L_{P_1^l,P_2^l}$ loose. Now recall that $L_{P_1^i,P_2^i}$ becomes loose after exactly n_{i-1} positive stabilizations and $L_{P_1^{i-1},P_2^{i-1}}$ will be come loose after exactly n_{i-2} positive stabilizations. Moreover, we just saw that $S_+^{n'_{i-1}}(L_{P_1^i,P_2^i})$ is isotopic to $S_-^{n'_{i-1}}(L_{P_1^{i-1},P_2^{i-1}})$. We claim that

$$n_{i-2} = n_{i-1} - n'_{i-1}.$$

If this is true then it is clear that the line defining the lower edge of the wing of $L_{P_1^i,P_2^i}$ and $L_{P_1^{i-1},P_2^{i-1}}$ will be the same, and the same argument works for all adjacent wings. It is not

hard to see from the Farey graph that $s'_{i-1} = s_{i-1} \oplus s_{i-2}$. Since s_{i-1} and s_{i-2} are on opposite sides of q/p, their intersection number with q/p will have opposite sign. Thus we have

$$\left|s'_{i-1} \bullet \frac{q}{p}\right| = \left|(s_{i-1} \oplus s_{i-2}) \bullet \frac{q}{p}\right| = \left|s_{i-1} \bullet \frac{q}{p}\right| - \left|s_{i-2} \bullet \frac{q}{p}\right|.$$

□

Proposition 7.11. *With the notation above and in Proposition 7.10, let*

$$\overline{W} = \bigcup_{k=2}^{i} W_{-P_1^k, -P_2^k}.$$

No Legendrian element in W is equivalent to an element of $\overline{W}$.

Remark 7.12. In Section 7.7 below we will see that when $pq < 0$, W is disjoint from $\overline{W}$ and hence $W \cup \overline{W}$ is coarsely Legendrian simple. However when $pq > 0$ $W \cap \overline{W} \neq \emptyset$ and hence $W \cup \overline{W}$ is not Legendrian simple.

Proof. Notice any element in W will become loose after a finite number of negative stabilizations, while elements of $\overline{W}$ will stay non-loose after any number of negative stabilizations so no element in W can be equivalent to an element of $\overline{W}$. □

7.2.2. *Diamonds in ξ_1 when $pq > 0$.* Let (P_1, P_2) be a pair of paths for that represent q/p with $pq > 0$ and assume all the signs in the paths are the same, say negative. From Lemma 7.4 we know that ξ_{P_1,P_2} is ξ_1.

Proposition 7.13. *Given P_1 and P_2 as above, the Legendrian knots $S_\pm^k S_\mp^l(L_{\pm P_1, \pm P_2})$ are non-loose if and only if $k < p$ and $l < q$.*

We call the set

$$D(L_{\pm P_1, \pm P_1}) = \{S_\pm^k S_\mp^l(L_{\pm P_1, \pm P_2}) : k < p, l < q\}$$

the *diamond of* $L_{\pm P_1, \pm P_1}$ and think of these as the non-loose Legendrian knots generated from $L_{\pm P_1, \pm P_1}$.

Proof. Notice that the path $\overline{P_1}$ starts at $\lfloor q/p \rfloor$ goes clockwise in some number of jumps to q/p and represents a tight contact structure on a solid torus with lower meridian ∞ and convex boundary with dividing slope q/p. By Lemma 2.6 we can represent this contact structure by the unique contact structure on the solid torus with convex boundary 0 and then a contact structure on $T^2 \times [0,1]$ given by the path $0, 1, \dots, \lfloor q/p \rfloor$ followed by $\overline{P_1}$ and the signs on the edges between 0 and $\lfloor q/p \rfloor$ can be chosen arbitrarily. In particular we can choose them to be negative (that is the same sign as the signs in P_1 and P_2). Thus inside V_1 we have a convex torus T_0 with two dividing curves of slope 0 such that the path from 0 to q/p consists of all negative signs. Similarly, we have a convex torus T_∞ of slope ∞ inside V_2 and again the path from q/p to ∞ consists of all negative signs. Let L_0 and L_∞ be ruling curves of slope q/p on the tori T_0 and T_∞, respectively. By Lemma 7.8 we know that L_0 is $S_-^q(L_{P_1,P_2})$ and that L_∞ is $S_+^p(L_{P_1,P_2})$. Notice that T_0 separates S^3 into two solid tori one of which has meridional slope 0 and hence we see a dividing curve on T_0 bounds an

overtwisted disk in this solid torus and hence L_0 is loose. Similarly L_∞ is also loose. Thus we see that $S_+^k S_-^l(L_{P_1,P_2})$ is loose if either $k \geq p$ or $l \geq q$.

Now if $k < p$ and $l < q$, then the Legendrian knot $S_\pm^k S_\mp^l(L_{\pm P_1,\pm P_2})$ cannot be put on either T_0 or T_∞ and the same isotopy discretization argument as in the proof of Proposition 7.5 shows that $S_\pm^k S_\mp^l(L_{\pm P_1,\pm P_2})$ is non-loose.

A similar argument establishes the result for $L_{-P_1,-P_2}$. □

Proposition 7.14. *Given P_1 and P_2 as above, the union $D' = D(L_{P_1,P_2}) \cup D(L_{-P_1,-P_2})$ is coarsely Legendrian simple, that is, any two Legendrian knots in D' with the same* tb *and* rot *are equivalent. See Figure 23.*

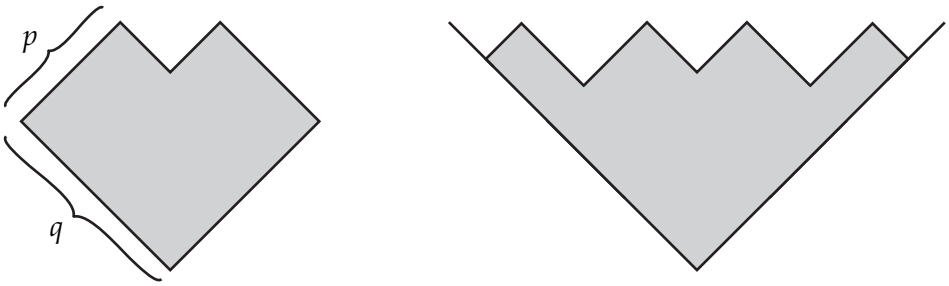

FIGURE 23. The union D' of the diamonds associated with to completely consistent paths describing q/p for $pq > 0$ is shown on the left. The peaks occur at pq and the central valley occurs after stabilizing a peak $q - p$ times. The union of the diamonds of all pairs of paths compatible with the original paths is shown on the right. Each integral point in the shaded region, whose coordinates sum to be odd, is realized by a unique non-loose Legendrian knot with tor = 0.

Proof. As argued in the proof of the previous proposition, inside V_1 we find a convex torus T_1 with two dividing curves of slope 1. Let L_1 be a ruling curve on T_1 with slope q/p. Lemma 7.8 tells us that L_1 is $S_-^{q-p}(L_{P_1,P_2})$.

Notice that T_1 breaks S^3 into two solid tori V_1' and V_2' each having two longitudinal dividing curves, so there is a unique tight contact structure on each, the first described by a path that goes from ∞ clockwise to 1 and the other going from 0 anti-clockwise to 1. As argued above we can break the first path into a path from ∞ to 0 and then 0 to 1. The fist edge describes the unique tight contact structure on a solid torus with longitudinal divides and the second edge can have any signs and here, we choose a positive sign. Similarly for the second path we may subdivide the edges from 1 to $\lfloor q/p \rfloor$ and then the edges in $\overline{P_1} \cup P_2$ that are from $\lfloor q/p \rfloor$ to ∞ and we may assume that all the edges have a positive sign. This shows that L_1 also sits in the contact structure $\xi_{-P_1,-P_2}$ and in particular is $S_+^{q-p}(L_{-P_1,-P-2})$ and we see that $S_-^{q-p}(L_{P_1,P_2})$ is Legendrian isotopic to $S_+^{q-p}(L_{-P_1,-P_2})$. Since all other stabilizations of L_{P_1,P_2} and $L_{-P_1,-P_2}$ with the same classical invariants are stabilizations of $S_-^{q-p}(L_{P_1,P_2}) = S_+^{q-p}(L_{-P_1,-P_2})$, the result follows. □

As all the signs in all the paths P_1 and P_2 are the same, we can shorten $\overline{P}_1 \cup P_2$ to a path going from $\lfloor q/p \rfloor$ clockwise to ∞. Inside the contact structure on $T^2 \times [0,1]$ described by this path we can find a torus T with dividing slope $\lceil q/p \rceil$. Now T divides (S^3, ξ_{P_1,P_2}) into two tight solid tori. One with lower meridian ∞ and convex boundary of slope $\lceil q/p \rceil$ and the other with upper meridian 0 and convex boundary of slope $\lceil q/p \rceil$. So the first solid torus has longitudinal dividing curves and hence there is only one possible contact structure on it. Moreover, by Lemma 2.6 we may split this torus into one with boundary slope $\lfloor q/p \rfloor$ and basic slice with boundary slopes $\lfloor q/p \rfloor$ and $\lceil q/p \rceil$ and the sign of the basic slice can be chosen arbitrarily. We choose the sign to be positive and then subdivide the path to $\overline{P_1} \cup P_2$ so that all the basic slices are positive except the last one in P_2 going from $\lceil q/p \rceil$ to ∞ which is still negative. Denote the paths with the new signs by P_1^{2m-1}, P_2^{2m-1}. Break the paths into their continued fraction blocks

$$(A_2^{2m-1}, \dots, A_{2n}^{2m-1}) \text{ and } (B_1^{2m-1}, \dots, B_{2m-1}^{2m-1})$$

as in Section 2.3. Then this new pair of paths is $(2m-1)$-inconsistent (that is, maximally inconsistent). We leave the almost identical case when the continued blocks in P_2 have even subscripts to the reader. As we saw in Section 2.3 we will now get k-inconsistent pairs of paths P_1^k, P_2^k for $k = 2, 3, \dots, 2m-1$ that are all compatible. Notice that all the signs of the basic slices in P_1^2 are negative, except the first one which is positive, and all the basic slices of P_2^2 are positive, except the first one which is negative.

Proposition 7.15. *With the notation above, consider the V formed by the two rays starting at the bottom vertex of D', tangent to the lower boundary of D', and with the top of the V at* $\mathrm{tb} = pq$. *Each pair of paths $(\pm P_1^k, \pm P_2^k)$ constructed above gives a Legendrian knot $L_{\pm P_1^k, \pm P_2^k}$ with* $\mathrm{tor} = 0$ *and* $\mathrm{tb} = pq$, *and stabilizations of it will remain non-loose exactly when the resulting Legendrian has its classical invariants on or above the V described above. The set of non-loose stabilizations of $L_{\pm P_1^k, \pm P_2^k}$ gives the diamond $D(L_{\pm P_1^k, \pm P_2^k})$ of $L_{\pm P_1^k, \pm P_2}$. The union*

$$D = D' \cup \bigcup_{k=2}^{2m-2} D(L_{\pm P_1^k, \pm P_2^k})$$

is coarsely Legendrian simple, i.e. any two Legendrian knots in D with the same tb *and* rot *are equivalent. See the right-hand side of Figure 23.*

Proof. We first relate a stabilization of $L_{P_1^{2m-1}, P_2^{2m-1}}$ and a stabilization of L_{P_1,P_2}. To this end, we use the notation from the paragraph preceding the statement of the proposition and notice that in the contact structure ξ_{P_1,P_2} we see that inside of V_2 there is a convex torus $T_{\lceil q/p \rceil}$ with two dividing curves of slope $\lceil q/p \rceil$. Let $L_{\lceil q/p \rceil}$ be a ruling curve on $T_{\lceil q/p \rceil}$ with slope q/p. By Lemma 7.8 we know that $L_{\lceil q/p \rceil}$ is isotopic to the result of positively stabilizing L_{P_1,P_2} exactly $|\lceil \frac{q}{p} \rceil \cdot \frac{q}{p}|$ times. As noted in the paragraph above, we also know that $T_{\lceil q/p \rceil}$ is a convex torus inside $\xi_{P_1^{2m-1}, P_2^{2m-1}}$ and from this we see that $L_{\lceil q/p \rceil}$ is also the result of negatively stabilizing $L_{P_1^{2m-1}, P_2^{2m-1}}$ exactly $|\lceil \frac{q}{p} \rceil \cdot \frac{q}{p}|$ times, thus all further stabilizations of these knots will remain isotopic.

Now just as in the proof of Proposition 7.5 we see that $L_{P_1^{2m-1},P_2^{2m-1}}$ positively stabilized $n_{2n} = |s_{2n} \bullet \frac{q}{p}|$ times is loose but stabilizing any fewer times remains non-loose (here, $2n = 2m-2$). Also, as in the proof of Proposition 7.10 we see that $S_-^{n_{2n}-1}(L_{P_1^{2m-1},P_2^{2m-1}})$ can be negatively stabilized some number of times to agree with the left corner of D'. From this we see that we get the diamond of $L_{P_1^{2m-1},P_2^{2m-1}}$ and when an element shares classical invariants with D' it is isotopic to the corresponding element of D'.

The diamonds for the other paths P_1^k, P_2^k follow from the same arguments as in Propositions 7.5 and 7.10 and the arguments above. □

7.3. **Non-loose torus knot with** tb $\geq pq$**.** In this section, we will classify non-loose (p,q)–torus knots with tb $\geq pq$ and tor $= 0$, which stabilize to L_{P_1,P_2} for some 2-inconsistent (P_1,P_2).

Proposition 7.16. *Let (P_1,P_2) be a 2-inconsistent pair of paths representing q/p. If $pq > 0$, then we assume that (P_1,P_2) are not $\pm(P_1',P_2')$ in Lemma 7.4. Then L_{P_1,P_2} and $L_{-P_1,-P_2}$ contribute an infinite X, that is there are non-loose Legendrian knots L_-^k and L_+^k, for $k \in \mathbb{Z}$ with invariants*

$$\mathrm{tb}(L_\pm^k) = k \text{ and } (L_\pm^k) = \pm r_0 \mp k$$

for some r_0, and such that

$$S_\pm^i(L_\pm^k) = L_\pm^{k-i} \text{ and } S_\mp(L_\pm^k) \text{ is loose.}$$

See the left-hand side of Figure 24.

The classification of $(p, np+1))$-torus knots with tb $= np2+p+1$ and $(p,-(np-1))$-torus knots with tb $= -np2+p+1$ was also established in [25].

Remark 7.17. We will see in the proof that L_{P_1,P_2} is either L_+^{pq} or L_-^{pq} and the other one is $L_{-P_1,-P_2}$, so the two pairs produce the same knots $L_\pm^k$.

Remark 7.18. Notice that $L_+^{r_0}$ and $L_-^{r_0}$ both have rotation number zero, but are not equivalent since they behave differently under stabilization.

Remark 7.19. From the paragraph before Proposition 7.15 we see that the excluded 2-inconsistent pair of paths in the proposition is compatible with the pair of paths whose signs are all the same and hence by Lemma 7.2 we know the contact structure is ξ_1.

Proof. From Proposition 7.5 we get the Legendrian knots $L_\pm^k$ for $k \leq pq$ with the desired properties. We now recall that Lemma 6.10 says that there is a tight contact structure ξ on the complement C of the (p,q)–torus knot that has convex boundary with two dividing curves of slope ∞ and no convex Giroux torsion such that adding a basis slice $(T^2\times I, pq, \infty)$ to (C,ξ) will result in the complement of a standard neighborhood of L_{P_1,P_2}. Suppose this basis slice was negative. Then given any integer $n > pq$ we can factor $T^2\times[0,1]$ into negative basic slices given by the path $pq,\dots,n-1,n,\infty$ in the Farey graph. That is there is a convex torus T_n in $T^2\times[0,1]$ with two dividing curves of slope n. This torus separates $C\cup T^2\times[0,1]$ into two pieces, one, denoted C_n, is diffeomorphic to C and clearly the complement of a Legendrian (p,q)–torus knot L_-^n with tb $= n$. Moreover, since the complement of $L_{P_1,P_2} = L_-^{pq}$ is obtained by attaching $n-pq$ negative basic slices to C_n,

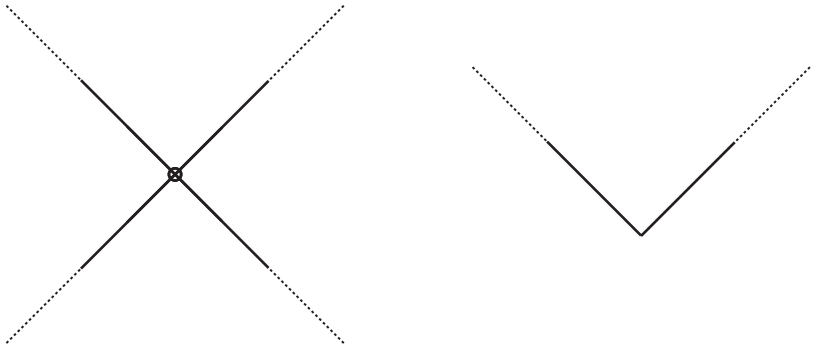

FIGURE 24. On the left are the Legendrian realizations of a (p,q)–torus knot related to the 2-inconsistent pairs $\pm(P_1,P_2)$ when $(P_1,P_2) \neq \pm(P_1',P_2')$ (see Lemma 7.4). On the right we see the same when $(P_1,P_2) = \pm(P_1',P_2')$. For each integral point on each of the lines on the left or on the infinite V on the right whose entries sum to an odd integer, there is a unique non-loose Legendrian, except that the crossing point of the X were there are exactly two non-loose Legendrian knots.

we see that $L_{P_1,P_2} = S_-^{n-pq}(L_-^n)$. Similarly, all the tori T_k for $k \in [pq,n] \cap \mathbb{Z}$ give rise to Legendrian knots L_-^k with the desired properties. Since n was arbitrary we see that we have constructed L_-^k for any $k \in \mathbb{Z}$. Notice that one attaches a positive basic slice to C_n with dividing slopes n and $n-1$, then in the result we have a contact structure on $T^2\times[0,1]$ given by the path $\infty, n, n-1$ in the Farey graph and the signs on each edge are different. Since the path can be shortened the contact structure is overtwisted. Thus a positive stabilization of L_-^n is loose. So we have constructed L_-^k with the desired properties for all k. Similarly we can get the L_+^k from $L_{-P_1,-P_2}$. □

Proposition 7.20. *Suppose that $pq > 0$ and let (P_1,P_2) be the pair of decorated paths (P_1',P_2') in Lemma 7.4. The Legendrian knots L_{P_1,P_2} and $L_{-P_1,-P_2}$ contributes an V of non-loose Legendrian (p,q)–torus knots in ξ_{P_1,P_2}. That is, there are non-loose Legendrian knots $L_\pm^k$ for $k > pq - r_0$, where $r_0 = |R(P_q,P_2)|$ (see Lemma 2.19), and L^{pq-r_0} in ξ_{P_1,P_2}, with invariants*

$$\mathrm{tb}(L_\pm^k) = k, \text{ and } \mathrm{rot}(L_\pm^k) = (\pm pq \mp r_0) \mp k$$
$$\mathrm{tb}(L^{pq-r_0}) = pq - r_0, \text{ and } \mathrm{rot}(L^{pq-r_0}) = 0,$$

such that

$$S_\pm(L_\pm^i) = L_\pm^{i-1} \text{ and } S_\pm(L_\pm^{pq-r_0+1}) = L^{pq-r_0},$$

and

$$S_\mp(L_\pm^i) \text{ and } S_\pm(L^{pq-r_0}) \text{ are loose.}$$

See the right-hand side of Figure 24.

The classification for the right handed trefoil with tb = 7 was also established in [25].

Remark 7.21. Notice that L_{P_1,P_2} is either L_+^{pq} or L_-^{pq} and the other one is $L_{-P_1,-P_2}$. So (P_1,P_2) and $(-P_1,-P_2)$ determine the same V. Moreover, it is also clear that the Legendrian knots in the V are determined by their tb and rot.

Proof. The Legendrian knots $L^k_\pm$ for $k \leq pq$ are given by Proposition 7.14 and those for $k > pq$ are founds exactly as in the proof of Proposition 7.16. □

7.4. **The extra torus knot when** $pq < 0$**.** By Lemma 6.7, when $pq < 0$ there exists one extra contact structure ξ_e in $\mathrm{Tight}_0(C; |pq| - |p| - |q|)$. If we glue a tight solid torus to C to obtain S^3, then the added solid torus is a standard neighborhood of a non-loose Legendrian knot L_e with tor = 0. We now study the properties of this extra Legendrian knot.

Proposition 7.22. *Suppose $pq < 0$. Let (P_1, P_2) be the paths describing a Legendrian L_{P_1,P_2} such that the edges in P_1 has only positive signs and the edges in P_2 has only negative signs. Let $\xi_{p,q}$ be the contact structure supported by the open book with binding the (p, q)–torus knot. We have the following:*

(1) *The transverse push-off of L_{P_1,P_2} is the binding of an open supporting $\xi_{p,q}$.*
(2) $d_3(\xi_{p,q}) = |pq| - |p| - |q| + 1$.
(3) *In $\xi_{p,q}$, there are non-loose Legendrian knots $L^i_\pm$, $i \in \mathbb{Z}$ such that*
   (a) $\mathrm{tb}(L^i_\pm) = i, \mathrm{rot}(L^i_\pm) = \pm(|pq| - |p| - |q|) \mp i$,
   (b) $L^i_\pm = S_\pm(L^{i-1}_\pm)$, $S_\mp(L^i_\pm)$ *is loose, and*
   (c) $L^{pq}_\pm = L_{\mp P_1, \mp P_2}$.
(4) *The extra Legendrian L_e is in the contact manifold $(S^3, \xi_{p,q})$ such that*
   (a) $\mathrm{tb}(L_e) = |pq| - |p| - |q|$, $\mathrm{rot}(L_e) = 0$, *and*
   (b) $S_\pm(L_e) = L^{|pq|-|p|-|q|-1}_\pm$.

Proof. Item (1) and (2) are the content of Lemma 7.1 and its proof, while Item (3) is Proposition 7.16 except for the computation of the rotation numbers which will be done below. So we are left to check Item (4).

In Lemma 6.2, we saw that when $pq < 0$, there is an extra contact structure $\xi_e \in \mathrm{Tight}_0(C; |pq| - |p| - |q|)$ such that all convex tori parallel to ∂C have dividing slope $|pq| - |p| - |q|$. Thus if we glue a solid torus to C and extent ξ_e (there is a unique way to do this) then we get a Legendrian knot L_e with standard neighborhood the glued in solid torus. Clearly $\mathrm{tb}(L_e) = |pq| - |p| - |q|$. By Lemma 6.4, we also know that ξ_e is universally tight and remains so after gluing any amount of convex Giroux torsion. Thus if $\xi_\pm$ is the result of adding a $\pm$-basic slice in $\mathrm{Tight}^{min}(T^2 \times [0,1]; \infty, |pq| - |p| - |q|)$ to ξ_e, we know it is tight. Moreover, we may factor $\xi_\pm$ into a contact structure $\xi^i_\pm \in \mathrm{Tight}_0(C; i)$ and a $\pm$-basic slice with slopes ∞ and i for $i < |pq| - |p| - |q|$. Clearly $\xi^i_\pm$ the complement of a non-loose Legendrian knot $\widetilde{L}^i_\pm$ and $\widetilde{L}^i_\pm$ is a $(|pq| - |p| - |q| - i)$-fold $\pm$-stabilization of L_e. Notice that $\widetilde{L}^{pq}_\pm$ are non-loose Legendrian knots whose complements are universally tight and remain so after adding any amounts of convex Giroux torsion. Thus by the proof of Lemma 7.1, we know that $\widetilde{L}^{pq}_\pm$ is equivalent to $L^{pq}_\pm$ and thus all the $\widetilde{L}^i_\pm$ for $i < |pq| - |p| - |q|$ are equivalent to $L^i_\pm$ by Lemma 7.16 (indeed we know there are only $2n(p, q)$ non-loose knots with tor = 0 having these invariants and only one $L^i_\pm$ can stabilize to $L^{pq}_\pm$ so $\widetilde{L}^i_\pm$ must agree with this Legendrian knot). Since we know that $\mathrm{rot}(L^{pq}_-) = -\mathrm{rot}(L^{pq}_+)$ we see that $\mathrm{rot}(L_e)$ must be zero. This establishes Item (4).

The computation of the rotation numbers for the $L^i_\pm$ now follows since we know the rotation number of L_e and how it relates to the $L^i_\pm$. □

7.5. **The Giroux torsion of the examples above.** In this section, we will see that all the examples constructed in Section 7.2 have no convex Giroux torsion in their complement unless $pq > 0$ and we are in ξ_{pq-p-q}, in which case some of the Legendrian knots have convex half Giroux torsion.

Remark 7.23. For the Legendrian knots discussed in Section 7.3 and 7.4 that have $\mathrm{tb} \geq pq$ we already know they have no convex Giroux torsion in their complement because their complements are in $\mathrm{Tight}_0(C; n)$ for some $n \geq pq$ which by definition have no convex Giroux torsion.

Proposition 7.24. *Given a pair of decorated paths (P_1, P_2), any non-loose stabilization of L_{P_1,P_2} has* $\mathrm{tor} = 0$, *unless $pq > 0$ and (P_1, P_2) is the one from Lemma 7.1. In the latter case, the non-loose stabilizations of L_{P_1,P_2} will have* $\mathrm{tor} = 0$ *if* $\mathrm{tb} > pq - p - q$, *and* $\mathrm{tor} = 1/2$ *if* $\mathrm{tb} \leq pq - p - q$.

Proof. We consider three cases: first when (P_1, P_2) is 2-inconsistent, but not totally 2-inconsistent, then when (P_1, P_2) is 2-consistent, and finally when (P_1, P_2) is totally 2-inconsistent.

We deal with the first case. By possibly replacing (P_1, P_2) by $(-P_1, -P_2)$ if necessary, we can assume that $S^k_-(L_{P_1,P_2})$ is non-loose and $S_+(L_{P_1,P_2})$ is loose. (When we consider the paths with opposite signs the role of $\pm$ stabilizations is reversed). Let (C, ξ) be the complement of $S^k_-(L_{P_1,P_2})$ and assume ξ contains convex half Giroux torsion. By Lemma 6.5 and Lemma 7.25, we can split C into C' and $T^2 \times [0,1]$ where $\xi|_{C'} \in \mathrm{Tight}_0(C; pq)$ and $\xi|_{T^2\times[0,1]}$ has a convex Giroux torsion layer in it. Since ξ is tight and is obtained from $\xi|_{C'}$ by attaching a convex Giroux torsion layer, we know that $\xi|_{C'}$ must be associated to a totally 2-inconsistent pair of paths (P'_1, P'_2) by Lemma 6.13. Thus we can add an arbitrarily amount of convex Giroux torsion to $\xi|_{C'}$ and the result is still tight by Lemma 6.15. But this, of course, implies that we can add an arbitrary amount of convex Giroux torsion to ξ and the result is still tight, which contradicts Lemma 6.13. Thus $S^k_-(L_{P_1,P_2})$ has $\mathrm{tor} = 0$.

Now consider a pair of decorated paths (P_1, P_2) that is 2-consistent. We note that (P_1, P_2) is compatible with a 2-inconsistent pair of paths (P'_1, P'_2) that is not totally 2-inconsistent (see Section 2.3). Moreover, Proposition 7.10 and 7.15 say that any stabilization of L_{P_1,P_2} can be further stabilized to be a stabilization of $L_{P'_1,P'_2}$ and since the latter does not have any convex Giroux torsion in its complement, neither does the former.

We are left to consider totally 2-inconsistent pairs of paths, and the proof of Lemma 6.19 gives the result in this case. □

7.6. **Non-loose torus knots with convex Giroux torsion.** We begin by noticing that all non-loose torus knots have finite torsion.

Lemma 7.25. *If L is a non-loose Legendrian torus knot, then* $\mathrm{tor}(L) < \infty$.

Proof. Suppose $\mathrm{tor}(L) \neq 0$. Then we can stabilize or destabilize L and make $\mathrm{tb}(L) = pq$. Let C be the complement of L. As in Section 6.1, we can decompose C into $V_1 \cup (S^1 \times P) \cup V_2$ where P is a pair of pants and V_1, V_2 are solid tori. We use the coordinates system $\mathcal{F}_2$ from Section 6.1 so that (a push-off of) L is considered as a 0-twisting vertical Legendrian curve in $S^1 \times P$. Use this 0-twisting vertical Legendrian curve to thicken V_1 and V_2 so that their dividing slopes become 0. Perturb T_1, T_2 and T_3 so that ∂P is the ruling curves. After

that, perturb P to be convex and there exist two possible dividing set on P as shown in Figure 25.

We will first show that the dividing set shown in the first drawing of Figure 25 results in an overtwisted contact structure. In the first drawing of Figure 25, we can find a bypass for T_2 and thicken V_2 so that the dividing slope becomes ∞. However, $V_!$ contains a convex torus with slope $(q/p)^c$ measured in the coordinates system $\mathcal{F}_1$, which is ∞ measured in the coordinates system $\mathcal{F}_2$. Thus $V_!$ contains a half convex Giroux torsion after thickening and we can find an overtwisted disk in C.

Thus the dividing set on P should be the one shown in the second drawing of Figure 25. Choose a 0-twisting vertical Legendrian curve in $S^1 \times P$, which is in the I-invariant neighborhood of T_1. Then we can find a convex torus T which contains this curve and is smoothly isotopic to T_3, and its ruling curve sits on P and intersects the dividing curves at two points as shown in Figure 25. Now cut $S^1 \times P$ along the torus T and we obtain a contact structure on $S^1 \times P$ with boundary slope 0 and the dividing set on P being as shown in the first drawing of Figure 14. This T and T_1 and T_2 co-bound an $S^2 \times P$ and from Lemma 2.21, we know that there exists unique tight contact structure on this $S^1 \times P$ up to boundary twisting. Let C' be the union of this $S^1 \times P$ and V_1, V_2. Then C is decomposed into C' and a finite convex Giroux torsion layer. Clearly, the contact structure on C' is in $\text{Tight}_0(C; pq)$. According to Claim A in the proof of Lemma 6.19, the number of convex Giroux torsion added to a contact structure in $\text{Tight}_0(C; pq)$ is fixed, and there exist only finite number of dividing curves on P, so it must be finite. □

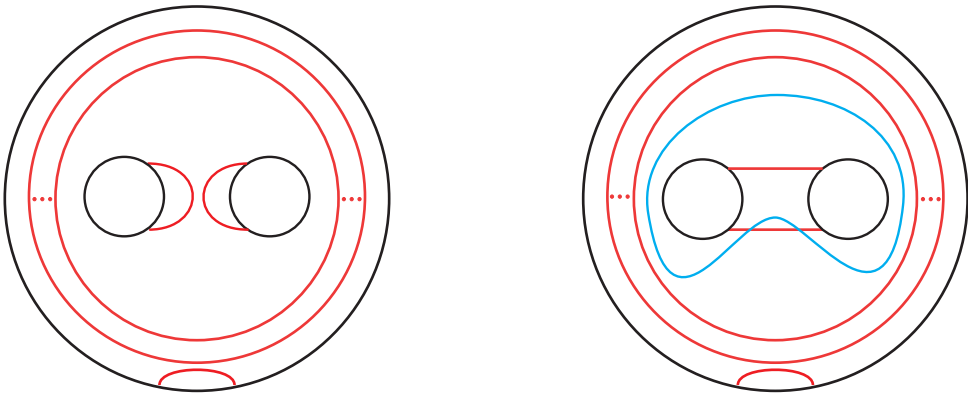

FIGURE 25. Some possible dividing sets on the pair of pants P. The blue curve is a Legendrian curve.

Proposition 7.26. *Let L be any non-loose (p, q)–torus knot in (S^3, ξ) with $\text{tor}(L) = n$. Then there is some pair of totally 2-inconsistent paths (P_1, P_2) representing q/p such that the complement of a standard neighborhood of L is obtained from the complement of a standard neighborhood of L_{P_1,P_2} by attaching a basic slice $(T^2 \times [0, 1]; \infty, pq)$ and then attaching a convex $(n - 1/2)$ Giroux torsion layer, and finally a basic slice $(T^2 \times [0, 1]; \text{tb}(L), \infty)$. In particular, the complement of a standard neighborhood of L is in a contact structure in $\text{Tight}_n(C; \text{tb}(L))$ and any element in $\text{Tight}_n(C; \text{tb}(L))$ gives a non-loose Legendrian knot with $\text{tor}(L) = n$.*

In addition, $\xi = \xi_{P_1,P_2}$ if n is an integer, or ξ is obtained from ξ_{P_1,P_2} by a half Lutz twist on the transverse push-off of L_{P_1,P_2} if n is a half integer (recall that by Proposition 7.5 either L_{P_1,P_2} or $L_{-P_1,-P_2}$ remains non-loose after arbitrarily many negative stabilizations, we assume that it is L_{P_1,P_2} that has this property).

Proof. This follows directly from Lemma 6.19 and its proof. □

7.7. **Proof that the algorithm gives a complete classification.** We will now show that the algorithm from Section 3 does indeed give all non-loose torus knots.

We first consider non-loose Legendrian (p,q)–torus knots with tor $= 0$. We first note that any such knot with tb $= pq$ will be of the form L_{P_1,P_2} for some pair of decorated paths (P_1,P_2) representing q/p by Lemma 6.8. Moreover, if a non-loose Legendrian knot with tor $= 0$ has tb $< pq$, then it will stabilize to one with tb $= pq$ by Lemma 6.5. Thus we know that it will be in a Wing or a Diamond of L_{P_1,P_2} for some decorated pair (P_1,P_2) by Propositions 7.5 and 7.15.

Now if a non-loose Legendrian (p,q)–torus knot with tor $= 0$ has tb $= n > pq$, then its complement is in $\mathrm{Tight}_0(C;n)$ and hence is a destabilization of some L_{P_1,P_2} for some decorated pair of paths by Lemma 6.7, and moreover they must be 2-inconsistent by Lemma 6.10. Thus we see that such a knot must be in an infinite X or V from Propositions 7.16 and 7.20.

These observations show that the classification algorithm in the generic case (Steps 1 and 3 of the algorithm) give the desired result except when $pq > 0$ and we are in the situation where P_1 has all one sign and P_2 has all the other sign. The only things that might not be immediately clear is the rotation numbers of $L^{pq}_{k,\pm}$. However, those easily follow from the computation of $R(P_1,P_2)$ for the 2-inconsistent paths according to Lemma 2.19, and the proofs of Proposition 7.5 and Proposition 7.15 that indicates when compatible pairs of decorated paths stabilize to become the same. In the excluded case, we will not have an infinite X associated to L_{P_1,P_2} and $L_{-P_1,-P_2}$ with tor $= 0$. Only the knots in the X with tb $> pq - p - q$ will have no convex Giroux torsion. Those with tb $\leq pq - p - q$ will have convex half Giroux torsion by Proposition 7.24.

Remark 7.27. To see that the generic X-wings are as depicted in Figure 3, we need to see that the crossing of the X is above pq when $pq < 0$ and otherwise is below pq. This is actually clear by considering the inequalities in Theorem 1.19 (shown graphically in Figure 10). Indeed, suppose the crossing of the X was below pq when $pq < 0$ then the top part of the X would not fit through the allowable range when tb $= 0$ (we see that when tb $= 0$ we must have rot between $-|pq| + |p| + |q|$ and $|pq| - |p| - |q|$). We can similarly argue for $pq > 0$.

In the exceptional cases (Step 2), we first consider $pq > 0$. In this case, the above discussion shows that in ξ_1, we have an infinite V together with some other diamonds. The only thing to consider is the claimed values for the rotation numbers. To see this we first consider the pair of paths (P_1,P_2) with all signs the same. We saw in Proposition 7.14 that the diamonds associated to L_{P_1,P_2} and $L_{-P_1,-P_2}$ have a common lowest vertex that has tb $= pq - p - q + 2$. Now for the 2-inconsistent pairs of decorated paths that are compatible with these paths, we see that they must be stabilized either strictly positively or strictly

negatively to get to this lowest vertex (see Proposition 7.15). Thus we get the desired rotation numbers for these two Legendrian knots and the rotation numbers for the others follow from the proof of Proposition 7.15.

We now consider the exceptional case when $pq < 0$. Here the classification follows directly from the above discussion and Proposition 7.22.

Finally, the classification of non-loose torus knots with convex Giroux torsion in their complement follows directly from Proposition 7.26.

8. General results of non-loose torus knots

Theorem 1.1 claims that any Legendrian (p, q)–torus knot destabilizes if $\mathrm{tb} \neq pq$ except for one with $\mathrm{tb} = |pq| - |p| - |q|$ when $pq < 0$ and some with $\mathrm{tb} = pq$ do but others do not.

Proof of Theorem 1.1. This follows directly from Lemma 6.5 and Lemmas 6.10 and 6.2. □

The parity of the d_3-invariants of contact structures supporting non-loose torus knots is given in Theorem 1.2 which we now prove.

Proof of Theorem 1.2. If (P_1, P_2) are a pair of decorated paths such that ξ_{P_1,P_2} supporting a non-loose (p, q)–torus knot with $\mathrm{tb} = pq$ (and all contact structures supporting non-loose torus knots have such a non-loose Legendrian knot), then we can draw a surgery diagram for ξ_{P_1,P_2} as described in Section 2.4 and then use Equation (3) to compute its d_3-invariant. Notice that in that equation the only term that depends on the decorations on (P_1, P_2) is c^2. Recall that c is the vector of rotation numbers of the link in the surgery presentation of ξ_{P_1,P_2} and c^2 is computed with the intersection pairing given by the linking matrix M of the surgery diagram. The class c is a characteristic element of the pairing M (see the proof of Corollary 3.6 in [9], where they show that c is related to c_1 of a complex structure, which is known to be characteristic by $9q$ where q is the number of (+1)-contact surgeries in the diagram. Since $q = 2$ in our case we see c is characteristic). Now since the surgery diagram presents S^3 we know that M is unimodular, we know that c^2 is congruent to the signature of M modulo 8. Hence all the decorated paths (P_1, P_2) have the same d_3-invariant modulo 2.

Since for $pq > 1$ we know there are always non-loose L_{P_1,P_2} in ξ_1, see Section 7.2.2, we know that all d_3-invariants of contact structures supporting non-loose Legendrian knots with $\mathrm{tor} = 0$ must have odd d_3-invariants. Moreover, those with $\mathrm{tor} = n \in \mathbb{N}$ will have the same d_3-invariants since full Lutz twists do not change the d_3-invariant and those with $\mathrm{tor} = (2n - 1)/2$ will have even d_3-invariants since half Lutz twists will change the d_3-invariant by the self-linking number of the transverse knot which is Lutz twisted about, see Section 3.2, and we know these are all odd. We have a similar result for $pq < 0$ since there is always some non-loose representative with $\mathrm{tor} = 0$ in the contact structure $\xi_{|pq|-|p|-|q|+1}$, see Lemma 7.1. □

Theorem 1.3 details all the possible Legendrian knots with $\mathrm{tor} = 0$ and $\mathrm{tb} > pq$.

Proof of Theorem 1.3. This follows directly from the classification given in Section 7.7, or more specifically Propositions 7.16, 7.20, and 7.22.

We are left to show that all $L^i_{\pm,k}$ can be realized as a Legendrian knot in Figure 1. We start with $i = pq + 1$. First, a simple Kirby calculus shows that L_- and L_+ are smooth (p, q)–torus knots. See Figure 26 (if in the first figure of row two, the green curve is slide

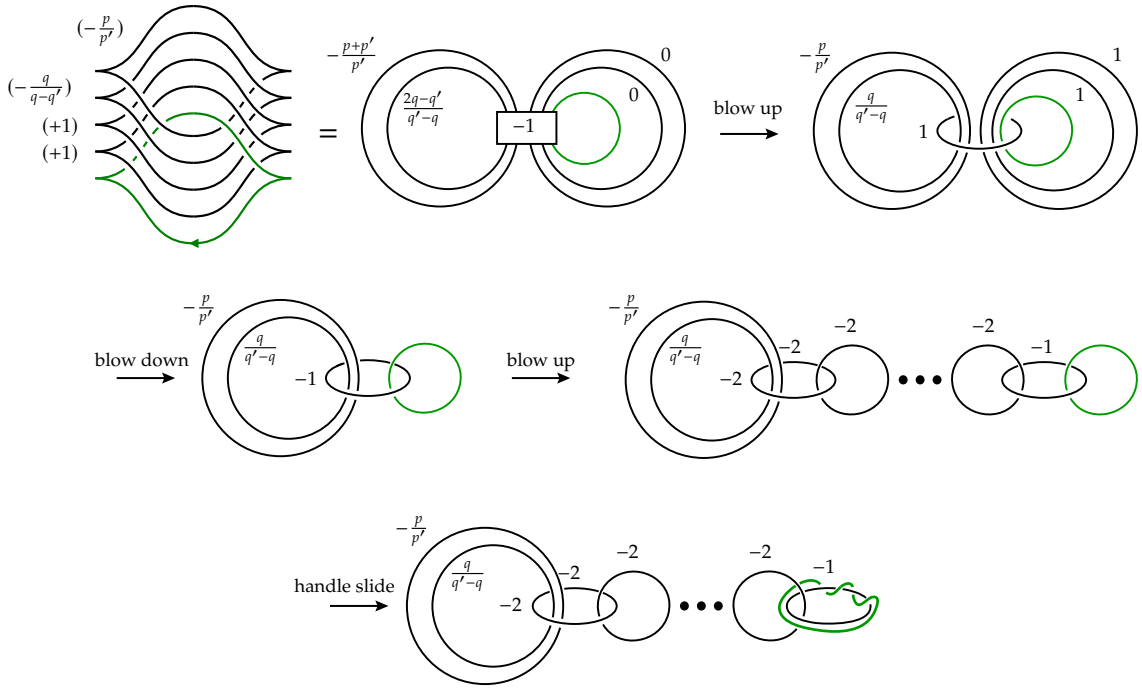

FIGURE 26. Various Kirby diagrams of a (p, q)–torus knot. As shown in Section 2.4, in the upper left we see a contact surgery presentation for the (p, q)–torus knot with tb $= pq$.

over the -1-framed curve, then the resulting diagram can be realized as a contact surgery diagram in the top row of Figure 1). If we perform a Legendrian surgery on $L_\pm$ in the first row of Figure 1, then we obtain tight $L(p, -q)\#L(q, -p)$. Thus $\mathrm{tor}(L_\pm) = 0$. Since $S^3_{pq}(T_{p,q}) \cong L(p, -q)\#L(q, -p)$ and $S^3_m(T_{p,q}) \ncong S^3_n(T_{p,q})$ for $m \neq n$, the smooth surgery coefficient on $L_\pm$ (with respect to the Seifert framing) must be pq, which is tb -1. Thus $\mathrm{tb}(L_\pm) = pq + 1$. Clearly there exist $n(p, q)$ different L_- and the same for L_+. Now suppose some L_- and L_+ are equivalent. This implies that the Legendrian surgery on them results in the same contact structure. We can calculate the rotation numbers of these $L_\pm$ using the Formula (4). Clearly, $\mathbf{rot}, M, \mathbf{lk}$ are the same for both $L_\pm$. The only difference is r_0. Thus $\mathrm{rot}(L_-) \neq -\mathrm{rot}(L_+)$, so they cannot be equivalent. Thus the first row of Figure 1 represents $2n(p, q)$ non-loose torus knots with $\mathrm{tb} = pq + 1$ and $\mathrm{tor} = 0$. Since we have already established that there are exactly $2n(p, q)$ non-loose Legendrian (p, q)-torus knots with $\mathrm{tor} = 0$ and $\mathrm{tb} = pq + 1$, they must all be represented by a contact surgery diagram in Figure 1.

Now consider $i = pq + m$ for $m > 1$. If we perform a Legendrian surgery on $L_\pm$ in the second row of Figure 1, then we obtain Stein fillable contact manifolds and it is diffeomorphic to $S^3_{pq+m-1}(T_{p,q})$. Thus the smooth surgery coefficient on $L_\pm$ is $pq + m - 1$ and

$\mathrm{tb}(L_\pm) = pq + m$. The Legendrian surgery on each $L_\pm$ produces $n(p,q)$ different contact structures distinguished by the Spin^c structures on the Stein filling given by the surgery diagrams in Figure 1 without the (+1)–surgery components, see [39, Theorem 1.2]. Finally, each L_- and L_+ are not equivalent since we can calculate their rotation numbers as above and they are different. Thus the second row of Figure 1 represents $2n(p,q)$ non-loose torus knots with $\mathrm{tb} = pq + m$ and $\mathrm{tor} = 0$. Since we now there are exactly $2n(p,q)$ (p,q)-torus knots with $\mathrm{tb} > pq$, except with $pq < 0$ and $\mathrm{tb} = |pq| - |p| - |q|$, we have established the theorem except in the exceptional case.

In the case that $pq < 0$ and $\mathrm{tb} = |pq| - |p| - |q|$, we know there are $2n(p,q) + 1$ non-loose Legendrian knots, the extra one we are denoting L_e. We claim that none of the surgery diagrams in Figure 1 give L_e, given this we have completed the proof of Theorem 1.3. To see this recall that $S_\pm(L_e)$ is non-loose for either choice of stabilization, but for all the other non-loose Legendrian knots with $\mathrm{tb} = |pq| - |p| - |q|$ one sign of stabilization will give a loose knot, while the other will remain non-loose. So we will establish our claim by showing that all the Legendrian knots in Figure 1 become loose after one stabilization of the correct sign.

To this end consider the lower left diagram in Figure 1. Let S be a standard neighborhood of a $\mathrm{tb} = -1$ unknot that contains the bottom Legendrian unknot with contact framing (+1) which we will call K. We can assume that L_+ is contained in this neighborhood too. We will show that the complement of $S_-(L_+)$ in S is overtwisted and thus the complement of $S_-(L_+)$ in S^3 is also overtwisted. Let S' be a standard neighborhood of K in S, notice that L_+ sits on $\partial S'$ as a Legendrian divide. So $S \setminus S'$ is a positive basic slice with dividing slopes -2 and -1. When we perform contact (+1) surgery on K we remove S' from S are replace it with a solid torus S_{-1} with lower meridian -1 and dividing slope -2, call the result S_K. Clearly S_K is overtwisted, but when we remove S_{-1} from S_K we get a tight basic slice. Notice that S_{-1} is a standard neighborhood of L_+ in S_K (since it sits on ∂S_{-1} as a Legendrian divide). If we negatively stabilize L_+ in S_{-1} the result will have a standard neighborhood with boundary slope $-\infty$ (and lower meridian -1) and the complement of the standard neighborhood in S_{-1} will be a negative basic slice with dividing slopes $-\infty$ and -2. Thus the complement of this neighborhood in S_K will be the union of a positive basic slice with dividing slopes -2 and -1 and a negative basic slice with dividing slopes $-\infty$ and -2. Since the path from $-\infty$ to -2 to -1 can be shortened and our basic slices have opposite sign, we see that the complement of $S_-(L_+)$ in S_K is overtwisted as claimed. □

Remark 8.1. We note that according to our classification of non-loose Legendrian torus knots we know that $S_\pm(L_\pm)$ must be non-loose, but one can put the whole surgery diagram in Figure 1 and $S_\pm(L_\pm)$ on an open book and then (using a lantern relation) show that Legendrian surgery on $S_\pm(L_\pm)$ is supported by an open book with positive monodromy. Thus it is tight and $S_\pm(L_\pm)$ is non-loose.

Theorem 1.4 gives the number of non-loose Legendrian knots $\mathrm{tor} = 0$ and $\mathrm{tb} = pq$.

Proof of Theorem 1.4. From Lemma 6.8, we know that the number of Legendrian (p,q)–torus knots with tight complement and $\mathrm{tor} = 0$ and $\mathrm{tb} = pq$ is $m(p,q)$. For $pq > 0$ there are no such Legendrian knots in (S^3, ξ_{std}) so in this case the number of non-loose such knots is $m(p,q)$. However, by [16], we know that there are $2\lceil q/p \rceil$ such knots in (S^3, ξ_{std})

and hence we have the claimed number of non-loose Legendrian knots. The fact that they come from the claimed surgery diagram was shown in Section 2.4. □

We discuss that there can be arbitrarily many peaks and deep valleys in Theorem 1.6.

Proof of Theorem 1.6. It is clear that one can choose q/p so that there are arbitrarily many continued fraction blocks in P_1 and P_2 and that these blocks are arbitrarily long except for the first one. According to Proposition 7.10 and 7.15, the result about the number of peaks now follows by that we can choose i-inconsistent decorated pair of paths for arbitrarily large i. According to the proof of Proposition 7.10, the depth of the valleys is determined by the difference between the lengths of two continued fraction blocks A_{i-1} and B_i, or B_{i-1} and A_i, which we can make arbitrarily large. □

In Theorem 1.8 we give an upper bound on the number of overtwisted contact structures supporting non-loose (p, q)–torus knots.

Proof of Theorem 1.8. Any non-loose Legendrian torus knot with tor = 0 is in a contact structure given by a 2-inconsistent pair of paths by the discussion in Section 2.3 and the classification given in Section 3. Moreover, there are $2n(p, q)$ of such pairs by Lemmas 6.7 and 6.10. Since (P_1, P_2) and $(-P_1, -P_2)$ give the same contact structures, we see an upper bound is $n(p, q)$ as claimed.

Now allow non-loose Legendrian knots with any convex Giroux torsion. According to Proposition 7.26, the extra contact structures only come from totally 2-inconsistent pairs of paths. According to Lemma 6.19, the number of totally 2-inconsistent pairs of paths is twice what we want. Again, since (P_1, P_2) and $(-P_1, -P_2)$ give the same contact structures, we see an upper bound in the formula is correct. □

We now establish Theorem 1.9 about the convex Giroux torsion in non-loose torus knot complements.

Proof of Theorem 1.9. This directly follows from Lemma 7.25 and Claim A, B in the proof of Lemma 6.19. □

We end by considering non-loose transverse knots by giving the proof of Theorem 1.10.

Proof of Theorem 1.10. As noted in the introduction the classification of transverse knots is equivalent to the classification Legendrian knots up to negative stabilization, [16, Theorem 2.10]. So any non-loose transverse knot will be the transverse push-off of non-loose Legendrian knot. Suppose ξ supports non-loose Legendrian knots with a mountain range given in Figure 3. Since we only need to consider Legendrian knots up to negative stabilization, we only need to consider the bottom lower left of the figure. If the "wings" are non-trivial (that is there is more than just an X in the mountain range) then none of the Legendrian knots can have Giroux torsion (since the 2-inconsistent pair of paths associated to the X cannot be totally 2-inconsistent if it is compatible with a 3-inconsistent pair of paths.) and we see the transverse push-offs of these Legendrian knots gives transverse knots as in Item (1) of Theorem 1.10. If the mountain range has just an X, then it might support non-loose knots with convex Giroux torsion or not. If there is no convex Giroux torsion then we are in the case above, if there is convex Giroux torsion then we know for

every point in the mountain range there are an infinite number of Legendrian knots with different convex Giroux torsion in their complement. Their transverse push-offs will give transverse knots as in Item (2) of the theorem. □

REFERENCES

[1] Kenneth L. Baker, John B. Etnyre, and Jeremy Van Horn-Morris. Cabling, contact structures and mapping class monoids. *J. Differential Geom.*, 90(1):1–80, 2012.

[2] Kenneth L. Baker and Sinem Onaran. Nonlooseness of nonloose knots. *Algebr. Geom. Topol.*, 15(2):1031–1066, 2015.

[3] Apratim Chakraborty, John B. Etnyre, and Hyunki Min. Cabling legendrian and transverse knots, 2020.

[4] Vincent Colin. Chirurgies d'indice un et isotopies de sphères dans les variétés de contact tendues. *C. R. Acad. Sci. Paris Sér. I Math.*, 324(6):659–663, 1997.

[5] James Conway and Hyunki Min. Classification of tight contact structures on surgeries on the figure-eight knot. *Geom. Topol.*, 24(3):1457–1517, 2020.

[6] Jennifer Dalton, John B. Etnyre, and Lisa Traynor. Legendrian torus and cable links, 2021.

[7] F. Ding, Y. Li, and Q. Zhang. Tight contact structures on some bounded Seifert manifolds with minimal convex boundary. *Acta Math. Hungar.*, 139(1-2):64–84, 2013.

[8] Fan Ding and Hansjörg Geiges. A Legendrian surgery presentation of contact 3-manifolds. *Math. Proc. Cambridge Philos. Soc.*, 136(3):583–598, 2004.

[9] Fan Ding, Hansjörg Geiges, and András I. Stipsicz. Surgery diagrams for contact 3-manifolds. *Turkish J. Math.*, 28(1):41–74, 2004.

[10] Fan Ding, Hansjörg Geiges, and András I. Stipsicz. Lutz twist and contact surgery. *Asian J. Math.*, 9(1):57–64, 2005.

[11] S. Durst and M. Kegel. Computing rotation and self-linking numbers in contact surgery diagrams. *Acta Math. Hungar.*, 150(2):524–540, 2016.

[12] Katarzyna Dymara. Legendrian knots in overtwisted contact structures on S^3. *Ann. Global Anal. Geom.*, 19(3):293–305, 2001.

[13] Y. Eliashberg. Classification of overtwisted contact structures on 3-manifolds. *Invent. Math.*, 98(3):623–637, 1989.

[14] Yakov Eliashberg and Maia Fraser. Classification of topologically trivial Legendrian knots. In *Geometry, topology, and dynamics (Montreal, PQ, 1995)*, volume 15 of *CRM Proc. Lecture Notes*, pages 17–51. Amer. Math. Soc., Providence, RI, 1998.

[15] John B. Etnyre. On knots in overtwisted contact structures. *Quantum Topol.*, 4(3):229–264, 2013.

[16] John B. Etnyre and Ko Honda. Knots and contact geometry. I. Torus knots and the figure eight knot. *J. Symplectic Geom.*, 1(1):63–120, 2001.

[17] John B. Etnyre and Ko Honda. On the nonexistence of tight contact structures. *Ann. of Math. (2)*, 153(3):749–766, 2001.

[18] John B. Etnyre, Douglas J. LaFountain, and Bülent Tosun. Legendrian and transverse cables of positive torus knots. *Geom. Topol.*, 16(3):1639–1689, 2012.

[19] John B. Etnyre, Hyunki Min, Lisa Piccirillo, and Agniva Roy. Embeddings of rational homology balls and lens spaces into complex projective space. *In preparation*.

[20] John B. Etnyre, Hyunki Min, and Bülent Tosun. Tight surgeries on torus knots. *In preparation*.

[21] John B. Etnyre and Agniva Roy. Symplectic fillings and cobordisms of lens spaces, 2021.

[22] John B. Etnyre and David Shea Vela-Vick. Torsion and open book decompositions. *Int. Math. Res. Not. IMRN*, 2010(22):4385–4398, 2010.

[23] Hansjörg Geiges. *An introduction to contact topology*, volume 109 of *Cambridge Studies in Advanced Mathematics*. Cambridge University Press, Cambridge, 2008.

[24] Hansjörg Geiges and Sinem Onaran. Legendrian rational unknots in lens spaces. *J. Symplectic Geom.*, 13(1):17–50, 2015.

[25] Hansjörg Geiges and Sinem Onaran. Exceptional Legendrian torus knots. *Int. Math. Res. Not. IMRN*, 2020(22):8786–8817, 2020.

[26] Hansjörg Geiges and Sinem Onaran. Legendrian Hopf links. *Q. J. Math.*, 71(4):1419–1459, 2020.
[27] Paolo Ghiggini. Infinitely many universally tight contact manifolds with trivial Ozsváth-Szabó contact invariants. *Geom. Topol.*, 10:335–357, 2006.
[28] Paolo Ghiggini. Ozsváth-Szabó invariants and fillability of contact structures. *Math. Z.*, 253(1):159–175, 2006.
[29] Paolo Ghiggini, Paolo Lisca, and András I. Stipsicz. Tight contact structures on some small Seifert fibered 3-manifolds. *Amer. J. Math.*, 129(5):1403–1447, 2007.
[30] Paolo Ghiggini and Stephan Schönenberger. On the classification of tight contact structures. In *Topology and geometry of manifolds (Athens, GA, 2001)*, volume 71 of *Proc. Sympos. Pure Math.*, pages 121–151. Amer. Math. Soc., Providence, RI, 2003.
[31] Emmanuel Giroux. Structures de contact en dimension trois et bifurcations des feuilletages de surfaces. *Invent. Math.*, 141(3):615–689, 2000.
[32] Robert E. Gompf. Handlebody construction of Stein surfaces. *Ann. of Math. (2)*, 148(2):619–693, 1998.
[33] Matthew Hedden. Some remarks on cabling, contact structures, and complex curves. In *Proceedings of Gökova Geometry-Topology Conference 2007*, pages 49–59. Gökova Geometry/Topology Conference (GGT), Gökova, 2008.
[34] Ko Honda. On the classification of tight contact structures. I. *Geom. Topol.*, 4:309–368 (electronic), 2000.
[35] Ko Honda. On the classification of tight contact structures. II. *J. Differential Geom.*, 55(1):83–143, 2000.
[36] Ko Honda. Factoring nonrotative $T^2 \times I$ layers. Erratum: "On the classification of tight contact structures. I" [Geom. Topol. **4** (2000), 309–368; mr1786111]. *Geom. Topol.*, 5:925–938, 2001.
[37] Ko Honda. Gluing tight contact structures. *Duke Math. J.*, 115(3):435–478, 2002.
[38] Ko Honda, William H. Kazez, and Gordana Matić. Convex decomposition theory. *Int. Math. Res. Not.*, 2002(2):55–88, 2002.
[39] P. Lisca and G. Matić. Tight contact structures and Seiberg-Witten invariants. *Invent. Math.*, 129(3):509–525, 1997.
[40] Paolo Lisca, Peter Ozsváth, András I. Stipsicz, and Zoltán Szabó. Heegaard Floer invariants of Legendrian knots in contact three-manifolds. *J. Eur. Math. Soc. (JEMS)*, 11(6):1307–1363, 2009.
[41] Paolo Lisca and András I. Stipsicz. Ozsváth-Szabó invariants and tight contact 3-manifolds. III. *J. Symplectic Geom.*, 5(4):357–384, 2007.
[42] Irena Matkovič. Classification of tight contact structures on small Seifert fibered L-spaces. *Algebr. Geom. Topol.*, 18(1):111–152, 2018.
[43] Irena Matkovič. Non-loose negative torus knots. *ArXiv e-prints 2001.07681*, 2020.
[44] Thomas Vogel. Non-loose unknots, overtwisted discs, and the contact mapping class group of S^3. *Geom. Funct. Anal.*, 28(1):228–288, 2018.

SCHOOL OF MATHEMATICS, GEORGIA INSTITUTE OF TECHNOLOGY, ATLANTA, GA
Email address: etnyre@math.gatech.edu
Email address: anubhavmaths@gatech.edu

DEPARTMENT OF MATHEMATICS, MASSACHUSETTS INSTITUTE OF TECHNOLOGY, CAMBRIDGE, MA
Email address: hkmin@mit.edu